Molecularly-targeted anti-cancer drug interactions of the human ABCG2 multidrug transporter

PhD thesis

Csilla Hegedüs

Eötvös Loránd University Faculty of Science
Doctoral School of Biology
Program of Immunology

Supervisors:	Balázs Sarkadi, MD, PhD, DSc
	Csilla Laczka, PhD
Head of the Doctoral School of Biology:	Anna Erdei, PhD, DSc
Head of the Program of Immunology:	Anna Erdei, PhD, DSc

Membrane Research Group of the Hungarian Academy of Sciences
Budapest, Hungary

2013

"Én értem a tudományokat, és egyelőre nem tudom megcsinálni a vállállást a korláton – de mi lesz, ha egyszer mégis megtanulom?"

Karinthy Frigyes

TABLE OF CONTENTS

1. ABBREVIATIONS

ABC:	ATP binding cassette
ABCP:	Placenta specific ABC transporter
Abl:	Abelson tyrosine kinase
ADME-Tox:	Absorption, distribution, metabolism, excretion and toxicity
ADP:	Adenosine diphosphate
AhR:	Aryl hydrocarbon receptor
ALL:	Acute lymphoid leukemia
AML:	Acute myeloid leukemia
ATP:	Adenosine triphosphate
Bcr:	Breakpoint cluster region protein
BCRP:	Breast cancer resistance protein
BSA:	Bovine serum albumin
CAR:	Constitutive androstane receptor
CFTR:	Cystic fibrosis transmembrane conductance regulator
CHO:	Chinese hamster ovary (cells)
CML:	Chronic myeloid leukemia
CSC:	Cancer stem cell
DB:	Disaggregating buffer
DNA:	Deoxyribonucleic acid
DOC:	Deoxycholate
DPBS:	Dulbecco's modified phosphate buffered saline
ECL:	Enhanced chemiluminescence
EDTA:	Ethylene diamine tetraacetic acid
EGF:	Epidermal growth factor
ER:	Endoplasmic reticulum
hEGF:	Human (recombinant) epidermal growth factor
huES:	Human embryonic stem cell
EGFR:	Epidermal growth factor receptor
FISH:	Fluorescent *in situ* hybridization

FTC:	Fumitremorgin C
GFP:	Green fluorescent protein
HPLC-MS:	High pressure liquid chromatography - mass spectrometry
MDR:	Multidrug resistance
MRP:	Multidrug resistance associated protein
mTOR:	Mammalian target of rapamycin
MX:	Mitoxantrone
MXR:	Mitoxantrone resistance protein
NBD:	Nucleotide binding domain
NSCLC:	Non-small cell lung cancer
PDK1:	Phosphoinositide-dependent protein kinase-1
PE:	Phycoerythrin
PFA:	Paraformaldehyde
Pgp:	P-glycoprotein
PhIP:	2-amino-1-methyl-6-phenylimidazo[4,5-b]pyridine
Pi:	Inorganic phosphate
PI3K:	Phosphatidylinositol 3-kinase
PIP3:	Phosphatidylinositol (3,4,5) trisphosphate
PVDF:	Polyvinylidene difluoride (membrane)
PXR:	Pregnane X receptor
RTK:	Receptor tyrosine kinase
SD:	Standard deviation
SDS:	Sodium dodecyl sulfate
SE:	Standard error
Sf9:	*Spodoptera frugiperda* (ovarian cells)
SP:	Side population
SUR1:	Sulfonylurea receptor
TCA:	Trichloro acetic acid
TEMED:	N,N,N′,N′- tetramethyl ethylene diamine
TMD:	Transmembrane domain
WGA:	Wheat germ agglutinin

2. INTRODUCTION

2.1. Multidrug resistance (MDR) and the discovery of P-glycoprotein (Pgp/MDR1/ABCB1)

The appearance of drug resistance during the course of chemotherapy is a major impediment to successful cancer treatment that clinicians have long been facing (1). Extensive research on model cells *in vitro* cultured in increasing doses of anti-cancer drugs has revealed various cellular mechanisms of drug resistance. Cultured cells maintained under drug selection pressure might become resistant to a single agent or a small number of functionally related drugs by loss of a cell surface receptor or transporter for the drug, by alteration of the intracellular target of the drug or by increase of cellular repair mechanisms correcting the drug-induced fatal molecular damage (2,3). *In vitro* cellular exposure to a single anti-cancer drug might also lead to the emergence of ***multidrug resistance (MDR)***, when cells acquire resistance not only to the selecting agent but also develop cross resistance towards a wide variety of chemically and target-wise unrelated drugs (2,3). Studies on the mechanisms of MDR were initiated with the 1973 discovery of the active outward transport of the chemotherapeutic drug daunomycin from resistant tumor cells, described by *Keld Dano* (4). In 1974, a seminal study of *Ling and Thompson* characterized Chinese hamster ovary (CHO) cells which were subjected to stepwise selection with increasing doses of colchicine (5). Colchicine-resistant CHO cells showed cross resistance to several apparently unrelated compounds, and the degree of cross resistance positively correlated with that of colchicine resistance (5,6). Analysis of the isolated colchicine-resistant CHO cells revealed that reduced cellular drug uptake rather than altered intracellular colchicine binding was responsible for colchicine resistance (5), and it was further suggested that energy-dependent alterations in the permeability of the plasma membrane could account for the pleiotropic phenotype of the drug resistant cells (6,7). In 1976, a 170 kDa glycoprotein in the cell surface of resistant CHO cells was identified as the major molecular determinant of decreased drug permeability, which was hence designated as ***P-glycoprotein (Pgp)*** (MDR1, ABCB1) (8). The finding that the relative amount of Pgp in the cell membrane showed strong positive correlation with the degree of drug resistance also provided evidence that the presence of Pgp was functionally related to the drug resistant phenotype (8). In subsequent reports,

expression of Pgp was demonstrated in hamster, mouse and human tumor cell lines displaying simultaneous resistance to various drugs and in human tumor samples as well (9-14), suggesting a general molecular basis for the emergence of multidrug resistance and its potential relevance in cancer therapy. *Pgp* was cloned in 1986, and its predicted amino acid sequence was found to contain the consensus sequence for two potential ***ATP binding cassettes (ABC)***. The evolutionarily conserved ATP binding domain had already been known to couple the energy of ATP hydrolysis to various cellular functions in bacteria, including membrane transport processes (15). Based on the strong homology observed between Pgp and bacterial transporters, Pgp was proposed to function as an efflux pump responsible for the removal of various drugs by an ATP-dependent mechanism thereby causing multidrug resistance (16-22).

2.2. Atypical multidrug resistance and the discovery of BCRP/MXR/ABCP/ABCG2

Although the concept that the function of a single protein accounted for the MDR phenomenon initially seemed to hold out promising implications for cancer treatment, it soon became obvious that cellular factors other than Pgp also operated in multidrug resistant cells. The notion that vincristine-selected HL60 and doxorubicin-selected H69AR cells displayed a multidrug resistant phenotype but were devoid of Pgp expression led to the cloning of a novel ABC transporter termed as ***multidrug resistance associated protein (MRP)*** (MRP1, ABCC1) (23,24). An early study describing detailed pharmacological characterization of MRP revealed that forced expression of the protein also conferred a multidrug resistant phenotype which was similar but not identical to that caused by Pgp (25).

In search for alternate cellular factors involved in MDR, studies using the *in vitro* drug selection approach continued. In the 1990s, MCF-7 human breast carcinoma cells exposed to stepwise selection with doxorubicin (Adriamycin) in the presence of the Pgp inhibitor verapamil (MCF-7/AdrVp) were demonstrated to lack overexpressed Pgp and MRP and to show a unique (‘atypical’) cross-resistance pattern. MCF-7/AdrVp cells also displayed enhanced ATP-dependent efflux of daunomycin and rhodamine 123 implying the presence of an as yet unknown energy-dependent transport protein (26,27).

Investigations using these MCF-7/AdrVp cells, other mitoxantrone-selected cell lines showing an atypical drug resistance pattern; and analysis of a human cDNA library led to the discovery of the third ABC protein associated with the transport of various chemotherapeutics and multidrug resistance, that was named after the biological systems from which it was simultaneously but independently identified as ***breast cancer resistance protein (BCRP), mitoxantrone resistance protein (MXR)*** or ***placenta specific ABC transporter (ABCP)*** (28-30).

2.3. The ABCG2 protein: structure, function, tissue distribution and putative physiological role

BCRP/MXR/ABCP belongs to the superfamily of ***ATP binding cassette (ABC) transporter*** proteins which represents one of the largest and most diverse groups of transmembrane proteins. Members of the ABC protein superfamily share a structurally and functionally highly conserved protein module, the ATP binding cassette (ABC) (also known as nucleotide binding domain, NBD) , which is responsible for the binding and hydrolysis of ATP and thereby can energize inward (cellular or luminal accumulation, import) or outward (extrusion, export) transmembrane transport processes (15,31). ABC transporters are present in all species from microorganisms to man and are engaged in a variety of biological functions (31).

The human genome encodes 48 ABC transporters which, based on gene structure, amino acid sequence alignments and domain organization, can be grouped into seven subfamilies from A to G. Protein members of the subfamilies are further denoted by Arabic numerals, therefore BCRP/MXR/ABCP which is the second member of the ABCG subfamily was designated as ***ABCG2*** according to the standard nomenclature (32). The vast majority of human ABC proteins function as active transporters moving their substrates against a concentration gradient, but proteins functioning as channels (the cystic fibrosis transmembrane conductance regulator CFTR/ABCC7 which functions as a chloride ion channel) or receptors (the sulfonylurea receptors SUR1/ABCC8 and SUR2/ABCC9 which regulate an ATP-dependent potassium channel) are also present in the superfamily (32,33). Mutations in 18 of the human ABC genes have been linked to human diseases or phenotypes (34).

The human *ABCG2* gene, which was mapped to be located on chromosome 4q22, spans over 66 kb and consists of 16 exons (30,35). Its gene product is a 655 amino acid 72 kDa protein, which, similarly to all members of the ABC superfamily is built from two structurally and functionally characteristic units: the nucleotide binding domain and the transmembrane domain (Fig. 1). The ***nucleotide binding domain (NBD)*** which is responsible for ***releasing the energy of ATP hydrolysis*** carries three evolutionarily conserved sequence motifs, the ***Walker A*** (GXXGXGKS/T), the ***Walker B*** (hhhhD) and the ***ABC signature motif*** (LSGGQQ/R/KQR) (28-30,36). While the Walker A and Walker B motifs can be found in other nucleotide binding proteins as well (37), the ABC signature motif is a hallmark of the ABC transporter superfamily (36). The ***transmembrane domain (TMD)*** of ABCG2 is predicted to consist of six membrane spanning helices (38-40), and is most probably responsible for the ***recognition and handling of substrates***. The hydrophilic amino terminal of ABCG2 contains the NBD, while the TMD is located in the relatively hydrophobic carboxyl terminal of the protein. This molecular configuration corresponds to one half of the Pgp polypeptide in a reverse domain arrangement (Fig. 1).

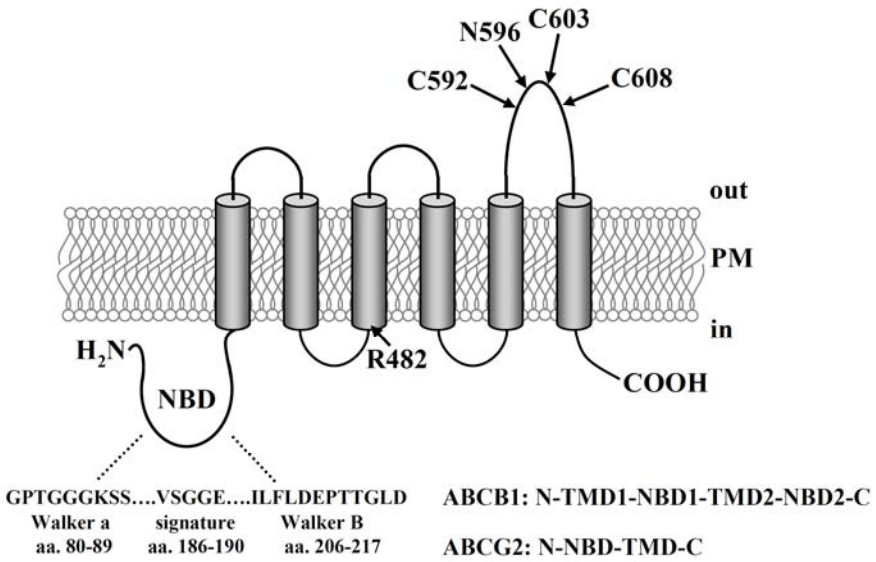

Figure 1. Predicted membrane topology of ABCG2. *ABCG2 is built from a nucleotide binding domain (NBD) and a transmembrane domain (TMD) of six membrane spanning helices. NBD consensus motifs are Walker A, Walker B and the signature. C592, C608 and C603 are involved in intra- and intermolecular disulfide bridge formation; amino acid at position 482 affects substrate specificity (see text for details). Domain organization of ABCG2 compared with ABCB1 is shown. PM: plasma membrane; aa: amino acid.*

It is widely accepted that a fully functional ABC transporter requires the presence of at least two NBDs and two TMDs, therefore the ABCG2 protein is recognized as a ***half-transporter*** and is currently considered to work as a ***homodimer or homo-oligomer*** (28-31,41-44).

Similarly to all ABC proteins, the transport process performed by ABCG2 is energized by the hydrolysis of ATP. The two L-shaped ***NBDs dimerize*** in a head-to-tail orientation to form two ***composite catalytic sites***; each involving the Walker A sequence of one and the ABC signature motif of the other NBD and sandwiching the nucleotides at the NBD dimer interface (45,46). The functional interaction and the formation of the substrate translocation pathway by two TMDs are also required for proper transporter function (47-49). The ***ATP hydrolytic (catalytic) cycle*** has been profoundly investigated using the first discovered human MDR-ABC transporter molecule, Pgp. According to the ***alternating catalytic sites*** hypothesis first proposed by Senior et al in 1995, ATP binding at one catalytic site promotes the hydrolysis of ATP at the other catalytic site and ATP hydrolysis induces a conformation which prohibits ATP hydrolysis at the other site. Relaxation of this intermediate bearing high chemical potential results in the translocation of the bound substrate (50). A revised and extended model of the catalytic cycle of Pgp was presented by Sauna et al, suggesting that two hydrolysis events are required in each transport cycle (51). This model proposes that the first step of the catalytic cycle is the binding of the drug on the 'ON' drug-binding site, and the binding of ATP molecule(s) at one or both of the catalytic sites. There is no energetic requirement for this step. Hydrolysis of the first ATP molecule generates a conformational change that reduces the affinity of both the drug (possibly moving to the 'OFF' drug-binding site) and the nucleotide for Pgp. With the release of inorganic phosphate (Pi), the drug is extruded from Pgp. The subsequent release of ADP generates a conformation displaying high affinity for nucleotides but low affinity for drug and hydrolysis of the second ATP is initiated. The second ATP hydrolysis event is required for re-setting the transporter to regain its high affinity drug binding state and to enter a new cycle (51). The basic principles established by these models still guide further refinements.

The *classical pump* model suggests that MDR-ABC transporters would remove their substrates from the cytoplasm, which apparently seem to conflict with the promiscuous

drug recognition and the high abundance of lipophilic substrates for both Pgp and ABCG2. Two alternative models therefore suggested that drug recognition by MDR-ABC transporters occur in the lipid phase, and the protein translocates the drug directly from the membrane (*hydrophobic vacuum cleaner*) or extracts its substrate from the inner to the outer membrane leaflet similarly to lipid *floppases* (Fig. 2). A kinetic model describing the ***hydrophobic vacuum cleaner*** mechanism fit best with the experimental data obtained by microscopic analysis of the GFP-ABCG2-mediated cellular extrusion of mitoxantrone, indicating that ABCG2 removes mitoxantrone directly from the cell membrane (52).

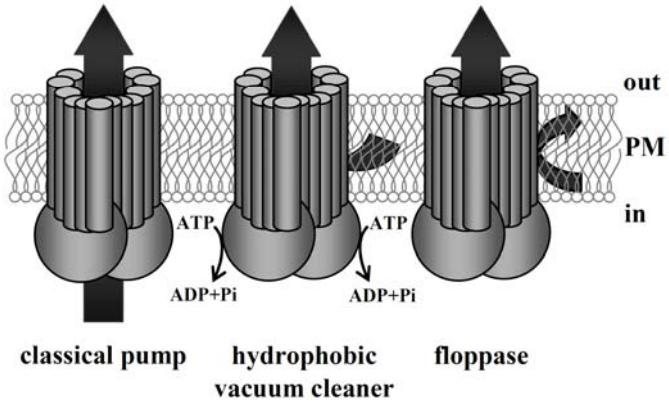

Figure 2. Transport models of MDR-ABC proteins. *Instead of removing substrates from the cytoplasm as classical pumps, MDR-ABC proteins were suggested to interact with their substrates in the lipid phase. According to the hydrophobic vacuum cleaner model, MDR-ABC transporters extract their substrates directly from the plasma membrane. Alternatively, they might work similarly to lipid floppases. ABCG2 was shown to expel mitoxantrone directly from the plasma membrane (52). The energy of ATP hydrolysis is used for transport in all cases, which, for clarity is only shown in the hydrophobic vacuum cleaner model. PM: plasma membrane.*

The exact molecular mechanism of ***coupling the energy of ATP hydrolysis with the transport of substrates*** and the molecular basis of ***polyspecific drug binding*** of MDR-ABC transporters are still unclear. Crystal structures of cytoplasmic NBDs or full polypeptides of several bacterial ABC transporters have been solved, including the entire Sav1866 multidrug exporter of *Staphylococcus aureus*, which is the bacterial homolog of human Pgp (53,54). The molecular snapshot of Sav1866 caught an outward facing conformation in an ADP-bound state, with the two NBDs in close proximity sandwiching the bound nucleotides. The structure indicates that residues from all transmembrane

helices are involved in forming a large cavity at the interface of the two TMDs, which serves as the translocation pathway for drugs. Rather than aligned side-by-side, the subunits are twisted so that and each NBD contacts both TMDs. To date, high resolution structural information regarding mammalian ABC transporters is only available for murine Pgp which shows 87% sequence identity with human Pgp (55). Structures of the apo and drug-bound murine Pgp revealed an inward facing conformation with a large intramembrane cavity bearing distinct drug-binding sites and two portals open to the inner leaflet and the cytoplasm that allow entry of hydrophobic drugs. Nevertheless, as each of the solved murine Pgp structures is in the absence of bound nucleotides and the two NBDs seem to locate unreasonably far apart, it can be debated whether these crystal structures have any physiological relevance.

Gene expression of human *ABCG2* is regulated by the binding of numerous transcription factors (56) and also by the usage of three ***alternative promoters***. The transcribed ABCG2 mRNA species with ***different 5' UTRs*** (untranslated regions) (exon 1a, b and c) have been reported to display a tissue specific and tumor type specific expression pattern (57-60). ABCG2 transcripts carrying ***distinct 3' UTRs*** were also reported in human embryonic stem cells (huES cells) and drug selected tumor cells, and stability and translation of these 3' UTR ABCG2 mRNA variants were suggested to undergo miRNA-mediated control (58,61,62). The translated ABCG2 polypeptide undergoes folding and ***N-glycosylation*** at N596 in the endoplasmic reticulum (ER) and transits *via* the Golgi to the plasma membrane (Fig. 1). Full glycosylation at N596 is not prerequisite either for plasma membrane localization or for proper function of the transporter (41,63-65). The ***third extracellular loop*** of ABCG2 is relatively large and exposes three cysteine residues (C592, C603 and C608) which are involved in the formation of ***intra- and intermolecular disulfide bridges*** in the ER (Fig. 1). The intramolecular disulfide bridge (between C592 and C608) influences the plasma membrane targeting and the substrate specificity of ABCG2 (66-69) and the extracellular epitope formation for the anti-ABCG2 5D3 antibody as well (70,71). The intermolecular disulfide bridge covalently links two ABCG2 molecules via their C603 residues, thus generating a homodimer (66,72). Interestingly, the presence of C603 and the resulting intermolecular disulfide bond between two ABCG2 molecules is not essential for the

expression and proper function of the transporter (43,66,67,72,73). The third extracellular loop of ABCG2 has also been suggested to play role in the transmembrane transport and extracellular transfer of porphyrines (74). Regulation of the localization or function of ABCG2 by phosphorylation is currently controversial, as functional ABCG2 was shown to be unphosphorylated in epithelial and ovarian carcinoma cell lines (64); however, in prostate cancer cells phosphorylation of the transporter at T362 by Pim-1 kinase was reported (75). Involvement of signaling cascades in the expressional and functional regulation of ABCG2 is poorly understood. The ERK/MAPK cascade (60,76,77), the PI3K/Akt cascade (78-84), the p53/NFkappa-B pathway (85) and Hedgehog (Hh) signaling (86,87) have been proposed to regulate ABCG2. Correctly processed functional ABCG2 is degraded *via* the lysosome, while ABCG2 that is misfolded, underglycosylated or lacks the intramolecular disulfide bond is targeted to the ubiquitin-mediated proteasomal proteolysis pathway (65).

ABCG2 is ***predominantly expressed in the plasma membrane*** (88-90), however presence of the transporter has also been reported in lysosomal and mitochondrial membranes (91-93). While surface ABCG2 is believed to be part of the first line cellular defense machinery eliminating xenobiotics at the cell membrane, ABCG2 located in lysosomal compartments has been suggested to be involved in vesicular sequestration of intracellularly accumulated drugs (91), whereas mitochondrial ABCG2 has been reported to transport mitoxantrone (92) and to decrease 5-aminolevulinic acid (ALA)-mediated mitochondrial accumulation of protoporphyrin IX (93). Nevertheless, the presence, functional activity and biological relevance of ABCG2 located in subcellular compartments await confirmation from further studies.

Northern blot, RT-PCR and immunohistochemistry revealed that human ABCG2 is highly expressed in placental syncytiotrophoblasts, in the epithelium of the small and large intestine and the colon, in biliary canaliculi, in the proximal tubule of the kidney, in the zona reticularis of the adrenal gland, in Sertoli/Leydig cells of the testis, in alveolar pneumocytes of the lung, in breast tissue, in veinous and capillary endothelium and in the endothelium of the central nervous system (28,94,95). The ***physiological tissue distribution*** of ABCG2 strongly ***indicates a general xenoprotective function*** for the transporter. ABCG2 is also expressed in the ***side population (SP) of stem cells*** of various

origins and is currently believed to maintain the undifferentiated state of stem cells and/or to contribute to their protection against endo- and exotoxins, various stress conditions and hypoxia (70,96-98). ABCG2 is also present in the cell membrane of erythrocytes, and defines the blood group system Junior (Jr) (99,100).

ABCG2 knockout (Bcrp1-/-) mice proved to be viable and fertile (101). Nevertheless, when Bcrp1 null mice were challenged with the dietary phototoxin pheophorbide a (a breakdown product of chlorophyll) they developed protoporphyria and (in some cases lethal) phototoxic lesions on light-exposed skin on the ear (102). Pheophorbide a was shown to be a transported substrate of ABCG2 (102,103). Bcrp null mice were also reported to display increased systemic exposure to the dietary carcinogen PhIP (104). Moreover Bcrp1-/- mice showed increased sensitivity to mitoxantrone (101). These data further suggest a key role of ABCG2 in protecting the body from endogenous and environmental toxins.

Recently, orchestrated co-operation of uptake transporters, drug metabolizing enzymes and efflux transporters, including MDR-ABC proteins, in cellular and systemic protection of the body has been suggested. As several features of this molecular machinery resemble those of the classical immune system (46,105), it has been designated as a ***chemoimmunity defense system*** (46) (Table 1).

	Immune system	**Chemoimmune system**
Target	Water-soluble antigens	Hydrophobic toxins
Physiological functions	Recognition, elimination	Recognition, elimination
Major types	Innate, adaptive	Innate, adaptive
Effectors	Huge repertoire of proteins	Limited number of proteins
Pathological functioning	Autoimmune disorders, allergy	Multidrug resistance

Table 1. Comparison of the classical immune system and the chemoimmune system.

Wet laboratory studies reporting upregulation of ABCG2 by xenobiotic sensing receptors (which also regulate expression of various uptake transporters, drug metabolizing enzymes and other MDR-ABC transporters) such as the aryl hydrocarbon

receptor (AhR) (106-109), the constitutive androstane receptor (CAR) (110,111) or the pregnane X receptor (PXR) (110) also support the concept that ABCG2 might be involved in a complex molecular chemoimmunity network.

2.4. ABCG2 in cancer

Following identification and cloning of ABCG2, its overexpression was soon demonstrated to be associated with the multidrug resistant phenotype of cancer cell lines of various origins, such as breast, colon, gastric and ovarian carcinoma, fibrosarcoma and myeloma (29,112,113). Nevertheless, whether or not functional ABCG2 is present and can be associated with drug resistance in human tumors has raised controversies. Samples from patients with ***hematological malignancies*** such as acute myeloid leukemia (AML) or acute lymphoid leukemia (ALL) were both reported to express relatively high and low or undetectable levels of ABCG2, questioning the prognostic significance of the transporter (90,114-121); while primitive chronic myeloid leukemia (CML) cells were shown to express functional ABCG2 (122,123). Similarly, immunohistochemical staining of ABCG2 in a panel of human ***solid tumor*** samples revealed ABCG2 expression in only a single case of small-intestinal adenocarcinoma (out of 57 cryosections of various tumor origins) in one study (90), whereas frequent expression of the transporter was described in a panel of 150 samples of 21 tumor origins in another paper (124). A case report also associated ABCG2 overexpression with acquired drug resistance in a non-small cell lung cancer (NSCLC) patient (125). Most probably due to the ***lack of validated standard methods to detect MDR-ABC transporter expression and function*** in human tumor tissues, ABCG2 (together with Pgp and MRP1) is still being attributed a ***controversial role in clinical oncology***. Importantly, as ABCG2 shows relatively high physiological expression at pharmacological tissue barriers (in the gut, the liver, the kidney, the blood-brain barrier, the blood-testis barrier or feto-maternal barrier) recent studies have also proposed its ***major influence on drug absorption, distribution, metabolism, excretion and toxicity (ADME-Tox)*** (126,127).

ABCG2 is the molecular determinant of the side population (SP) of normal stem cells under physiological conditions (70). The SP fraction has also been isolated from various hematological and solid tumors (81,128-130); and ***cancer SP cells*** were shown to

recapitulate several properties of normal stem cells such as self-renewal or ***resistance to chemotherapeutics*** (81,129,131,132). The ***cancer stem cell (CSC) hypothesis*** suggests that drug resistant cancer stem cells are driving tumor re-growth and ***ABCG2*** is probably a pivotal efflux transporter that ***contributes to preserving the CSC sanctuary under chemotherapeutic pressure*** (128,132). Notably, a small subpopulation of AML and CML cells were reported to show remarkably high expression of ABCG2. These cells were also $CD34^{+}CD38^{-}$ that is a surface antigen marker combination which is currently believed to define the cancer stem cell population in these leukemias (119,122,123).

2.5. Substrates and inhibitors of the ABCG2 protein

The hypothesis that ABCG2 has an essential physiological role (which would assume that it transports an important physiological substrate) can be challenged by the notions that *Bcrp1-/-* mice, at least in controlled sterile animal facilities, are viable and fertile; and human individuals of the Jr(a-) blood type who lack cell surface ABCG2 appear phenotypically normal (99-101). These observations could also be explained by MDR-ABC transporters having an overlapping physiological substrate spectrum and thus fulfilling a replaceable physiological function. Indeed, ***physiological substrates*** for ABCG2 have long remained elusive. Two genome-wide association studies identified a single nucleotide polymorphism (SNP) in the *ABCG2* gene as a major modulator of serum uric acid levels and as a potential risk factor for hyperuricemia and gout (133,134). In a follow-up report ABCG2 was shown to transport ***uric acid*** (135).

ABCG2 transports a remarkably wide spectrum of chemically and target-wise unrelated drugs (56,126,136,137). Selected ***drug substrates*** of ABCG2 are listed in Table 2. Accordingly, ABCG2 has been shown to confer cellular resistance against various clinically relevant anti-cancer drugs; however, correlation between results obtained in primary tumors and tumor cell lines has not always been straightforward. Importantly, ABCG2 substrates acting as competitive inhibitors might play an attractive role in chemo-sensitization of drug resistant cells during combination therapies. Interestingly, numerous drug-selected cancer cell lines were shown to overexpress mutant ABCG2 protein variants, namely ABCG2 R482G or ABCG2 R482T (28,29,138-140). Amino acid substitutions at the 482 position were shown to affect the substrate specificity of the

transporter (141,142). Interestingly, even though the R482G and R482T gain-of-function mutations frequently appeared in drug-selected cell lines, only the wild-type ABCG2 species carrying an arginine at position 482 has hitherto been found in the human population (143).

Antineoplastics	
Anthracyclines	Mitoxantrone
Antifolates	Methothrexate
Campthotecins	Topotecan, irinotecan, SN-38
Kinase inhibitors	Flavopiridol, quercetin, imatinib, danusertib, gefitinib, erlotinib, lapatinib, sorafenib, sunitinib
Antihypertensives	Prazosin
Antivirals	Zidovudine (AZT), lamivudine
Antibiotics	Ciprofloxacin, ofloxacin, norfloxacin

Table 2. Selected drug substrates of the wild-type ABCG2 multidrug transporter. *The list was compiled from (46,56,126,127,136).*

Fumitremorgin C (FTC), a mycotoxin extracted from *Aspergillus fumigatus* had been reported to reverse atypical drug resistance before ABCG2 itself was identified and cloned (144). Later, FTC was confirmed to ***selectively inhibit the function of ABCG2*** (145). FTC showed little toxicity *in vitro,* however was reported to cause tremors in cockerels, while two related compounds FTA and FTB also showed neurotoxic effects in mammals, precluding *in vivo* applicability of FTC (145). The ***FTC analogue compounds Ko132, Ko134 and Ko143*** were reported to be potent, specific and low-toxicity inhibitors of ABCG2 *in vitro,* and also inhibited the function of the transporter *in vivo* in mice (146). ***Multispecific MDR-ABC transporter inhibitors*** showing both *in vitro* and *in vivo* activity are also available, such as elacridar (GF120918) and tariquidar (XR-9576) which inhibit Pgp and ABCG2; or cyclosporine A (CSA) and biricodar (VX-710) which inhibit Pgp, MRP1 and ABCG2 (126). Most of these multispecific inhibitors have already had history as potential (Pgp-mediated) MDR reversal agents applied in clinical trials, which unfortunately all ended with disappointing results (126,136). Inefficiency and/or toxicity

of the MDR-ABC inhibitors observed are currently believed to have resulted from the recruitment of patient cohorts not biased for MDR-ABC transporter expression and from interference with the physiological xenoprotective function of the targeted transporters. Recently, several compounds have been identified to which drug resistant cancer cells overexpressing Pgp showed an unexpected hypersensitivity (collateral sensitivity) (147-149). Whether drugs that selectively kill ABCG2-expressing cancer cells exist is yet to be elucidated (150). Nevertheless, novel promising therapeutic strategies seem to emerge that aim to selectively target and exploit MDR-ABC transporter overexpression of cancer cells (136).

2.6. Targeted cancer therapy

Conventional chemotherapeutics, which target DNA replication, DNA uncoiling, nucleic acid metabolism or microtubule function, cannot distinguish between rapidly dividing normal and cancer cells. The notion that proliferation and survival of cancer cells often depend on a single activated oncogene (a phenomenon currently believed to render cancer cells especially susceptible to interference with the function of the oncogene and the oncogene-associated signaling pathways, recently also termed as ***oncogene addiction***) provided a rationale for the design and clinical application of ***molecularly-targeted cancer therapeutic strategies*** that would specifically eliminate the malignant cells (151-154). Oncogenes that can confer oncogene addiction most frequently code for ***kinases*** (152,155-157). The human kinome has been shown to contain 518 putative kinase genes which constitute about 1.7% of the human genes (158). Chromosomal mapping of the human kinase genes revealed that 164 kinases located to amplicons frequently appearing in tumors (158); furthermore, an unexpectedly large number of putative *driver (playing a causal role in oncogenesis) and passenger somatic mutations* in kinomes of various tumor origins has recently been described (159,160). Protein kinases which have been validated as major contributors to oncogenesis, and therefore have already served as promising drug targets include the Bcr-Abl and the Epidermal Growth Factor Receptor (EGFR) kinase enzymes.

2.6.1. Bcr-Abl signaling in cancer and its small molecule inhibitors

Bcr-Abl is an ***oncogenic non-receptor tyrosine kinase*** whose activity is required for the pathogenesis of ***chronic myeloid leukemia (CML)***, a clonal myeloproliferative disorder of hematopoetic stem cell (HSC) origin. The genetic hallmark of CML is the *Philadelphia chromosome* (a shortened chromosome 22) generated by the t(9;22)(q34;q11) reciprocal translocation, which can be detected in approximately 95% of CML patients. This chromosomal translocation fuses the *Abl* proto-oncogene (the human homologue of *v-Abl* carried by the Abelson murine leukemia virus) physiologically located on chromosome 9 to the *Bcr* (breakpoint cluster region) gene on chromosome 22, generating the *Bcr-Abl* hybrid gene. Depending on the exact location of the breakpoints in *Bcr* (designated as major, minor and micro breakpoint cluster regions; M-*bcr*, m-*bcr* and μ-*bcr* respectively) and on alternative splicing of the different transcripts, four fusion protein variants can be generated, with molecular weights of 190 kDa, 210 kDa or 230 kDa. Most CML patients carry the 210 kDa Bcr-Abl kinase (161,162). The fusion-mediated loss of the N-terminal myristoylation site of Abl and the Bcr coiled-coil motif-mediated interference with the kinase autoinhibitory domains (Src homology domains, SH2 and SH3) of Abl results in ***constitutive tyrosine kinase activity*** and leukemogenic potential of Bcr-Abl (163,164) (Fig. 3). The autophosphorylation of Bcr-Abl at Tyr177 links Bcr-Abl to mitogenic Ras signaling through its direct interaction with the adaptor protein Grb2 (growth factor receptor-bound protein 2), a phenomenon which is required for the transforming potential of the fusion kinase (165-167) (Fig. 3). Bcr-Abl also transduces pro-survival and anti-apoptotic signals, and signals resulting in altered cell adhesion and migration (163,168).

Since ***Bcr-Abl plays a pivotal role in leukemogenesis***, it was soon recognized as a promising ***molecular drug target***. The first identified ***small molecule inhibitor*** showing potent *in vitro* and *in vivo* Abl inhibitory activity was ***imatinib*** (Gleevec/Glivec/imatinib-mesylate/CGP57148/STI-571) (169). Imatinib was soon reported to suppress proliferation and induce apoptosis of Bcr-Abl positive primary and model cells, setting the stage to its translation to clinical use (170-173). Imatinib displays an additional inhibitory activity on c-KIT (stem cell factor receptor, CD117) and PDGFR (platelet-derived growth factor receptor) kinases (174). Imatinib received accelerated FDA (US

Food and Drug Administration) approval in 2001, and 5- and 6-year follow-up studies reported impressive response rates and outstanding estimated overall survival rates in CML patient cohorts receiving imatinib as initial therapy (175,176). Nevertheless, imatinib is observed to be less effective in the advanced phases of CML, disease persistence is detected in the majority of patients indicating that imatinib is unable to eradicate all of the malignant cells, and resistance to imatinib also develops in many cases (177).

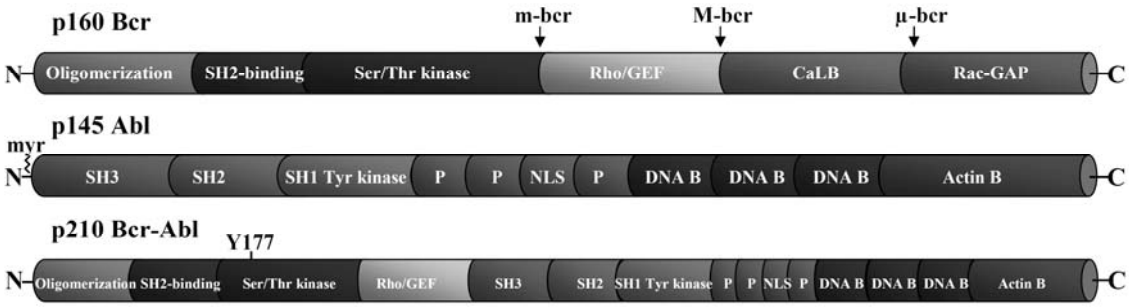

Figure 3. Domain organization of the Bcr (p160), Abl (p145) and Bcr-Abl (p210) proteins. *Actin B: Actin binding domain; CaLB: Calcium-dependent lipid binding domain; DNA B: DNA binding domain; NLS: Nuclear localization signal; P: Proline-rich domain; Rac/GAP: Rac GTPase activating protein homology domain; Rho/GEF: Rho guanine-nucleotide-exchange factor homology domain; SH: Src homology domain. Major (M), minor (m) and micro (µ) breakpoint cluster regions in Bcr, and Tyr177 residue in Bcr-Abl are shown. Myr: myristoylation site.*

To overcome the problems experienced with imatinib, second generation small molecule inhibitors of Bcr-Abl have been developed. The novel inhibitors include the selective Abl inhibitor ***nilotinib*** (Tasigna/ AMN107), and the dual inhibitors of the Abl and Src kinases ***dasatinib*** (Sprycel/ BMS-354825) and ***bosutinib*** (Bosulif/ SKI-606). Similarly to imatinib, nilotinib and dasatinib also inhibit c-KIT and PDGFR (174). Nilotinib and dasatinib are currently approved as a frontline therapy of CML and as a second-line treatment option in CML patients who are resistant or intolerant to imatinib; while bosutinib has recently been approved to treat CML patients who failed on prior treatments with multiple Bcr-Abl inhibitors (178,179). Resistance against second generation inhibitors of Bcr-Abl also occurs but has yet been less characterized (177).

2.6.2. EGFR signaling in cancer and its small molecule inhibitors

The ***Epidermal Growth Factor Receptor*** (EGFR/ErbB1/HER1) belongs to the ErbB subclass of the ***receptor tyrosine kinase*** (RTK) superfamily. ErbB receptors are physiologically expressed in various tissues of epithelial, mesenchymal and neuronal origins and play an essential role in embryogenesis. ErbBs are single-pass transmembrane receptors having an extracellular domain responsible for the binding of polypeptide ligands of the EGF (Epidermal Growth Factor) family and an intracellular region containing a tyrosine kinase catalytic domain. ErbB receptors homo-or heterodimerize upon ligand binding that results in activation of the intrinsic kinase domain and subsequent phosphorylation of tyrosine residues in the cytoplasmic tail. The phosphotyrosine residues serve as docking sites for adaptor proteins or enzymes with Src homology-2 (SH2) or phosphotyrosine-binding (PTB) domains, recruitment of which mediates the activation of multiple downstream signaling cascades involved in various cellular programs, such as proliferation, differentiation, survival, migration and adhesion. Under physiological conditions, ErbB receptor activity is tightly controlled by the spatial and temporal ligand accessibility (180,181).

EGFR (and ErbB2/HER2/Neu as well) has been reported to be ***constitutively active*** in numerous cancer types including ***glioma, breast cancer, ovarian cancer, colorectal cancer (CRC), squamous-cell carcinoma of head and neck (SCCHN) and non-small cell lung cancer (NSCLC)***. Aberrant activation of EGFR was reported to result from *autocrine ligand production* or *overexpression or mutation of the receptor* itself and was associated with poor clinical outcomes (180). Accordingly, EGFR has intensively been pursued as a molecular drug target. Therapeutic inhibition of EGFR can be achieved by ***monoclonal antibodies (mAbs)*** that either neutralize ligands or target the extracellular ligand binding domain of the receptor thus preventing dimerization-mediated activation and causing receptor internalization. Another therapeutic option is the administration of ***small molecule inhibitors*** which target the intracellular tyrosine kinase domain of the receptor (181,182). Small molecule inhibitors of EGFR include ***gefitinib*** (Iressa/ ZD1839) and the second generation inhibitors ***vandetanib*** (Zactima/ ZD6474), ***pelitinib*** (EKB-569) and ***neratinib*** (HKI-272) (154,183). Second generation EGFR inhibitors are multi-kinase specific and/or irreversibly bind to the target receptor that is believed to

enable augmentation of drug efficacy and the targeting of multiple types of solid tumors. Vandetanib is a potent inhibitor of vascular endothelial growth factor receptor 2 and 3 (VEGFR-2,3), and shows additional inhibitory activity against EGFR (184). Pelitinib covalently binds to and inhibits EGFR (185). Neratinib, another irreversible inhibitor of EGFR was synthesized on the chemical scaffold of pelitinib, and has additional inhibitory activity against ErbB2/HER2/Neu (186). Gefitinib, vandetanib, pelitinib and neratinib are presently under clinical evaluation or use either as monotherapy or in combination for a histologically diverse range of tumors, including lung cancer (183), breast cancer (187-189) and colorectal cancer (190). Notably, resistance to small molecule inhibitors of EGFR has also been reported to occur in several cases and represents a major impediment to the successful management of the relevant solid tumors (183,191,192).

2.7. Relevance of ABCG2 in resistance to small molecule kinase inhibitors applied in targeted cancer therapies

Target-dependent and ***target-independent molecular mechanisms causing resistance*** to small molecule inhibitors of Bcr-Abl and EGFR have both been described. *Point mutations* in the kinase domain of Bcr-Abl and EGFR, *overexpression* of Bcr-Abl and *engagement of redundant signaling molecules* (such as increased signaling by Lyn kinase or the MET receptor kinase in CML and lung cancer, respectively) are currently recognized as causal factors of drug resistance in the relevant tumor types (174,177,181-183,191,192). As small molecule kinase inhibitors have to pass the cell membrane to exert their intracellular kinase inhibitory action, involvement of the ***MDR-ABC efflux transporters*** has also been implicated in the emergence of drug resistance. On one hand, MDR-ABC proteins which are physiologically expressed at ***pharmacological tissue barriers*** might ***modify the bioavailability*** of the orally administered small molecule kinase inhibitors. On the other hand, exploiting the physiological protective function of the transporters, targeted ***cancer cells*** which overexpress MDR-ABC proteins might ***develop (multiple) drug resistance***. Furthermore, the specific function of ABCG2 might also ***protect the cancer stem cell (CSC) population*** leading to replenishment of the tumor. ABCG2 has been shown to interact with numerous clinically relevant small molecule kinase inhibitors (Table 2). The current literature on these interactions has

recently been reviewed by us (193,194); therefore, here I focus on data regarding interaction between ABCG2 and small molecule inhibitors of Bcr-Abl or EGFR.

Initially, data regarding the interaction of ABCG2 and imatinib were conflicting. Imatinib was reported to modulate the ATPase activity of ABCG2, which indicated that ABCG2 recognized and interacted with imatinib (195); however, at the time, imatinib had been recognized either as a substrate (196) or as an inhibitor (197) of the transporter. In subsequent reports, mostly published when our project had already been running, the ABCG2 ATPase modulatory effect of imatinib was confirmed (198,199), and ABCG2 was shown to transport lower concentrations of imatinib and to confer *in vitro* cellular imatinib resistance (78,196,198). Parallelly, imatinib at higher doses was reported to reverse ABCG2-mediated cellular resistance to the ABCG2 substrates mitoxantrone (195), topotean and SN-38 (197) and to inhibit the ABCG2-mediated transport of mitoxantrone (196), pheophorbide a (200,201) and Hoechst 33342 (195,198). Information about the interaction of ABCG2 and second generation inhibitors of Bcr-Abl were scarce. Both nilotinib and dasatinib were suggested to be transported by ABCG2 (198,202), and nilotinib was further shown to inhibit ABCG2-mediated Hoechst 33342 transport (198).

The first successful EGFR inhibitor gefitinib was characterized in detail with respect to its *in vitro* interaction with ABCG2. Gefitinib was shown to stimulate the ATPase activity of ABCG2 (195,203); however, similarly to imatinib, discrepancies soon emerged regarding the nature of the interaction between gefitinib and the transporter. Following the initial controversies concerning whether this compound is a substrate of ABCG2 or not (203-206), subsequent studies confirmed that ABCG2 transports lower concentrations of gefitinib and thereby causes *in vitro* cellular gefitinib resistance (203,204,207,208), while higher doses of gefitinib re-sensitize drug resistant cells to mitoxantrone, topotecan and SN-38 and inhibit ABCG2-mediated Hoechst 33342 and topotecan transport (195,206). The issue whether ABCG2 interacts with second generation inhibitors of EGFR has only been addressed in the case of vandetanib and the clinically irrelevant ABCG2 R482G variant (209).

3. AIMS

Since at the very beginning of the *first project* presented in my thesis, data regarding the interaction of ABCG2 with imatinib were controversial, and no information was available about the interaction of ABCG2 and second generation inhibitors of Bcr-Abl, we aimed to

- investigate whether imatinib can interfere with the ATPase activity of human wild-type ABCG2,
- set up and characterize a Bcr-Abl+ K562 cellular model system showing stable overexpression of the human wild-type ABCG2 multidrug transporter,
- clarify whether the function of human wild-type ABCG2 can influence the intracellular effects of imatinib,
- applying the Sf9 insect membrane- and Bcr-Abl+ K562 cell-based model systems which we validated by the analysis of the ABCG2-imatinib interaction, perform a comparative biochemical characterization on the interaction profile between human wild-type ABCG2 and the second generation Bcr-Abl inhibitors nilotinib, dasatinib and bosutinib.

In the *second project* presented in my thesis, using gefitinib as a well-characterized control, we set out to

- screen the potential interaction between ABCG2 and the second generation EGFR inhibitors vandetanib, pelitinib and neratinib using Sf9 insect membranes containing human wild-type ABCG2,
- explore whether ABCG2 influences the intracellular effects of vandetanib, pelitinib and neratinib in EGFR+ A431 cells showing stable overexpression of human wild-type ABCG2,
- study whether vandetanib, pelitinib and neratinib are capable of inhibiting the function of human wild-type ABCG2,
- investigate whether gefitinib exposure influences the expression of ABCG2,
- elucidate the role of the PI3K/Akt signaling axis in the rapid regulation of ABCG2.

4. MATERIALS AND METHODS

4.1. Materials

All chemicals were obtained from Sigma-Aldrich, unless stated otherwise. The investigated small molecule inhibitors of Bcr-Abl and EGFR kinases were synthesized and validated by VICHEM Chemie (Budapest, Hungary). Acrylamide/Bis solution, TEMED and PVDF membranes were purchased from Bio-Rad Laboratories. Acetonitrile and water used in the HPLC-MS experiments were HPLC grade and were obtained from Sigma-Aldrich. Acetic acid was purchased from Reanal. Purospher STAR RP-18 endcapped column (3 μm, 2 × 55 mm) was obtained from Merck. Human recombinant epidermal growth factor (hEGF) was purchased from Cell Signaling Technology. Alexa-Fluor-conjugated antibodies, wheat germ agglutinin (WGA), TOPRO-3 and DAPI were obtained from Invitrogen. Ko143 was obtained from Tocris Bioscience. Phycoerythrin-conjugated secondary antibodies were purchased from Beckman Coulter.

4.2. Cell lines

Stable human wild-type ABCG2 (referred to as ABCG2 hereafter) expressing derivatives of K562, A431 and PLB985 (PLB) cells were generated by retroviral transgene delivery by the laboratory of Katalin Német as described in detail previously (195,203,210). MDCKII cells stably expressing the N-terminally GFP-tagged version of human wild-type ABCG2 (referred to as GFP-ABCG2 hereafter) (211) were generated by the laboratory of Tamás Orbán, employing the Sleeping Beauty transposon-based transgene delivery system (212,213). Gefitinib resistant subclones of NCI-H1650 cells were generated by Kwak et al (214). Cell cultures were maintained in the appropriate medium (RPMI for K562, PLB and NCI-H1650 cells, α-MEM for A431 cells and D-MEM for MDCKII cells, all media purchased from Gibco) supplemented with 10% heat-inactivated fetal bovine serum (Gibco), 50 units/mL penicillin, 50 units/mL streptomycin and 5 mmol/L glutamine, at 37 °C in 5% CO_2. Cells were regularly monitored for Mycoplasma infection with the MycoAlert® Mycoplasma Detection Kit (Lonza). Total and plasma membrane expression of ABCG2 was checked by Western blot using the anti-ABCG2 BXP-21 antibody (kind gift of Drs. George Scheffer and Rik Scheper) (139), and by flow cytometry using the anti-ABCG2 5D3 antibody (kind gift of Brian P.

Sorrentino) (70,215), respectively, as described in section 4.7. Specific ABCG2 function in the applied cell lines was routinely tested by Hoechst 33342 transport measurements (139) according to the protocol detailed in section 4.12.

4.3. Fluorescent in situ hybridization

In order to analyze *bcr-abl* chimeric genes in the applied K562 cell lines, fluorescent in situ hybridization (FISH) was performed by András Kozma using the universal FISH protocol of Q-BIOgene Molecular Cytogenetics. To visualize the genes of interest in the isolated nuclei of K562 or K562/ABCG2 cells, the Vysis LSI BCR/ABL Dual Color, Dual Fusion Translocation Probe (Abbott) was used.

4.4. Heterologous expression of ABCG2

To express human ABCG2 or GFP-ABCG2 in *Spodoptera frugiperda* (Sf9) insect cells, the baculovirus expression vector system was used. Baculovirus transfer vectors (pAcUW21-L) carrying ABCG2 or its GFP-tagged variant and recombinant baculoviruses (generated using the BaculoGold Transfection Kit, Pharmingen according to the manufacturer's instructions) were generated by Csilla Laczka as described previously (41,211).

Amplified viral stocks (1-2*10^8 pfu/mL) were used to infect Sf9 cells and to produce recombinant ABCG2 or GFP-ABCG2. 3*10^7/175 cm^2 cell culture flask of Sf9 cells in 5 mL insect cell culture media were incubated with 3 mL recombinant baculovirus supernatant for 1 hour at room temperatue. After addition of 15 mL insect cell culture media to the flasks, Sf9 cells were further incubated with the recombinant baculoviruses for 72 hours at 27 °C. Cells expressing the proteins of interest were then harvested and their membranes were isolated according to the protocol described in section 4.5.

4.5. Membrane preparation procedure

ABCG2-containing Sf9 membranes were isolated using the protocol described earlier (216), with minor modifications. 72 hours post-infection, Sf9 cells were harvested and were washed twice with ice cold washing buffer (50 mM TRIS pH=7.0, 300 mM mannitol, 50 µg/mL phenylmethylsulfonyl fluoride) at 4 °C. Cells were then collected in

TMEP buffer (50 mM TRIS pH=7.0, 50 mM mannitol, 2 mM EGTA-TRIS, 8 µg/mL aprotinin, 10 µg/mL leupeptin, 50 µg/mL phenylmethylsulfonyl fluoride, 2 mM dithiothreitol) and lysed and homogenized in a teflon glass tissue potter for 10 minutes on ice. Cellular debris was removed by centrifugation at 450 g for 10 minutes at 4 °C. Homogenization and centrifugation was repeated. The supernatant containing the membrane fragments was then transferred into ultracentrifuge tubes and was incubated with 2 mM random methylated beta cyclodextrin loaded with cholesterol (CycloLab) for 20 minutes at 4 °C on a tube roller (217). After centrifugation at 45000 g for 60 minutes at 4 °C, the pellet containing the isolated membrane fragments was resuspended in TMEP buffer to obtain approximately 4-6 mg/mL total protein concentrations. Membrane samples were stored at -70 °C in aliquots until further analysis.

4.6. Determination of protein concentrations

Total protein concentration of the samples was determined by the modified Lowry method (218), using bovine serum albumin (BSA) solutions with known concentrations to obtain standard curves.

Briefly, 5 µL of Sf9 membrane preparation samples was incubated in 1.5 mL Lowry reagent (0.19 M Na_2CO_3 in 1 M NaOH solution supplemented with 1% (v/v) 2% sodium tartrate solution and 1% (v/v) 1% $CuSO_4$ solution) and 0.15 mL 1 N Folin-Ciocalteu's phenol reagent for 45 minutes at room temperature. Absorbance of the samples was read at 660 nm (using the Perkin Elmer UV/Vis Spectrometer Lambda R).

To determine total protein concentration of samples stored in sample buffer (disaggregating buffer, DB, see section 4.7 or Laemmli sample buffer, see section 4.11), 2.5 or 5 µL samples were diluted in 1.5 or 2 mL distilled water, respectively. 20 µL 2% deoxycholate (DOC) solution was added to each sample. Following incubation for 15 minutes at room temperature, samples were precipitated by addition of 750 µL 25% trichloro acetic acid (TCA) solution. Following centrifugation at 4000 g for 45 minutes at 4 °C, precipitates were incubated in 1.5 mL Lowry reagent and 0.15 mL 1 N Folin-Ciocalteu's phenol reagent for 45 minutes at room temperature. Absorbance of the samples was read at 660 nm.

4.7. Immunodetection of ABCG2

ABCG2 protein yields of the heterologous Sf9 expression system were estimated by Western blot. Sf9 membrane preparations with previously determined protein concentrations (see section 4.6) were diluted in disaggregating buffer (DB; 50 mM TRIS-PO_4 pH=6.8, 2% SDS, 2% β-mercaptoethanol, 2 mM EDTA pH=6.8, 20% glycerol, 0.02% bromphenol blue), and 1-10 μg total proteins were loaded onto 10% Laemmli-type SDS gels. Gel electrophoresis and protein transfer onto PVDF membranes were carried out using standard methodology. Blots were developed using the monoclonal anti-ABCG2 BXP-21 antibody at 125 ng/mL concentration.

Total ABCG2 protein levels in the model cells applied were also measured by Western blot. 2-10*10^6 cells were collected in DB. After one freeze-thaw cycle, samples were sonicated and their protein concentrations were determined by the modified Lowry method as described in section 4.6. 10-50 μg total proteins were resolved using 10% Laemmli-type SDS gels. Gel electrophoresis and protein transfer onto PVDF membranes were carried out using standard methodology. Blots were developed using the monoclonal anti-ABCG2 BXP-21 antibody at 500 ng/mL concentration.

For visualization of the immunoblots, goat anti-mouse horseradish peroxidase-conjugated secondary antibodies at 1:10000 or 1:20000 dilution (Jackson Immunoresearch) and the enhanced chemiluminescence (ECL) detection system were used (Amersham Biosciences/GE Healthcare).

Cell surface ABCG2 expression in the model cells applied was followed by labeling with the monoclonal anti-ABCG2 5D3 antibody that recognizes an external epitope of the transporter (70,215). For flow cytometry measurements, 5D3 labeling was carried out using aliquots of 2-5*10^5 intact cells suspended in HPMI buffer (120 mM NaCl, 5 mM KCl, 400 μM $MgCl_2$, 40 μM $CaCl_2$, 10 mM HEPES, 10 mM $NaHCO_3$, 10 mM glucose and 5 mM Na_2HPO_4) containing 0.5% bovine serum albumin (BSA). For indirect labeling, cells were incubated with 1 μg/mL 5D3 or 1 μg/mL mouse IgG2b (isotype control) in a final reaction volume of 100 μL for 45 minutes at 37 °C. After washing, either 3 μg/mL phycoerythrin (PE) - or 200x diluted Alexa-Fluor-647 (A647)-conjugated goat-anti mouse secondary antibodies were applied in 50 μL HPMI-0.5% BSA for 30 minutes at 37 °C, and their fluorescence was determined at 488 nm excitation and 585/42

nm emission (FL2) or 635 nm excitation and 661/16 nm emission (FL4) wavelengths, respectively, in a FACSCalibur flow cytometer (BD Biosciences). For direct labeling, cells were incubated with 2 μg/mL Alexa-Fluor-647 (A647)-conjugated 5D3 or isotype control antibodies in a final reaction volume of 100 μL for 45 minutes at 37 °C, and their fluorescence was determined at 635 nm excitation and 661/16 nm emission (FL4) wavelengths. For the ABCG2 localization experiments, 1% paraformaldehyde (PFA)-containing solution was applied for 10 minutes at 37 °C for fixation before the above mentioned labeling procedures.

The effect of drugs on the conformation and the related changes in the 5D3 binding affinity of ABCG2 ('5D3-shift' phenomenon introduced in (215)) were investigated using the same labeling protocol, except that following a pre-incubation for 5 minutes at 37 °C, drugs were also present throughout labeling with 5D3 or mouse IgG2b in HPMI buffer. In these experiments, 1 μM Ko143 was used to achieve maximum 5D3 binding of ABCG2. Except for PFA-fixed samples, TOPRO-3 (in case of applying PE fluorophore-conjugates) or propidium iodide (in case of applying A647 fluorophore-conjugates) staining was also performed as the final step of the labeling procedure, to allow exclusion of dead cells.

For 5D3 labeling of cells for confocal microscopy studies, $4*10^4$ cells/well were seeded onto 8-well Nunc Lab-Tek II chambered coverglass (Nalge Nunc International) and were grown for 48 hours in 400 μL/well complete medium. Following multiple washing steps with 37 °C Dulbecco's modified phosphate buffered saline (DPBS) cells were fixed in 1% PFA in DPBS for 15 minutes at 37 °C. Blocking was achieved by incubation of cells with DPBS-0.5% BSA for 1 hour at room temperature. 5D3 or mouse IgG2b was applied at a final concentration of 2 μg/mL in DPBS-0.5% BSA for 1 hour at room temperature. Following three washing steps with DPBS, Alexa-Fluor-488 conjugated goat anti-mouse secondary antibodies were administered at a dilution of 1:250 in blocking buffer for 1 hour at room temperature. After washing with DPBS, samples were stored at 4 °C in DPBS containing 0.46 mM sodium-azide. For visualization of nuclei, cells were stained with 10 μM DAPI for 10 minutes at room temperature. Images were captured with an Olympus IX-81/FV500 laser scanning confocal microscope and analyzed by the FluoView 4.7 software.

4.8. Measurement of the ATPase activity of ABCG2

Vanadate-sensitive ATPase activity was measured using membrane fragments isolated from ABCG2- or GFP-ABCG2-expressing Sf9 insect cells (see section 4.4 and 4.5 for details) by determining the liberation of inorganic phosphate from ATP with a colorimetric reaction (41,216). The reaction pre-mix (kept on ice) containing 10 μg/mL membrane protein and the investigated small molecule inhibitors, 1 μM quercetin (positive control), 0.5 μM Ko143 (negative control) or 1.3 mM sodium orthovanadate in reaction buffer (40 mM MOPS–TRIS pH=7.0, 50 mM KCl, 2 mM dithiothreitol, 500 μM EGTA–TRIS, 5 mM sodium-azide, 1 mM ouabain) was incubated at 37 °C for 5 minutes in shaker water bath. The reaction was started with the addition of 3.3 mM MgATP and the reaction mixture (in a final volume of 150 μL) was further incubated at 37 °C for 20 minutes. The reaction was stopped by addition of 100 μL 5% SDS solution. The subsequent colorimetric reaction was performed at room temperature. Samples were supplemented with 300 μL phosphate reagent (2.5 M H_2SO_4, 1% ammonium molybdate, 0.014% antimony potassium tartrate), 750 μL 20% acetic acid and 150 μL 1% ascorbic acid, and were incubated for 30 minutes at room temperature. Optical densities were read at 880 nm in a Perkin Elmer UV/Vis Spectrometer Lambda R. K_2HPO_4 solutions were used to obtain calibration curves, measurements were performed in duplicates.

4.9. Cellular viability assays

To measure the cellular toxicity of the investigated Bcr-Abl inhibitors, $1*10^5$/well K562 or K562/ABCG2 cells (growing in suspension culture) were seeded in 1 mL/well complete medium in 24-well plates. Cells were exposed to increasing doses of Bcr-Abl inhibitors in the absence or the presence of the specific ABCG2 inhibitor FTC (applied at 5 μM final concentration) for 48 hours at 37 °C in 5% CO_2. Cellular viability in 500 μL thoroughly suspended samples was determined by cellular staining with 50 nM TOPRO-3 and subsequent flow cytometry analysis. The assay was carried out in duplicates.

Cellular viability of drug-treated A431 and NCI-H1650 cells and their ABCG2-expressing counterparts (growing in monolayer culture) was determined by the MTT (3-[4,5-dimethylthiazol-2-yl]-2,5-diphenyltetrazolium) assay. $4*10^3$ cells/well were seeded in 100 μL/well complete medium in 96-well plates, and were let to adhere. The following

day, drugs were added in 100 µL medium, to achieve the indicated final concentrations in the 200 µL final volume. Cells were incubated with drugs for 72 hours at 37 °C in 5% CO_2, and then were stained with 0.5 mg/mL MTT dissolved in PBS. Following incubation for 4 hours at 37 °C in 5% CO_2, the formed formazan crystals were solubilized by addition of 100 µL of 9:1 isopropanol-hydrochloric acid solution. Absorbance was measured at 540 nm using a Perkin Elmer Victor X3 2030 Multilabel Plate Reader. Experiments were carried out in quadruplicates. Where appropriate, IC50 values were determined using the Prism software (GraphPad Software, Inc.) by fitting curves using nonlinear least-squares regression in a sigmoidal dose-response model with variable slope.

4.10. Measurement of hemoglobin production

$2*10^5$/mL K562 and K562/ABCG2 cells were exposed to 2 µM FTC or 0.5 µM imatinib administered as a single agent or in combination for 72 hours at 37 °C in 5% CO_2. Cellular viability in 500 µL thoroughly suspended samples was determined by cellular staining with 50 nM TOPRO-3 and subsequent flow cytometry analysis. The remaining cells were washed with PBS and then were collected in PBS-1% Nonidet-P40 solution. Samples were sonicated and centrifuged at 11000 g for 35 minutes at 4 °C. Hemoglobin content in the supernatant was determined by benzidine-staining (219) performed in duplicates for each sample. Briefly, 100 µL 1% benzidine solution in 90% acetic acid and 100 µL 1% hydrogen peroxide solution was added to 25 µL of the supernatant fractions. Following incubation for 20 minutes at room temperature, 1 mL 10% acetic acid was administered to each sample and absorbance at 512 nm was determined in a Perkin Elmer UV/Vis Spectrometer Lambda R. Hemoglobin concentration of the samples was calculated using bovine hemoglobin calibration curves. Data were normalized to the number of live cells in each sample, and were plotted relative to the amount of hemoglobin measured in vehicle-treated control samples.

4.11. Detection of kinase phosphorylation by Western blot

In order to test the intracellular efficiency of the investigated Bcr-Abl inhibitors at the target kinase site, $4*10^5$/mL K562 or K562/ABCG2 cells were seeded in Petri dishes.

Cells were exposed to 500 nM imatinib, 25 nM nilotinib, 5 nM dasatinib or 50 nM bosutinib in the absence or in the presence of 5 μM FTC for 48 hours at 37 °C in 5% CO_2.

In order to test the intracellular efficiency of the investigated inhibitors of EGFR, PI3K and mTOR at the target or downstream kinase sites, $7.5*10^5$/mL A431 or A431/ABCG2 cells were seeded in serum-free or complete media in 6-well plates and were let to adhere. After 16 hours, cells were either stimulated with 20 ng/mL hEGF for 15 minutes and then were exposed to the small molecule inhibitors at the indicated concentrations for additional 15 minutes at 37 °C in 5% CO_2, or were treated with 100 nM wortmannin for 90 minutes at 37 °C in 5% CO_2.

Protein samples were prepared according to the protocol described previously (220), with minor modifications. Following washing with ice cold PBS, cells were collected in lysis buffer (50 mM TRIS-HCl, 150 mM NaCl, 1 mM EDTA-Na, 1 mM EGTA-Na, 1 % Nonidet-P40) containing various inhibitors of phosphatase enzyme activities (40 mM β-glycerophosphate, 1 mM p-nitrophenyl-phosphate, 20 mM sodium fluoride, 1 mM sodium orthovanadate, 10 mM sodium pyrophosphate) and various inhibitors of protease enzyme activities (10 mM benzamidine, 10 μg/mL antipain, 10 μg/mL aprotinin, 10 μg/mL leupeptin, 10 μg/mL pepstatin A, 1 mM phenylmethylsulfonyl fluoride). After 10 minutes shaking at 4 °C, cellular debris was removed by centrifugation at 17000 g for 12 minutes at 4 °C. The supernatant containing the cellular proteins was diluted in Laemmli sample buffer (62.5 mM TRIS-HCl pH=6.8, 2% SDS, 10% glycerol, 2% β-mercaptoethanol, 0.02% bromphenol blue, 25 mM dithiothreitol; final concentrations are indicated). Samples were boiled for 5 minutes and were stored at -20 °C until further analysis. Protein concentration of the samples was determined by the modified Lowry method, as detailed in section 4.6.

20-40 μg total proteins were resolved using Laemmli-type SDS gels. Gel electrophoresis and protein transfer onto PVDF membranes were carried out using standard methodology. Blots were probed with the following antibodies: phospho-Bcr (Tyr177) (Cell Signaling Technology) at 1:1000 dilution, 0.2 μg/mL c-Abl (24-11) (Santa Cruz Biotechnology), 0.5 μg/mL c-Abl (K-12) (Santa Cruz Biotechnology), phospho-EGFR (Tyr1068) at 1:4000 dilution (Cell Signaling Technology), 0.4 μg/mL phospho-

Akt 1/2/3 (Ser 473) (Santa Cruz Biotechnology), 0.4 µg/mL phospho-p70S6 kinase alpha (Thr 389) (Santa Cruz Biotechnology) and 0.5 µg/mL beta actin. For visualization of the immunoblots, horseradish peroxidase-conjugated secondary antibodies at 1:10000 or 1:20000 dilution (Jackson Immunoresearch) and the enhanced chemiluminescence (ECL) detection system were used (Amersham Biosciences/GE Healthcare).

4.12. Fluorescent dye accumulation and uptake studies

Intracellular accumulation of the Hoechst 33342 dye was followed real-time using the Perkin Elmer Luminescence Spectrometer LS 50B at 350 nm excitation and 460 nm emission wavelengths, as described previously (139). Briefly, $5*10^5$ parental or ABCG2-expressing cells suspended in 2 mL HPMI buffer (120 mM NaCl, 5 mM KCl, 400 µM $MgCl_2$, 40 µM $CaCl_2$, 10 mM HEPES, 10 mM $NaHCO_3$, 10 mM glucose and 5 mM Na_2HPO_4) were pre-incubated at 37 °C for 3-6 minutes. Cells were then incubated with 1 µM Hoechst 33342 for additional 7-8 minutes followed by the administration of the specific ABCG2 inhibitors 1 µM Ko143 or 2 µM FTC. As a last step, for standardization, membrane permeabilization and subsequent full cellular staining was achieved by incubation of cells with 10 µM digitonin. The kinetics of Hoechst 33342 accumulation was analyzed with the FL WinLab (Perkin Elmer) software. Transport activity of ABCG2 was calculated as (Fi-Fo)/Fi*100 (221); where F_0 is the rate of dye accumulation in the absence of an ABCG2 inhibitor and Fi is the rate of dye accumulation in the presence of a specific ABCG2 inhibitor. The impact of the investigated small molecule inhibitors on the Hoechst 33342 transport capacity of ABCG2 was followed using the same approach. After pre-incubation of the ABCG2-expressing cells at 37 °C in HPMI buffer, cells were incubated with 1 µM Hoechst 33342 for 7-8 minutes (Fo), then co-incubated with Hoechst 33342 and the investigated small molecule inhibitor administered at a certain concentration for 4-5 minutes (Fx). Finally, cells were co-incubated with Hoechst 33342, the investigated compound and 1 µM Ko143 or 2 µM FTC (Fi) for another 3-5 minutes. ABCG2 transport activities under the different conditions were calculated with the FL WinLab software and ABCG2 inhibitory effect of the investigated small molecule inhibitors relative to the Ko143- or FTC-mediated maximum inhibition was calculated as $(F_x-F_0)/(F_i-F_0)*100$ (195).

The uptake of mitoxantrone (MX) was measured by flow cytometry (139). $2*10^5$ cells were washed and resuspended in HPMI buffer. Cells were pre-incubated in the absence or the presence of the specific ABCG2 inhibitor 1 μM Ko143 for 5 minutes at 37 °C in shaker water bath. The transport reaction was started by addition of 2 μM MX in a final reaction volume of 200 μL. Following incubation with MX for 30 minutes at 37 °C, cells were washed with 500 μL ice cold PBS and were resuspended in 200 μL ice cold PBS containing 12.5 μg/mL propidium iodide. Cells were kept on ice until flow cytometry analysis. To investigate the effect of small molecule inhibitors on the MX transport capacity of ABCG2, $2*10^5$ ABCG2-expressing cells in HPMI buffer were pre-incubated in the absence or in the presence of the investigated drug and 1 μM Ko143 administered alone or in combination for 5 minutes at 37 °C in shaker water bath. Cells were then incubated with 5 μM MX for 30 minutes at 37 °C. Cells were then washed and resuspended in ice cold PBS-12.5 μg/mL propidium iodide solution. Cells were kept on ice until flow cytometry analysis. MX fluorescence in live cells was analyzed in a FACSCalibur flow cytometer (BD Biosciences) at 635 nm excitation and 661/16 nm emission (FL4) wavelengths.

4.13. Determination of the intracellular accumulation of the investigated Bcr-Abl inhibitors by HPLC-MS

$4*10^5$/mL K562 or K562/ABCG2 cells were exposed to 25 nM nilotinib, 5 nM dasatinib or 10 nM bosutinib at 37 ºC for 60 minutes. After incubation, cells were collected in 5 mL ice-cold PBS. Cells were kept on ice throughout the sample preparation procedure. Following three washing steps with 5 mL PBS, cells were precipitated with 500 μL acetonitrile containing 30 nM imatinib as an internal standard. After centrifugation at 8000 g for 5 minutes, the supernatant was transferred into eppendorf tubes and acetontirile was evaporated in a heated vacuum concentrator centrifuge (UNIVAPO 100 H, UniEquip). HPLC-MS analysis of the samples was performed by the laboratory of Zoltán Takáts. Nilotinib, dasatinib, bosutinib and imatinib were separated using a RP-18 column on a XLC binary HPLC pump system (Jasco International). 20 μL of reconstituted sample was injected; flow rate of HPLC eluent was set to 200 μL/min. Mobile phases used were: (A) 0.1% acetic acid in 100 mM ammonium acetate buffer and

(B) 0.1% acetic acid in acetonitrile. The total HPLC run time was 9 min, using the following gradient: 0–1 min.: 80% A, 1-6 min.: 5% A, 6-7 min.: 5% A, 7-9 min.: 80% A. The Bcr-Abl inhibitors were detected using a TSQ Quantum Discovery (Thermo Finnigan) triple quadrupole mass spectrometer operated in positive ion electrospray mode. Protonated molecular ions of analytes were detected in multiple reaction monitoring (MRM) mode using m/z 530→289 and m/z 530→261 fragmentation channel for nilotinib, m/z 488→232 and m/z 488→401 for dasatinib, m/z 530→141 and m/z 530→113 for bosutinib and m/z 494→217 and m/z 494→394 for the internal standard imatinib. Amount of Bcr-Abl inhibitors in the samples were calculated from the respective Bcr-Abl inhibitor calibration curves and were normalized to the amount of imatinib. Experiments were carried out in duplicates.

4.14. Determination of the subcellular distribution of GFP-ABCG2 by confocal microscopy

To study subcellular distribution of GFP-ABCG2 in polarized cells, $2*10^4$ MDCKII/GFP-ABCG2 cells/well were seeded onto Nunc Lab-Tek II chambered coverglass (Nalge Nunc International) and were grown for 5 days. Following treatment with 100 nM wortmannin, 10 nM rapamycin or 10 μM rapamycin for 90 minutes at 37 °C, cells were fixed with 4% PFA and were stained with 5 μg/mL Alexa-Fluor-633-conjugated wheat germ agglutinin (WGA) and 1 μM DAPI. Subcellular distribution of GFP-ABCG2 relative to the apical marker WGA was evaluated by confocal microscopy. Images were captured with an Olympus IX-81/FV500 laser scanning confocal microscope and analyzed by the FluoView 4.7 software.

4.15. Data analysis

All experiments were repeated at least two times and mean +/- SD or SE values or representative images are presented. Differences were determined using Student's *t* test at 95% confidence interval.

5. RESULTS

5.1. Interaction of ABCG2 and small molecule inhibitors of Bcr-Abl

At the beginning of the first project presented in my thesis, literature data regarding the interaction between the ABCG2 multidrug transporter and the first successful Bcr-Abl inhibitor imatinib were conflicting. It was clear that ABCG2 recognized and interacted with imatinib (195); however, imatinib had initially been described either as a substrate (78,196) or as an inhibitor (197) of the transporter. Data regarding interaction of ABCG2 with newly developed second generation Bcr-Abl inhibitors were not available at the time. Therefore, besides aiming to clarify the nature of the interaction between imatinib and ABCG2, we also decided to investigate whether ABCG2 interacted with the novel Bcr-Abl inhibitors nilotinib, dasatinib and bosutinib (Table 3).

	Imatinib	**Nilotinib**	**Dasatinib**	**Bosutinib**
Aliases	Gleevec/ STI-571	Tasigna/ AMN107	Sprycel/ BMS-354825	Bosulif/ SKI-606
Target	Abl, c-KIT, PDGFR	Abl, c-KIT, PDGFR	Abl, c-KIT, PDGFR, Src family kinases	Abl, Src family kinases
Clinical indication	CML, Ph+ ALL, MDS/MPD, ASM, HES, CEL, GIST	CML	CML, Ph + ALL,	CML

Table 3. Bcr-Abl inhibitors investigated in this study. *C-KIT: Stem cell factor receptor; PDGFR: Platelet-derived growth factor receptor; Ph+ ALL: Philadelphia positive acute lymphoid leukemia; ASM: Advanced solid malignancies; CEL: Chronic eosinophil leukemia; CML: Chronic myeloid leukemia; GIST: Gastrointestinal stromal tumor; HES: Hypereosinophilic syndrome; MDS/MPD: Myelodysplastic syndrome/myeloproliferative disorders.*

5.1.1. Effect of imatinib on the ATPase activity of ABCG2

In the first set of experiments, we aimed to give detailed characterization of the interaction between ABCG2 and imatinib. ABCG2 expressed in Sf9 insect membranes generates high membrane ATPase activity (41). Many substrates of ABCG2 can stimulate the ATPase activity of the transporter, and modulation (stimulation or inhibition) of the ABCG2 ATPase indicates interaction between the drug and the protein

(41,127,222). Therefore, as a first step, we studied whether imatinib could modulate the ATPase activity of ABCG2. Membrane fragments were isolated from insect Sf9 cells overexpressing ABCG2 as described in section 4.5. Cholesterol enrichment of the cholesterol-poor insect membranes was suggested to improve the sensitivity of the ATPase assay (217), therefore throughout this study we also performed cholesterol loading of the membrane preparations. As shown in Fig.4, ABCG2 exhibited a relatively high basal ATPase activity in the absence of any compounds. Imatinib decreased this basal ATPase activity in a concentration-dependent manner, suggesting that ABCG2 indeed interacted with this drug. We also measured the effect of imatinib on the drug-stimulated ATPase activity of ABCG2. In this experimental setup, high turnover of the ABCG2 ATPase was triggered by administration of quercetin, which is a high affinity substrate for the transporter (223). As expected (222), imatinib decreased the quercetin-stimulated ATPase activity of ABCG2 (Fig. 4). Collectively, these data support the interaction of ABCG2 and imatinib; however, cannot give a clear-cut picture about the nature of this interaction. While specific ABCG2 inhibitors significantly decrease the high basal ABCG2 ATPase activity in isolated Sf9 membrane fragments (139,223), inhibition of the basal ABCG2 ATPase in a similar experimental system has also been reported in the case of ABCG2 substrates which are transported at a lower rate (41,139). Therefore, the ATPase assay cannot necessarily distinguish between ABCG2 substrates and inhibitors (127,222).

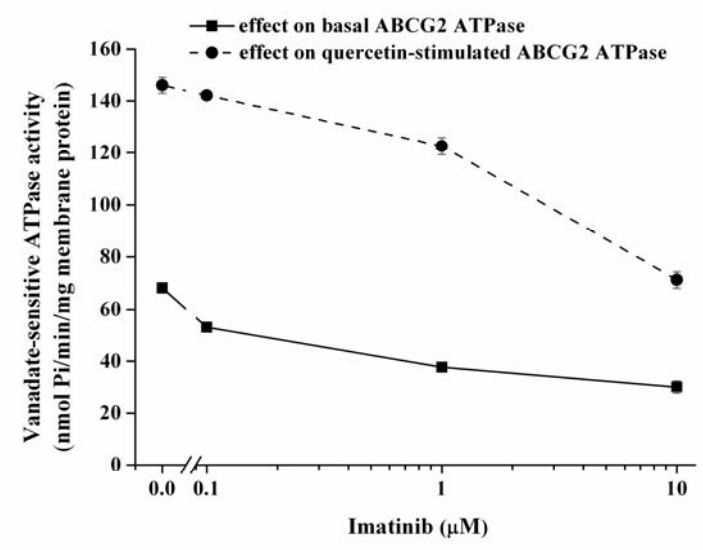

Figure 4. Modulation of the ATPase activity of ABCG2 by imatinib. *Concentration-dependent effect of imatinib on the basal and the stimulated (with 1 μM quercetin) ATPase activity of ABCG2 were measured using isolated cholesterol-loaded Sf9 membranes containing ABCG2. Mean ± SE values of three independent experiments (each performed in duplicates) are shown.*

5.1.2. Characterization of the Bcr-Abl+ K562 and K562/ABCG2 cell lines

In order to reveal whether the ABCG2-imatinib interaction suggested by the ATPase measurements is also relevant in a cellular context, and to clarify whether or not imatinib is a substrate of ABCG2, we generated and characterized a Bcr-Abl+ K562 cell based model system. K562 was the first CML-derived cell line which showed a persistent positive Philadelphia chromosome after prolonged *in vitro* culturing (224). K562 cells express the 210 kDa Bcr-Abl fusion protein bearing tyrosine kinase activity (225-227), and therefore are sensitive to inhibition of this kinase (228). K562 cells stably expressing human wild-type ABCG2 were generated using retroviral transgene delivery (210), by the laboratory of Katalin Német. Chimeric *bcr-abl* genes in the parental K562 and K562/ABCG2 cells were visualized by FISH. As shown in Fig. 5, the K562 cells applied in our experiments carry more copies of the *bcr-abl* hybrid gene.

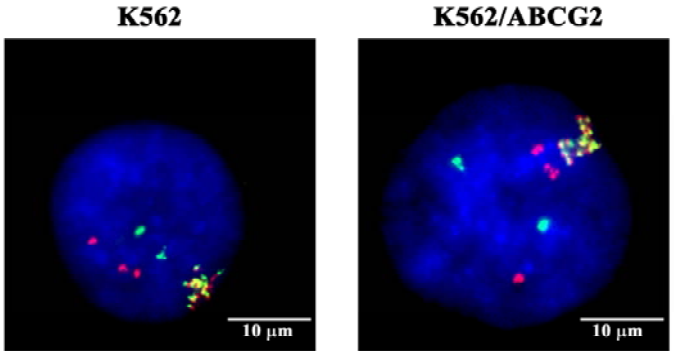

Figure 5. Chimeric bcr-abl genes in K562 and K562/ABCG2 cells visualized by fluorescent in situ hybridization. *Slides were prepared from isolated nuclei of $1*10^6$ K562 or K562/ABCG2 cells. The genes c-abl located on chromosome 9 (red), bcr located on chromosome 22 (green) and the chimeric gene bcr-abl located on chromosome 22 (yellow) were visualized by hybridization of fluorescently-labeled specific probes. Nuclei were counterstained with DAPI (blue).*

Total expression levels of the ABCG2 protein in the K562 cells applied were measured by Western blot (Fig. 6A), whereas cell surface levels of the transporter were studied by labeling with the 5D3 antibody followed by flow cytometry analysis (Fig. 6B). As documented, K562/ABCG2 cells showed strong total and plasma membrane ABCG2 protein expression. In contrast, no endogenous ABCG2 transporter expression could be detected in the parental K562 cells (Fig. 6A-B).

Specific function of the ABCG2 transporter in the model cells was tested by following the intracellular accumulation of the Hoechst 33342 dye. Hoechst 33342 passively permeates the cell membrane and its fluorescence intensity significantly increases upon

its binding to DNA. Hoechst 33342 is a transported substrate of ABCG2 (139,229). As the increase in Hoechst 33342 fluorescence directly reflects the rate of intracellular dye accumulation, real-time detection of cellular Hoechst 33342 uptake has been suggested to allow for sensitive, rapid and reliable evaluation of ABCG2 transport function (139,211). Hoechst 33342 is also a substrate for ABCB1 (230), another key transporter involved in multidrug resistance; however, contribution of this protein to cellular Hoechst 33342 extrusion can be excluded by using the ABCG2 specific inhibitor Ko143.

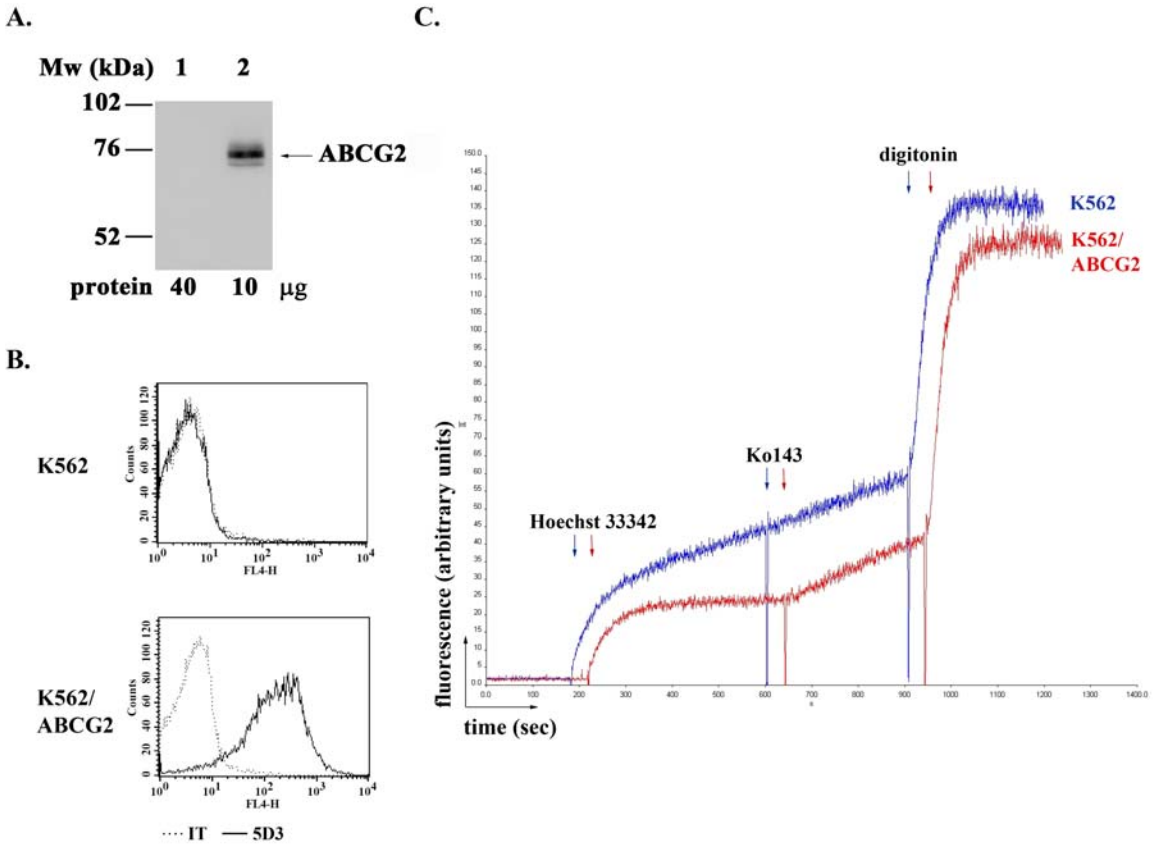

Figure 6. ABCG2 expression and function in K562 and K562/ABCG2 cells. (A) *Total ABCG2 protein levels of (lane 1) K562 and (lane 2) K562/ABCG2 cells were determined by Western blot using the BXP-21 antibody.* ***(B)*** *Cell surface expression of ABCG2 in K562 and K562/ABCG2 cells was measured by flow cytometry using the Alexa-Fluor-647-conjugated-IgG2b (isotype control, IT) or -5D3 antibodies* ***(C)*** *Specific ABCG2 function in K562 and K562/ABCG2 cells was followed by real-time spectrofluorometric detection of the cellular accumulation of the ABCG2 substrate dye, Hoechst 33342. Representative images of at least three independent experiments are shown.*

As shown in Fig. 6C, the uptake of Hoechst 33342 resulted in a rapid initial increase in cellular fluorescence in both K562 and K562/ABCG2 cells, which can partially be

explained by nuclear staining of dead cells and the increase of Hoechst 33342 fluorescence in the membrane lipid phase (139). However, in K562/ABCG2 cells, the rate of further Hoechst 33342 uptake and the subsequent increase of fluorescence intensity were much slower than those measured in K562 cells, most probably due to active ABCG2-mediated dye extrusion. Indeed, when ABCG2 function was blocked by the administration of Ko143, the rate of Hoechst influx in K562/ABCG2 cells became similar to that observed in K562 cells. In correlation with the ABCG2 expression data (Fig. 6A-B), we could not detect any endogenous ABCG2 function in the parental K562 cells, since we measured similar Hoechst 33342 dye uptake rates both in the absence and in the presence of Ko143 (Fig. 6C).

5.1.3. ABCG2 confers cellular resistance to imatinib

Imatinib displays a growth inhibitory effect on tumor cells expressing Bcr-Abl (170-172), and induces their apoptosis through dephosphorylation of Bcr-Abl and subsequent inhibition of its kinase activity and downstream signaling (228,231,232).

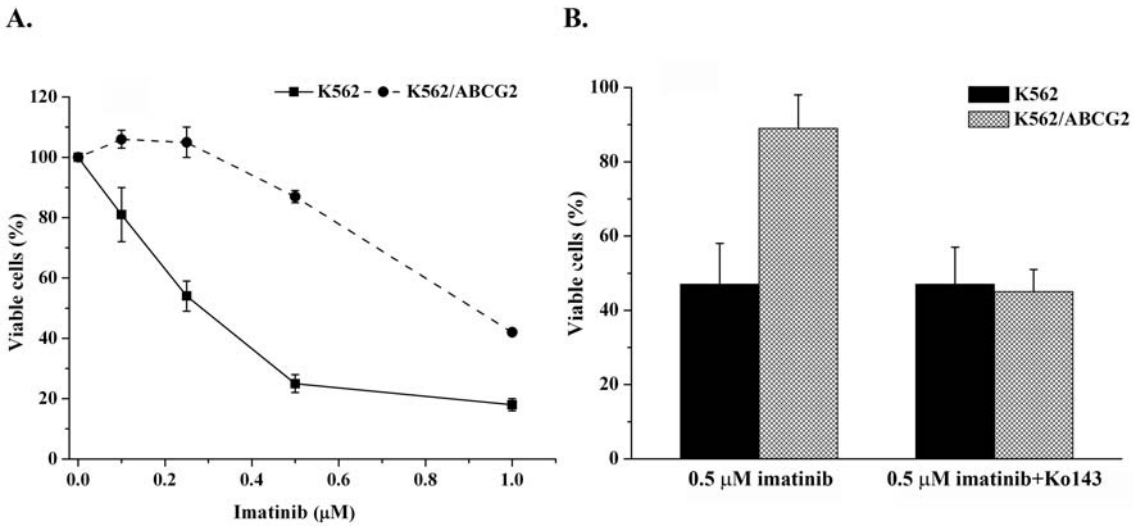

Figure 7. Cellular toxicity of imatinib in K562 and K562/ABCG2 cells. (A) *$1*10^5$/mL cells were exposed to increasing concentrations of imatinib for 48 hours.* ***(B)*** *To determine the specific effect of ABCG2, $4*10^5$/mL cells were exposed to 0.5 μM imatinib in the absence or presence of 1 μM Ko143 for 48 hours. The number of viable cells was determined by TOPRO-3 staining and subsequent flow cytometry analysis. Data were normalized to the number of viable cells measured in vehicle-treated samples. Mean ± SE values of three or two independent experiments (each performed in duplicates) are shown, respectively.*

In the next set of experiments, we compared the toxicity of imatinib in K562 and K562/ABCG2 cells. After a 48-hour drug exposure, imatinib significantly decreased the viability of K562 cells in a concentration dependent manner. In contrast, K562/ABCG2 cells displayed resistance to imatinib (Fig. 7A), which could be fully reverted by blocking the function of the transporter by Ko143 (Fig. 7B). The observed specific ABCG2-mediated decrease of the intracellular cytotoxic efficiency of imatinib strongly supports the previous findings of others (78,196) suggesting that this drug is actively extruded by ABCG2.

5.1.4. ABCG2 function prevents imatinib-induced erythroid differentiation in K562 cells

Besides inducing apoptosis, imatinib also triggers erythroid differentiation of K562 cells (228,232). As a next step, we studied whether ABCG2 function also prevented imatinib-induced erythroid differentiation of K562 cells. K562 and K562/ABCG2 cells were exposed to 0.5 μM imatinib in the absence or the presence of the specific ABCG2 inhibitor FTC for 72 hours. Hemoglobin content of the live cells was determined by benzidine-staining and subsequent spectrophotometry analysis.

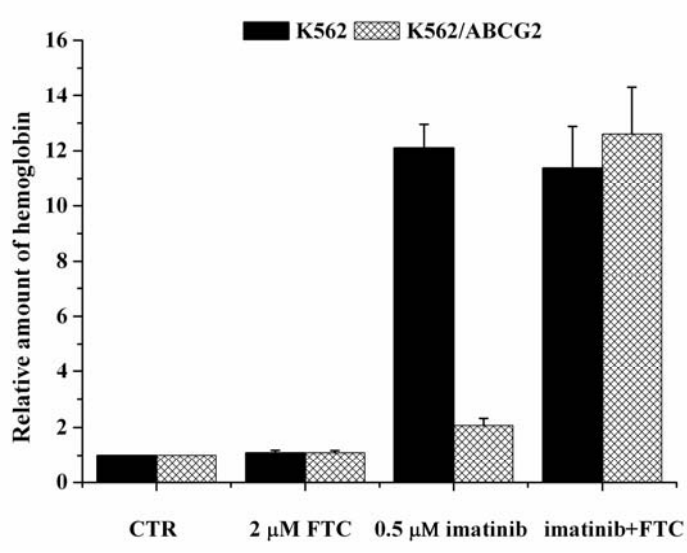

Figure 8. Imatinib-induced hemoglobin production of K562 and K562/ABCG2 cells. *$2*10^5$/mL cells were exposed to 2 μM FTC or 0.5 μM imatinib administered as a single agent or in combination for 72 hours. Hemoglobin production of the cells was determined by benzidine-staining and subsequent spectrophotometric analyis performed in duplicates for each sample. Data were normalized to the number of live cells in each sample, and were plotted relative to the amount of hemoglobin measured in vehicle-treated control samples. Mean ± SE values of two independent experiments are shown.*

As shown in Fig. 8, imatinib treatment resulted in an almost 12-fold elevation of hemoglobin levels in K562 cells as compared to the vehicle-treated control cells. In

contrast, only a slightly increased hemoglobin production could be observed in the case of imatinib-treated K562/ABCG2 cells. When cells were co-incubated with imatinib and FTC, similarly high hemoglobin levels could be detected in both K562 and K562/ABCG2 cells. The finding that the presence of the functional ABCG2 protein can also restrict the cellular effect of imatinib on the process of erythroid differentiation in K562 cells further implies that this compound is a substrate for the ABCG2 transporter.

5.1.5. Intracellular action of the second generation Bcr-Abl inhibitors nilotinib and dasatinib, but not that of bosutinib is restricted by ABCG2-mediated active efflux

In the experiments described above, the K562 cell based model system generated by us proved to be applicable to investigate whether ABCG2 function resulted in decreased intracellular efficiency of Bcr-Abl inhibitors, a phenomenon which strongly suggests active ABCG2-mediated transport of the drugs. In the next series of measurements, we therefore compared the cellular toxicities of the newly developed Bcr-Abl inhibitors nilotinib, dasatinib and bosutinib in K562 and K562/ABCG2 cells (Fig. 9).

Cells were incubated with the indicated drugs for 48 hours, and then were stained with TOPRO-3 in order to distinguish the population of live and dead cells. K562 cells showed sensitivity to increasing nanomolar concentrations of nilotinib (Fig. 9A), dasatinib (Fig. 9B) and bosutinib (Fig, 9C). In the case of nilotinib and dasatinib, however, we measured decreased drug sensitivity of K562/ABCG2 cells (Fig. 9A-B, respectively), which could be fully reversed by FTC-mediated specific pharmacological inhibition of ABCG2 function. In contrast, bosutinib was similarly effective in killing both K562 and K562/ABCG2 cells (Fig. 9C).

To explore the molecular basis of the measured cellular toxicities of nilotinib, dasatinib and bosutinib, we studied the phosphorylation pattern of their target kinase Bcr-Abl in K562 and K562/ABCG2 cells by Western blot. Imatinib, which was reported to induce apoptosis of Bcr-Abl positive cells *via* dephosphorylation of Bcr-Abl, inhibition of its kinase activity and subsequent inhibition of downstream signaling (228,231,232), was used as a positive control. The concentrations of the Bcr-Abl inhibitors were chosen according to the cellular toxicity measurements detailed above (Fig. 7 and 9).

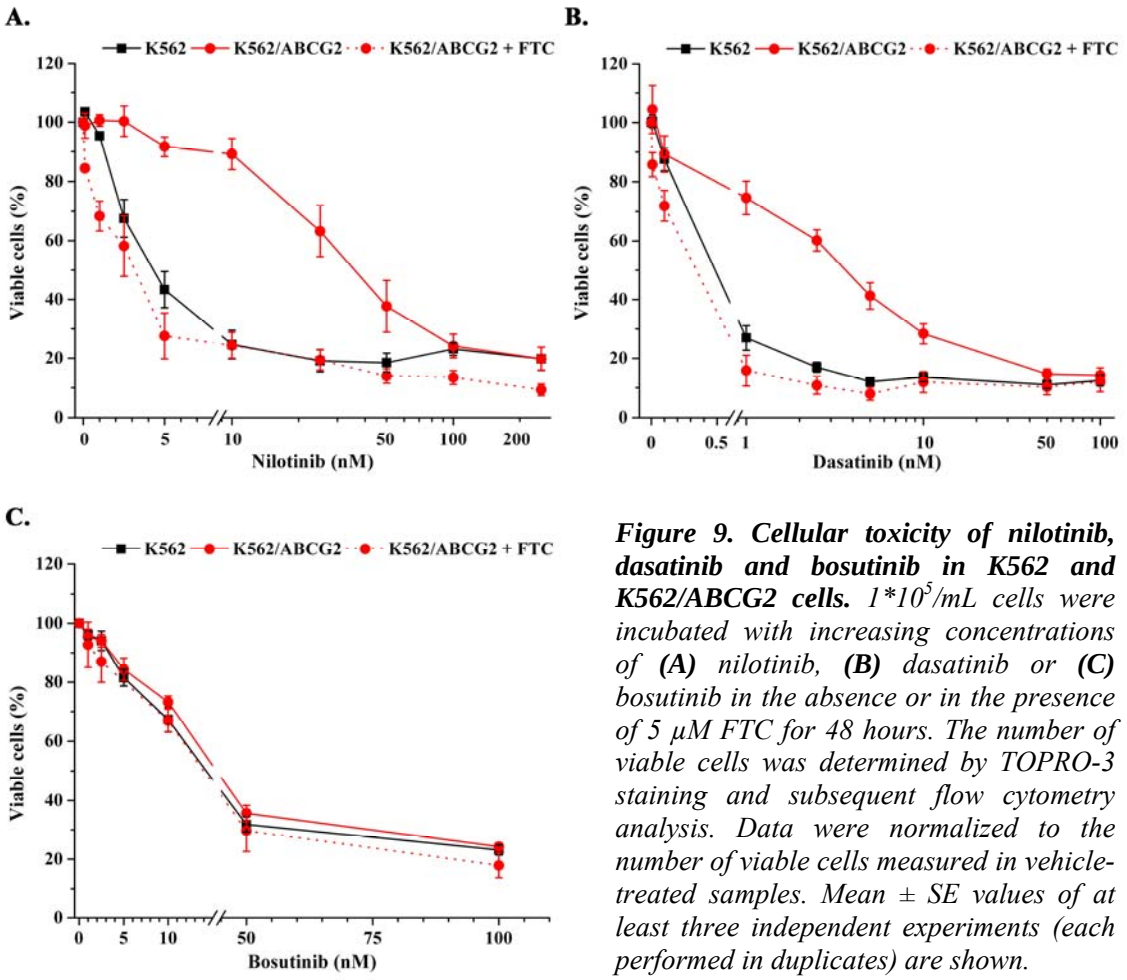

Figure 9. Cellular toxicity of nilotinib, dasatinib and bosutinib in K562 and K562/ABCG2 cells. *$1*10^5$/mL cells were incubated with increasing concentrations of* ***(A)*** *nilotinib,* ***(B)*** *dasatinib or* ***(C)*** *bosutinib in the absence or in the presence of 5 μM FTC for 48 hours. The number of viable cells was determined by TOPRO-3 staining and subsequent flow cytometry analysis. Data were normalized to the number of viable cells measured in vehicle-treated samples. Mean ± SE values of at least three independent experiments (each performed in duplicates) are shown.*

Cells were exposed to Bcr-Abl inhibitors in the absence or the presence of FTC for 48 hours. Phosphorylation of Bcr-Abl was probed using an antibody which recognizes the kinase when it is phosphorylated at Tyr177. As shown in Fig. 10, control K562 and K562/ABCG2 cells revealed high levels of constitutively phosphorylated Bcr-Abl, which is in accordance with the literature data (228). Exposure to all the investigated Bcr-Abl inhibitors resulted in decreased phospho-Bcr-Abl levels in K562 cells, and these phosphorylation patterns were similar both in the presence and in the absence of FTC. (Incubation of the cells with FTC alone had no impact on the phosphorylation of Bcr-Abl, data not shown.) In contrast, K562/ABCG2 cells treated with imatinib, nilotinib or dasatinib displayed high phospho-Bcr-Abl protein levels, which were comparable to the phospho-Bcr-Abl protein level detected in untreated K562/ABCG2 cells. However, when K562/ABCG2 cells were simultaneously treated with the Bcr-Abl inhibitors imatinib,

nilotinib or dasatinib and FTC, a pronounced decrease in phospho-Bcr-Abl levels could be measured. Notably, co-treatment of K562/ABCG2 cells with these Bcr-Abl inhibitors and FTC resulted in similar levels of phosphorylated Bcr-Abl to those measured in K562 cells. Bosutinib treatment of K562/ABCG2 cells caused a slight decrease in phospho-Bcr-Abl levels both in the absence and in the presence of FTC.

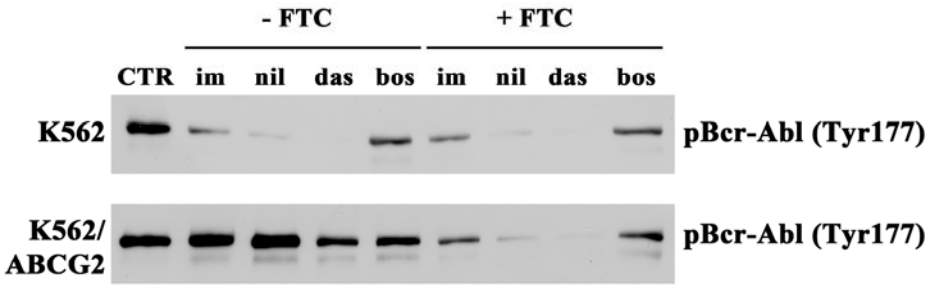

Figure 10. Phosphorylation of Bcr-Abl kinase in Bcr-Abl inhibitor-treated K562 and K562/ABCG2 cells. *$4*10^5$/mL cells were treated with 500 nM imatinib, 25 nM nilotinib, 5 nM dasatinib or 50 nM bosutinib in the absence or in the presence of 5 μM FTC for 48 hours. Cell lysates were prepared and 40 μg protein extracts were probed for phosphorylation of Bcr-Abl at Tyr177 by Western blot. Sample loading was checked by Coomassie Brilliant Blue staining of the gels (data not shown). A representative image of two independent experiments is shown.*

To check sample loading for the measurement presented in Fig. 10, first we performed Coomassie Brilliant Blue staining of the gels (data not shown). In addition, we developed the blots using the anti-c-Abl (K-12) antibody in order to visualize total Bcr-Abl protein levels in the samples (Fig. 11). The epitope of anti-c-Abl (K-12) maps within the kinase domain of the human c-Abl kinase, thus this antibody recognizes both the 210 kDa chimeric Bcr-Abl and the 145 kDa c-Abl proteins. Interestingly, we found that the 48-hour exposure of K562 cells to the investigated Bcr-Abl inhibitors decreased the levels of the Bcr-Abl fusion kinase, which was most pronounced in the case of nilotinib and dasatinib treatment (Fig. 11). This effect was completely abolished by the presence of functional ABCG2 as shown in the case of K562/ABCG2 cells treated with imatinib, nilotinib or dasatinib. When the function of ABCG2 was blocked with the administration of FTC in the K562/ABCG2 cells treated with the respective drugs, a decrease in Bcr-Abl protein levels could be detected similarly to that observed in K562 cells. Protein levels of

the c-Abl kinase were comparable in each sample, also verifying uniform sample loading. Similar results were obtained when the Western blots were probed with the anti-c-Abl (24-11) antibody, which recognizes a protein region within the C-terminus of the c-Abl kinase (data not shown).

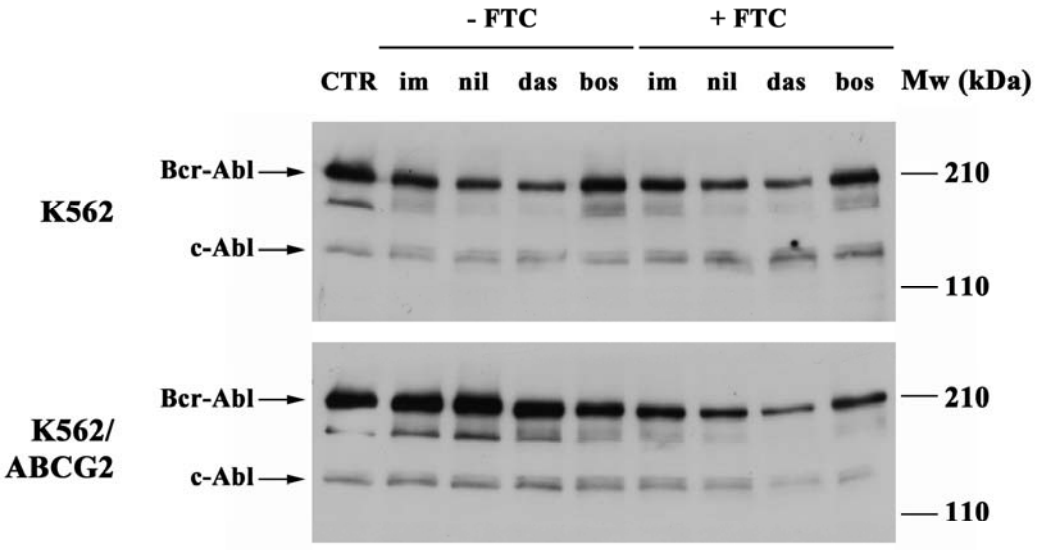

Figure 11. Levels of Bcr-Abl and c-Abl kinases in Bcr-Abl inhibitor-treated K562 and K562/ABCG2 cells. *4*10^5/mL cells were treated with 500 nM imatinib, 25 nM nilotinib, 5 nM dasatinib or 50 nM bosutinib in the absence or in the presence of 5 μM FTC for 48 hours. Cell lysates were prepared and 40 μg protein extracts were probed by Western blot using the anti-c-Abl (K-12) antibody. A representative image of two independent experiments is shown.*

Collectively, results of the cellular toxicity and Western blot experiments suggest that similarly to imatinib, ABCG2 can restrict the intracellular action of nilotinib and dasatinib as well, by preventing these compounds from reaching and inhibiting their intracellular target kinase Bcr-Abl. Contrarily, cellular toxicity and Bcr-Abl phosphorylation data obtained using bosutinib-treated K562 and K562/ABCG2 samples render it unlikely that ABCG2 transports bosutinib efficiently enough to reduce its intracellular concentration below the drug efficacy threshold.

In order to investigate direct ABCG2-mediated transport of nilotinib, dasatinib and bosutinib, we attempted to set up an experimental system which would not require radioactively or fluorescently labeled drugs for detection. K562 and K562/ABCG2 cells

were incubated with the Bcr-Abl inhibitors at 37 °C for 60 minutes at the concentrations indicated in Fig.12. Cells were then washed and precipitated in acetonitrile containing imatinib as an internal standard. The intracellular amount of Bcr-Abl inhibitors was then determined by HPLC-MS by the laboratory of Zoltán Takáts as described in section 4.13. As shown in Fig. 12, we found that K562/ABCG2 cells accumulated significantly less nilotinib and dasatinib than the parental K562 cells, whereas only a very slight decrease in intracellular drug levels could be detected in the case of bosutinib.

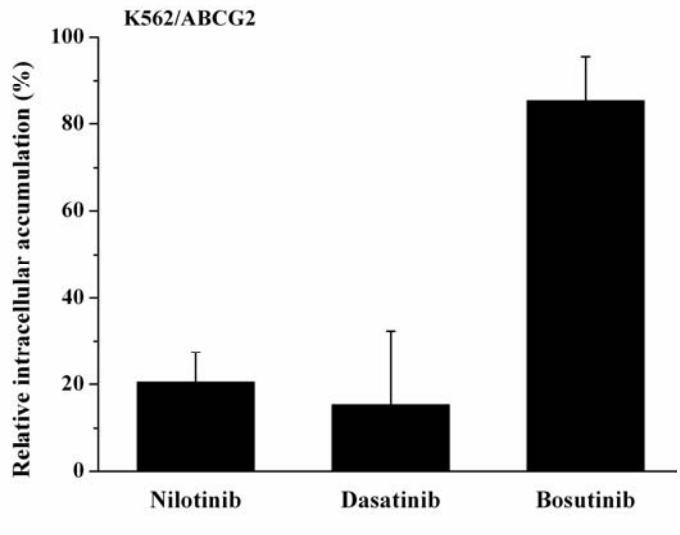

Figure 12. Intracellular accumulation of nilotinib, dasatinib and bosutinib in K562/ABCG2 cells. *$4*10^5$/mL K562 or K562/ABCG2 cells were incubated with 25 nM nilotinib, 5 nM dasatinib or 10 nM bosutinib at 37 °C for 60 minutes. Following multiple washing steps, cells were precipitated with acetonitrile containing 30 nM imatinib as an internal standard. Intracellular amount of the investigated Bcr-Abl inhibitors were determined by HPLC-MS. Data obtained from K562/ABCG2 samples were plotted relative to the respective drug amounts measured in K562 cells (100%). Mean ± SE values of at least two independent experiments (each performed in duplicates) are shown.*

In summary, we show that the Bcr-Abl kinase inhibitory effect of the second generation Bcr-Abl inhibitors nilotinib and dasatinib, but not that of bosutinib is restricted by ABCG2-mediated active efflux.

5.1.6. Effect of nilotinib, dasatinib and bosutinib on the ATPase activity of ABCG2

To gain further information about the interaction profile of ABCG2 and the investigated second generation Bcr-Abl inhibitors, we performed ABCG2 ATPase measurements using ABCG2-containing Sf9 membrane preparations. In these experiments, modulatory effect of the Bcr-Abl inhibitors on the ATPase activity of

ABCG2 could be tested over significantly wider concentration ranges than those applicable in the K562 cellular toxicity measurements. As shown in Fig. 13, low nanomolar concentrations of nilotinib stimulated the high basal ATPase activity of the transporter, which corresponds to our previous findings demonstrating that nilotinib is a transported substrate of ABCG2. Nevertheless, a decreasing ABCG2 ATPase activity could be detected in the presence of higher, micromolar concentrations of nilotinib. In the case of dasatinib and bosutinib, we measured no ABCG2 ATPase modulatory effect under 1 μM concentrations of the drugs. When administered at 10-20 μM concentrations, however, both dasatinib and bosutinib decreased the basal ABCG2 ATPase, with bosutinib displaying a more pronounced effect. Altogether, these data imply that higher concentrations of the investigated Bcr-Abl inhibitors might have an ABCG2 inhibitory effect.

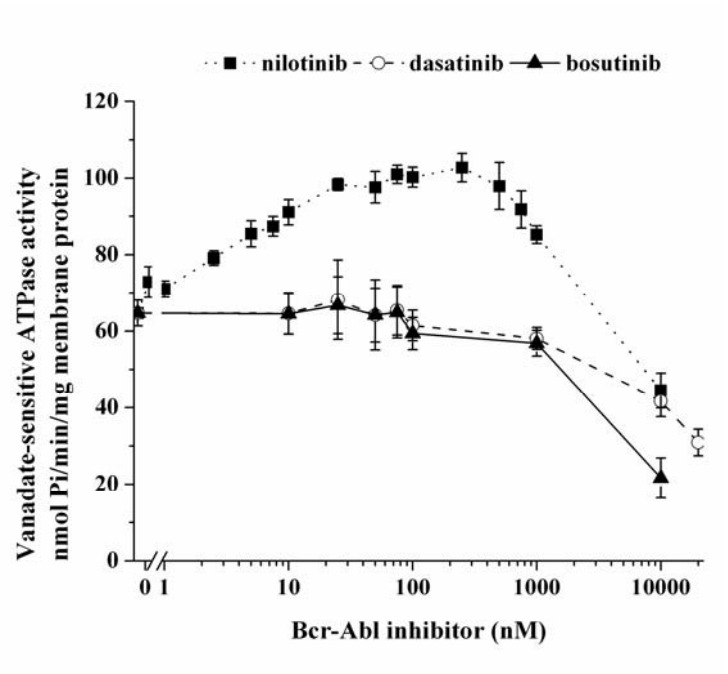

Figure 13. Modulation of the ATPase activity of ABCG2 by nilotinib, dasatinib and bosutinib. *Concentration-dependent effect of the investigated Bcr-Abl inhibitors on the basal ATPase activity of ABCG2 was measured using isolated cholesterol-loaded Sf9 membranes containing ABCG2. Mean ± SE values of at least three independent experiments (each performed in duplicates) are shown.*

5.1.7. Nilotinib, dasatinib and bosutinib inhibit ABCG2-mediated Hoechst 33342 transport

Inhibition of the function of ABCG2 by the investigated Bcr-Abl inhibitors which were suggested by the ATPase measurements (Fig. 13) might lead to re-senzitization of cells towards simultaneously administered ABCG2 substrate cytotoxic agents. To test this effect, we measured whether nilotinib, dasatinib or bosutinib could inhibit the

ABCG2-mediated transport of the Hoechst 33342 dye. Uptake of Hoechst 33342 was measured in K562/ABCG2 cells in the absence or in the presence of increasing concentrations of the Bcr-Abl inhibitors. ABCG2 inhibitory effect of the respective concentration of the Bcr-Abl inhibitors was plotted relative to the Hoechst 33342 uptake measured under maximal FTC-mediated inhibition of ABCG2 function. Similarly to imatinib (195), all of the investigated second generation Bcr-Abl inhibitors could inhibit the ABCG2-dependent Hoechst 33342 accumulation in a concentrations-dependent manner (Fig. 14). While nilotinib efficiently inhibited ABCG2-mediated Hoechst 33342 uptake in a nanomolar concentration range, dasatinib and bosutinib displayed their inhibitory effect only when they were applied at higher than 1 μM concentration. Collectively, these results suggest that the investigated Bcr-Abl inhibitors might also inhibit the function of the ABCG2 transporter most probably through potential drug-drug interactions in its substrate binding pocket, which might result in chemo-sensitization and efficient eradication of drug resistant cells.

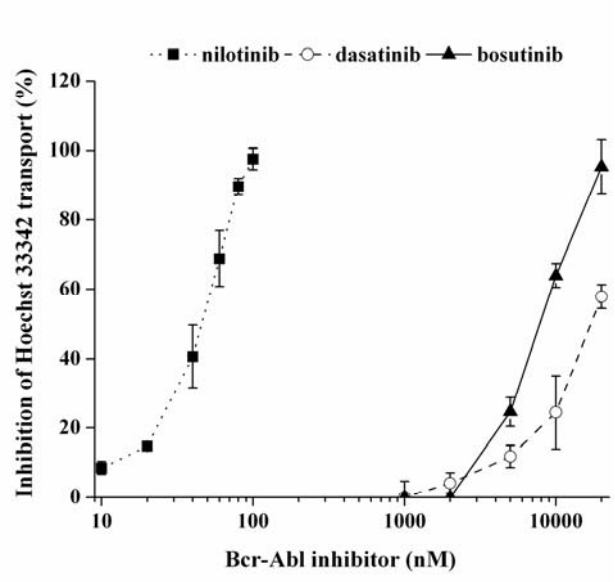

Figure 14. Inhibition of ABCG2-mediated Hoechst 33342 transport by nilotinib, dasatinib and bosutinib. *Concentration-dependent inhibitory potential of the investigated Bcr-Abl inhibitors on ABCG2-mediated Hoechst 33342 transport was measured in intact K562/ABCG2 cells. Changes in fluorescence corresponding to the intracellular accumulation of Hoechst 33342 were followed real-time using spectrofluorometry, in the absence of drugs (F_0), in the presence of the respective Bcr-Abl inhibitor (F_x) and in the simultaneous presence of the Bcr-Abl inhibitor and 2 μM FTC (F_i). Data representing the inhibitory potential of the Bcr-Abl inhibitors relative to the maximum FTC-mediated inhibition were calculated as $(F_x-F_0)/(F_i-F_0)*100$. Mean ± SD values of three independent experiments are shown.*

5.2. Interaction of ABCG2 and small molecule inhibitors of the EGFR/PI3K/Akt/mTOR cascade

The aim of the second project presented in my thesis was to give detailed biochemical characterization of the interaction between the ABCG2 multidrug transporter and small molecule inhibitors of the Epidermal Growth Factor Receptor (EGFR) and the downstream PI3K/Akt/mTOR signaling cascade.

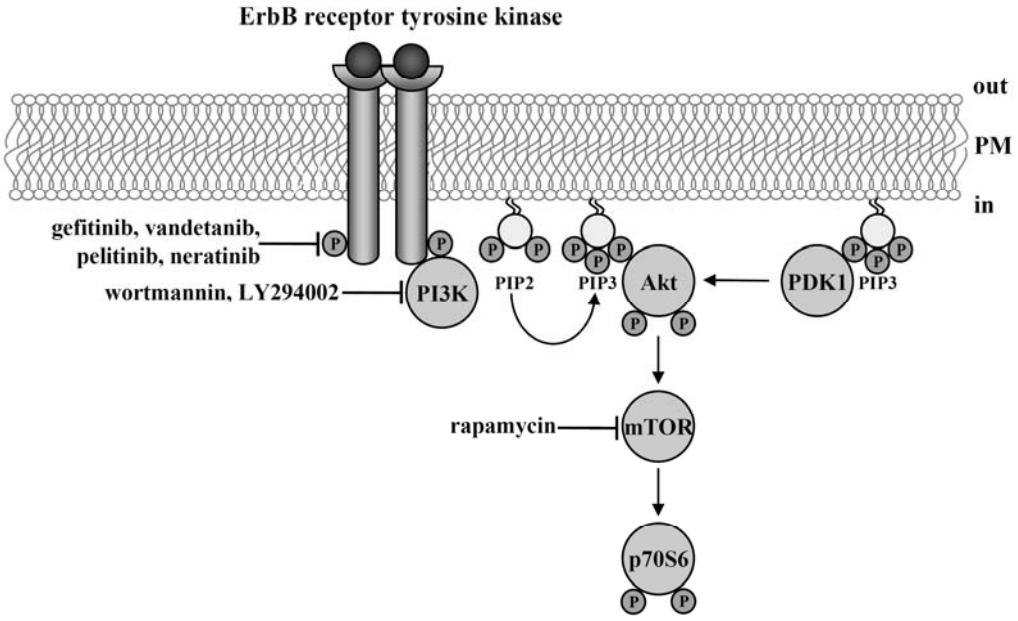

Figure 15. The EGFR/PI3K/Akt/mTOR signaling cascade and its small molecule inhibitors investigated in this study. *The Epidermal Growth Factor Receptor (EGFR) belongs to the ErbB family of receptor tyrosine kinases. Upon ligand binding followed by dimerization, the receptor is phosphorylated thus activating phosphatidylinositol 3-kinase (PI3K). PI3K generates phosphatidylinositol (3,4,5) trisphosphate (PIP3), which results in subsequent plasma membrane recruitment and phosphoinositide-dependent protein kinase-1 (PDK1)-mediated phosphorylation and activation of Akt kinase. Downstream targets of activated Akt include the mammalian target of rapamycin (mTOR) kinase, which can further phosphorylate p70S6 kinase. Small molecule inhibitors used in this study and their intracellular targets are indicated in the figure. PM: plasma membrane.*

EGFR has been described to display uncontrolled kinase activity in various solid tumors, therefore it soon emerged as a promising molecular drug target in cancer therapies (181-183,191). Papers reporting on the interaction of gefitinib, the first applied small molecule inhibitor of EGFR, and ABCG2 were soon published (195,203-208).

With gefitinib used as a positive control, we aimed to investigate whether ABCG2 interacted with the therapeutically relevant second generation EGFR inhibitors vandetanib, pelitinib and neratinib (Fig. 15, Table 4).

EGFR signaling (76) and also the PI3K/Akt/mTOR signaling axis (78-84,233) have been implicated in the regulation of ABCG2, therefore in these studies we also included pharmacological inhibitors of the PI3K/Akt/mTOR cascade, namely wortmannin and LY294002 which are inhibitors of the PI3K, and rapamycin which is an inhibitor of the mTOR kinase. Schematic representation of the EGFR/PI3K/Akt/mTOR signaling pathway and the intracellular targets of the small molecule inhibitors investigated in this study are shown in Fig. 15.

	Gefitinib	**Vandetanib**	**Pelitinib**	**Neratinib**
Aliases	Iressa/ZD1839	Zactima/ZD6474	EKB-569	HKI-272
Target	EGFR	EGFR/VEGFR	EGFR/HER2	EGFR/HER2
Clinical indication or trials	NSCLC	Medullary thyroid cancer, lung cancer	ASM, breast cancer, CRC, NSCLC	Breast cancer, NSCLC

Table 4. EGFR inhibitors investigated in this study. *ASM: Advanced solid malignancies; CRC: Colorectal cancer; NSCLC: Non-small cell lung cancer. (Information on drugs is also available in the Drug Dictionary of the US National Cancer Institute.)*

5.2.1. Characterization of the membrane- and cell-based model systems applied

For the biochemical characterization of the interaction between ABCG2 and the applied inhibitors of the EGFR/PI3K/Akt/mTOR signaling pathway, we employed both membrane- and cell-based model systems. Besides human wild-type ABCG2, in some experiments we also used the N-terminally GFP-tagged ABCG2 protein variant. GFP-ABCG2 has earlier been reported to show similar subcellular localization and functional characteristics to the untagged ABCG2 protein species (211).

Expression of the untagged or GFP-tagged ABCG2 protein in isolated Sf9 membrane fragments was tested by Western blot. As shown in Fig. 16A, both ABCG2 and GFP-ABCG2 were correctly expressed in the insect membranes in their core glycosylated forms (41,211). Total and cell surface expression levels of ABCG2 in parental A431, A431/ABCG2, PLB/ABCG2 and MDCKII/GFP-ABCG2 were compared by Western blot and by labeling with 5D3 and subsequent flow cytometry analysis, respectively (Fig.

16B -C). Both ABCG2 and GFP-ABCG2 were expressed in a fully glycosylated form in the applied ABCG2 expressing mammalian cells (Fig. 16B) (41,211). Correct plasma membrane localization of the transporter in A431/ABCG2, PLB/ABCG2 and MDCKII/GFP-ABCG2 cells was confirmed by immunostaining with the 5D3 antibody which recognizes an external epitope of ABCG2 (Fig. 16C).

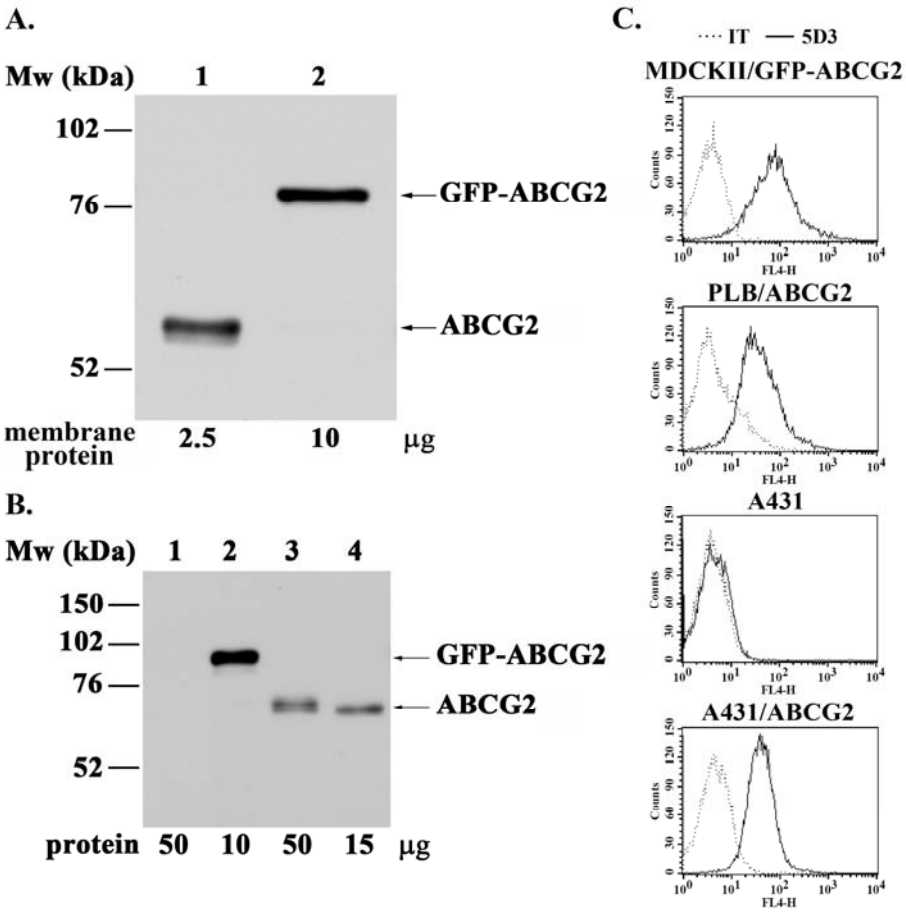

Figure 16. ABCG2 and GFP-ABCG2 expression in the model systems used. *Total ABCG2 protein levels were probed by Western blot using the BXP-21 antibody in* ***(A)*** *isolated Sf9 membranes containing (lane 1) ABCG2 or (lane 2) GFP-ABCG2; and in* ***(B)*** *the mammalian cell lines (lane 1) A431, (lane 2) MDCKII/GFP-ABCG2, (lane 3) PLB/ABCG2 and (lane 4) A431/ABCG2.* ***(C)*** *Cell surface expression of ABCG2 in the applied cell lines was measured by indirect labeling with IgG2b (isotype control, IT) or 5D3 antibodies and Alexa-Fluor-647-conjugated secondary antibodies, followed by flow cytometry analysis. Representative images of three independent experiments are shown.*

In the case of MDCKII/GFP-ABCG2 cells, the 5D3 positive ABCG2-expressing cells also showed homogenous and strong GFP fluorescence indicating no cleavage of the GFP tag (data not shown). No ABCG2 protein expression could be detected in parental A431 cells (Fig. 16B-C).

As shown in Fig. 16B-C, we found that expression levels of the ABCG2 protein varied between the applied ABCG2 expressing mammalian cell lines. These findings were confirmed in the Hoechst 33342 uptake experiments (Fig. 17), where A431/ABCG2 cells showed the highest Hoechst 33342 transport capacity. PLB/ABCG2 and MDCKII/GFP-ABCG2 cells displayed lower but significant ABCG2-dependent Hoechst 33342 transport capacity. In correlation with the ABCG2 expression data (Fig. 16B-C), no endogenous ABCG2 function could be measured in parental A431 cells (Fig. 17).

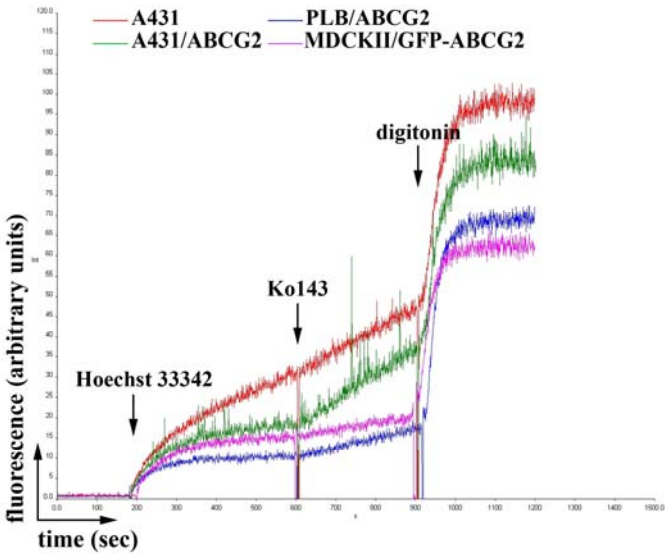

Figure 17. ABCG2 function in the model cell lines applied. *Specific ABCG2 function in the indicated model cells was followed by real-time spectrofluorometric detection of the cellular accumulation of the ABCG2 substrate dye, Hoechst 33342. Representative images of at least three independent measurements are shown.*

5.2.2. Effect of the investigated EGFR inhibitors on the ATPase activity of ABCG2

In order to screen the potential interaction between the investigated inhibitors of EGFR and ABCG2, we measured the concentration-dependent modulatory effect of the drugs on the ABCG2 ATPase activity. In these experiments, cholesterol-loaded Sf9 membrane fragments containing ABCG2 were used. As shown in Fig. 18A, pelitinib strongly stimulated the basal ATPase activity of ABCG2, similarly to gefitinib which is

known to be transported by ABCG2 (203,204,207,208). In contrast, we measured concentration-dependent decrease in the basal ATPase activity of ABCG2 by neratinib, which at higher than 5 μM doses, inhibited the ABCG2 ATPase to a similar extent as the specific ABCG2 inhibitor Ko143 (data not shown). Vandetanib displayed a slight inhibitory effect on the basal ATPase activity of ABCG2 (Fig. 18A).

We also tested whether the investigated EGFR inhibitors could affect the stimulated ATPase activity of ABCG2. In this experimental setup, we expected that compounds which interact with the transporter could decrease the quercetin-stimulated ABCG2 ATPase (127,222,223). We found that each EGFR inhibitor, when applied at micromolar concentrations, could inhibit the stimulated ATPase activity of ABCG2, with neratinib displaying the most pronounced effect (Fig. 18B). Altogether, these data suggest a potential interaction between the investigated drugs and the ABCG2 multidrug transporter.

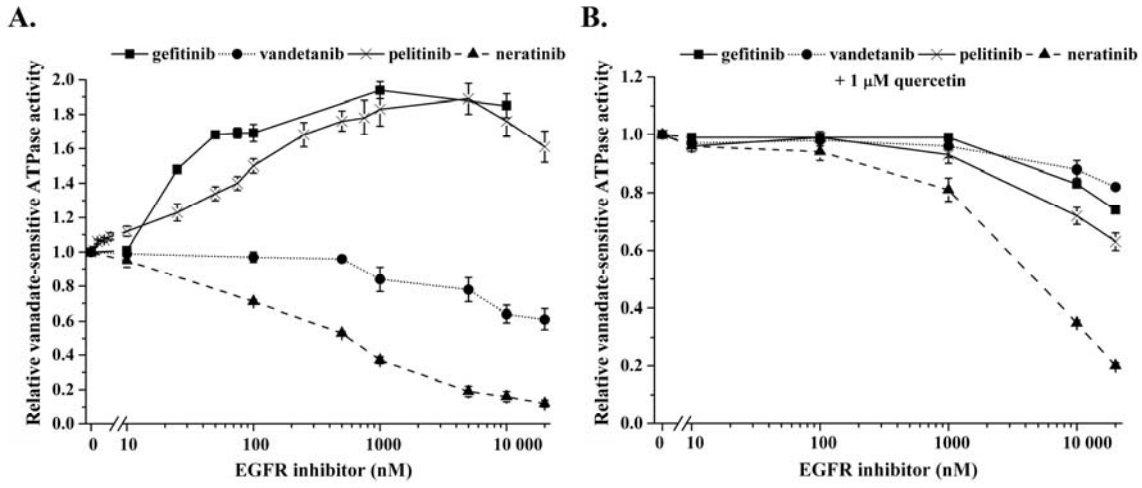

Figure 18. Modulation of the ATPase activity of ABCG2 by the investigated EGFR inhibitors. *Concentration-dependent effect of the investigated EGFR inhibitors on the* ***(A)*** *basal and the* ***(B)*** *stimulated (with 1 μM quercetin) ATPase activity of ABCG2 were measured using isolated cholesterol-loaded Sf9 membranes containing ABCG2. Data were normalized to the ABCG2 ATPase activities measured in the absence of EGFR inhibitors. Mean ± SE values of at least three independent experiments (each performed in duplicates) are shown.*

5.2.3. ABCG2 confers resistance to gefitinib and pelitinib, whereas intracellular action of vandetanib and neratinib is not restricted by the transporter

As a next step, we aimed to study whether the presence of ABCG2 could modify the action of the EGFR inhibitors in a cellular milieu. To this end, we measured the cellular toxicity of the drugs in A431 and A431/ABCG2 cells. A431 epidermoid carcinoma cells overexpress EGFR, rely on active EGFR signaling for survival and therefore show sensitivity to inhibition of the receptor (203). Cells were treated with increasing concentrations of the drugs for 72 hours in the absence or the presence of 5 μM FTC. Cellular viability was determined with the MTT assay (see section 4.9). IC50 values calculated from the respective killing curves are shown in Table 5.

Cellular IC50 (nM; mean ± SE)		Gefitinib	Vandetanib	Pelitinib	Neratinib
-FTC	A431 parental	106.1 ± 7.5	913.5 ± 61.3	23.2 ± 5.2	12.1 ± 2.2
	A431/ABCG2	197.7 ± 13.1	979.2 ± 79.2	133.2 ± 21.9	21.8 ± 5.4
+FTC	A431 parental	81.4 ± 7.4	n.d.	26.3 ± 3.2	11.7 ± 1.3
	A431/ABCG2	82.0 ± 1.6	n.d.	27.0 ± 4.8	22.7 ± 1.3

Table 5. Cellular toxicity of EGFR inhibitors in EGFR-overexpressing A431 and A431/ABCG2 cells.

As compared to parental A431 cells, we measured increased IC50 values for gefitinib and pelitinib in A431/ABCG2 cells. This decreased sensitivity of A431/ABCG2 cells towards gefitinib and pelitinib could be fully reversed by the specific blockade of ABCG2 function with FTC. Neratinib also showed slightly decreased cellular toxicity in A431/ABCG2 cells; however, this phenomenon was unaffected by the presence of the specific ABCG2 inhibitor FTC. A431 and A431/ABCG2 cells were similarly sensitive to vandetanib. These results imply that similarly to gefitinib, ABCG2 can confer cellular resistance to pelitinib, whereas cellular toxicity of neratinib and vandetanib is not restricted by the transporter.

To further investigate drug effects on a molecular level, we followed the phosphorylation status of EGFR in A431 and A431/ABCG2 cells treated with increasing concentrations of the applied EGFR inhibitors (Fig. 19). Serum-starved A431 or A431/ABCG2 cells were stimulated with hEGF for 15 minutes and then were exposed to

the indicated concentrations of EGFR inhibitors for additional 15 minutes. Cellular proteins were extracted as described in section 4.11, and phosphorylation of EGFR at Tyr1068 was probed by Western blot.

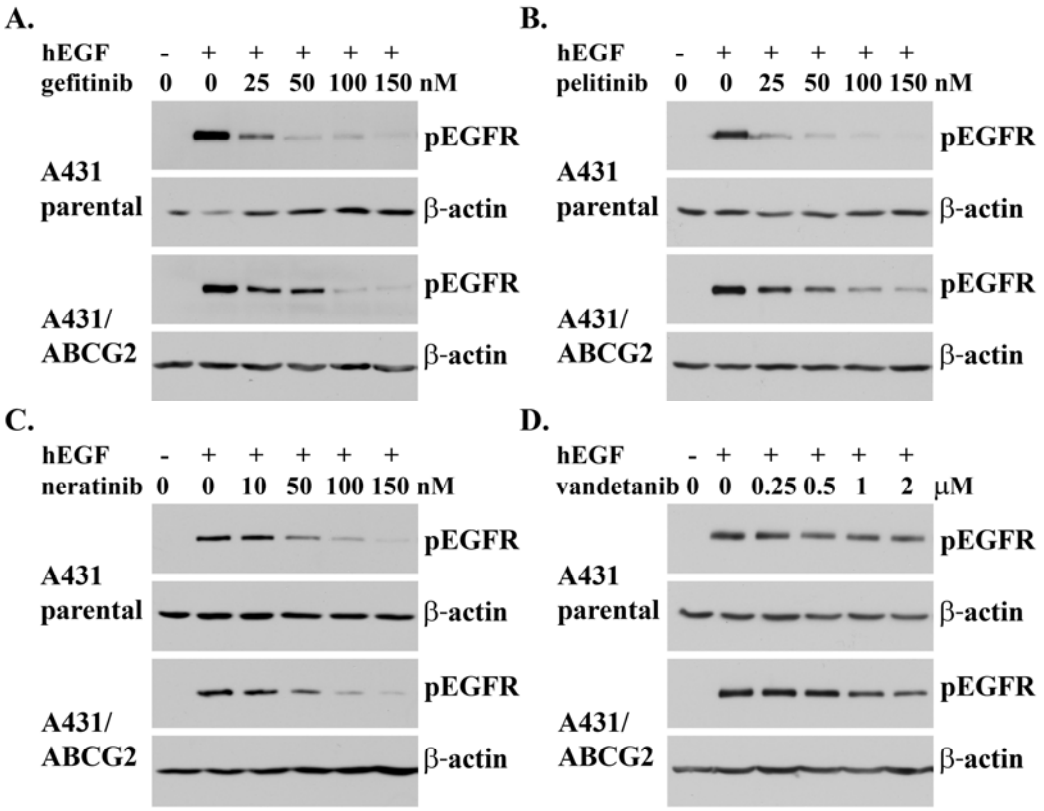

Figure 19. Phosphorylation of EGFR in EGFR inhibitor-treated A431 and A431/ABCG2 cells. *7.5*10^5/mL cells were seeded in serum-free medium. After 16 hours, cells were stimulated with 20 ng/mL hEGF for 15 minutes then were exposed to the EGFR inhibitors* ***(A)*** *gefitinib,* ***(B)*** *pelitinib,* ***(C)*** *neratinib or* ***(D)*** *vandetanib at the indicated concentrations for additional 15 minutes. Cell lysates were prepared and 20 μg protein extracts were probed for phosphorylation of EGFR at Tyr1068 by Western blot. Beta-actin was stained to check sample loading. Representative blots of three independent experiments are shown.*

As shown in Fig. 19, stimulation with hEGF resulted in strong phosphorylation of EGFR in both A431 and A431/ABCG2 cells. Consistently with the results obtained in the cellular toxicity measurements, we detected significantly higher levels of phosphorylated EGFR in A431/ABCG2 cells treated with gefitinib (Fig. 19A) or pelitinib (Fig. 19B) as compared to those measured in parental A431 cells. These findings strongly suggest that the presence of ABCG2 restrict the intracellular kinase inhibitory action of these drugs

most probably by active efflux. In the case of neratinib (Fig. 19C) or vandetanib (Fig. 19D) treatment, we measured similar levels of phosphorylated EGFR in A431 and A431/ABCG2 cells, further implying that the cytotoxic effect of these drugs is not modified by the presence of ABCG2.

5.2.4. The investigated EGFR inhibitors block ABCG2 function and enhance the cellular accumulation of ABCG2 substrates

In the next series of experiments, we studied whether the EGFR inhibitors used in this study could block the function of ABCG2, which could result in re-sensitization of cells resistant to simultaneously administered ABCG2 substrate drugs. It has been shown previously that conformational changes of ABCG2 can be monitored with the anti-ABCG2 5D3 antibody (70,215). ABCG2 has at least two distinct conformations exposing the extracellular 5D3 epitope displaying low or high affinity towards the antibody. The highly 5D3 immunoreactive form of ABCG2 corresponds to the PFA-fixed or the Ko143- or FTC-inhibited protein conformation (215). Therefore, drug-mediated increase in the 5D3 binding affinity of the transporter can be exploited to screen for compounds bearing ABCG2 inhibitory potential (223).

	Gefitinib	**Vandetanib**	**Pelitinib**	**Neratinib**
5D3 binding in A431/ABCG2 cells (% relative to Ko143; mean ± SD)	71.3 ± 12.7	9.3 ± 0.3	41.9 ± 6.5	26.0 ± 0.7
EC50 of inhibition of Hst 33342 efflux in PLB/ABCG2 cells (μM; mean ± SD)	0.6 ± 0.1	5.9 ± 0.5	0.9 ± 0.0	0.9 ± 0.0

Table 6. Effect of the investigated EGFR inhibitors on the 5D3 binding and Hoechst 33342 transport capacity of ABCG2.

Changes in the 5D3 binding capacity of ABCG2 in the presence of increasing concentrations of EGFR inhibitors was tested by flow cytometry in A431/ABCG2, PLB/ABCG2 and MDCKII/GFP-ABCG2 cells as described in section 4.7. The most pronounced effect was measured in the presence of 10 μM EGFR inhibitors. Statistical analysis of the data obtained using A431/ABCG2 cells and 10 μM EGFR inhibitors are summarized in Table 6. Geometric mean values of the histograms representing 5D3-

labeled cells were corrected with those representing isotype control (IgG2b) labeled cells of the corresponding treatment. Data were calculated as the percentage of the maximal 5D3 binding obtained in the presence of 1 μM Ko143. All of the investigated EGFR inhibitors provoked increased 5D3 binding of ABCG2 with gefitinib and pelitinib displaying the most pronounced effect in all of the investigated cell types. These findings indicate that the investigated EGFR inhibitors might efficiently block the function of the ABCG2 transporter. Therefore, as a next step, we studied the inhibitory potential of the EGFR inhibitors applied on the ABCG2-mediated transport of Hoechst 33342 in A431/ABCG2 and PLB/ABCG2 cells, and on the transport of mitoxantrone in A431/ABCG2 cells. All of the investigated EGFR inhibitors efficiently inhibited Hoechst 33342 transport in PLB/ABCG2 cells (Table 6) and A431/ABCG2 cells (data not shown) in a concentration-dependent manner. Furthermore, we found that 10 μM of gefitinib, pelitinib or neratinib completely blocked the ABCG2-mediated efflux of mitoxantrone from A431/ABCG2 cells (Fig. 20).Vandetanib at 10 μM concentration could also slightly inhibit mitoxantrone transport in A431/ABCG2 cells; however, to a lesser extent than the other EGFR inhibitors applied (Fig. 20). Collectively, these data suggest that gefitinib, pelitinib, neratinib and vandetanib might reverse ABCG2-associated drug resistance by inhibiting the function of the transporter.

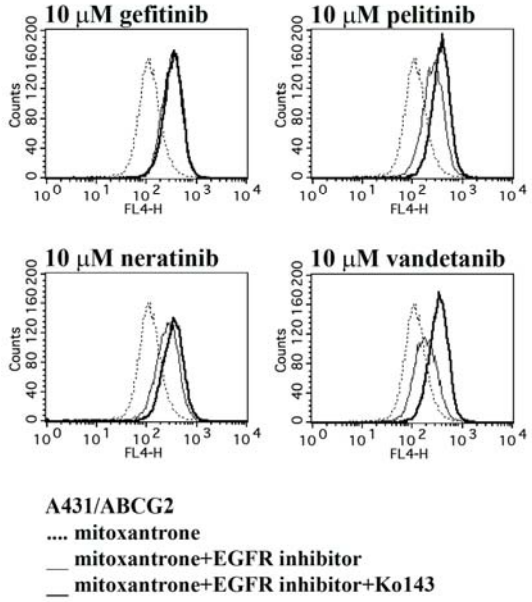

Figure 20. Inhibition of ABCG2-mediated mitoxantrone (MX) efflux by the investigated EGFR inhibitors. *$2*10^5$ A431/ABCG2 cells were incubated with 5 μM MX (dotted line), 5 μM MX with 10 μM of EGFR inhibitors (solid line) or 5 μM MX with 10 μM of EGFR inhibitors and 1 μM Ko143 (solid, bold line) at 37 °C for 30 minutes. Cellular fluorescence of MX in live cells was determined by flow cytometry. Representative histograms of three independent experiments are shown.*

5.2.5. Gefitinib exposure enhances ABCG2 protein expression and causes cellular resistance to mitoxantrone

In the next set of experiments, we aimed to investigate whether the exposure of cancer cells to the EGFR inhibitor gefitinib influences the expression of ABCG2. To this end, we analyzed ABCG2 protein expression and function in gefitinib-resistant NCI-H1650 cells. NCI-H1650 cells were exposed to gefitinib for 72 hours and the surviving gefitinib-resistant subclones (C11, G7, O11, P8 and P11, nomenclature of Kwak et al (214)) were isolated and characterized previously by Kwak et al (214).

First, we measured cell surface expression of ABCG2 in the parental NCI-H1650 cells and the C11, G7, O11, P8 and P11 gefitinib-resistant subclones by 5D3 labeling. We found detectable endogenous expression of the transporter in parental NCI-H1650 cells, and C11, G7 and P11 gefitinib resistant clones showed elevated plasma membrane protein levels of ABCG2 (data not shown). As clone G7 showed the highest increase in 5D3 binding as compared to parental NCI-H1650 cells, in the further measurements we analyzed expression and function of the ABCG2 protein in these cells.

Levels of the ABCG2 protein in NCI-H1650 and NCI-H1650 G7 cells were compared by Western blot. As shown in Fig. 21A, endogenous ABCG2 could be detected in parental NCI-H1650 cells by Western blot, and NCI-H1650 G7 cells showed an increase in total ABCG2 protein levels. Elevated levels of the transporter in the plasma membrane of NCI-H1650 G7 cells were further confirmed by 5D3 labeling and confocal microscopy measurements (Fig. 21B).

Next, we tested the function of ABCG2 in parental NCI-H1650 and the gefitinib-resistant NCI-H1650 G7 cells. Intracellular accumulation of mitoxantrone was measured in the absence and in the presence Ko143 by flow cytometry. As shown in Fig. 21C, in the absence of Ko143, NCI-H1650 G7 cells could accumulate less mitoxantrone than the parental NCI-H1650 cells, whereas administration of Ko143 enhanced mitoxantrone uptake in both cell types. Long-term consequences of enhanced expression of the ABCG2 protein in NCI-H1650 G7 cells were followed by measuring the cellular toxicity of mitoxantrone. NCI-H1650 and NCI-H1650 G7 cells were exposed to mitoxantrone in the absence or in the presence of Ko143 for 72 hours, and cellular viability was determined by the MTT assay. NCI-H1650 G7 cells showed increased resistance towards

mitoxantrone as compared to NCI-H1650 cells, and co-incubation with Ko143 restored mitoxantrone sensitivity of both cell types (Fig. 21D).

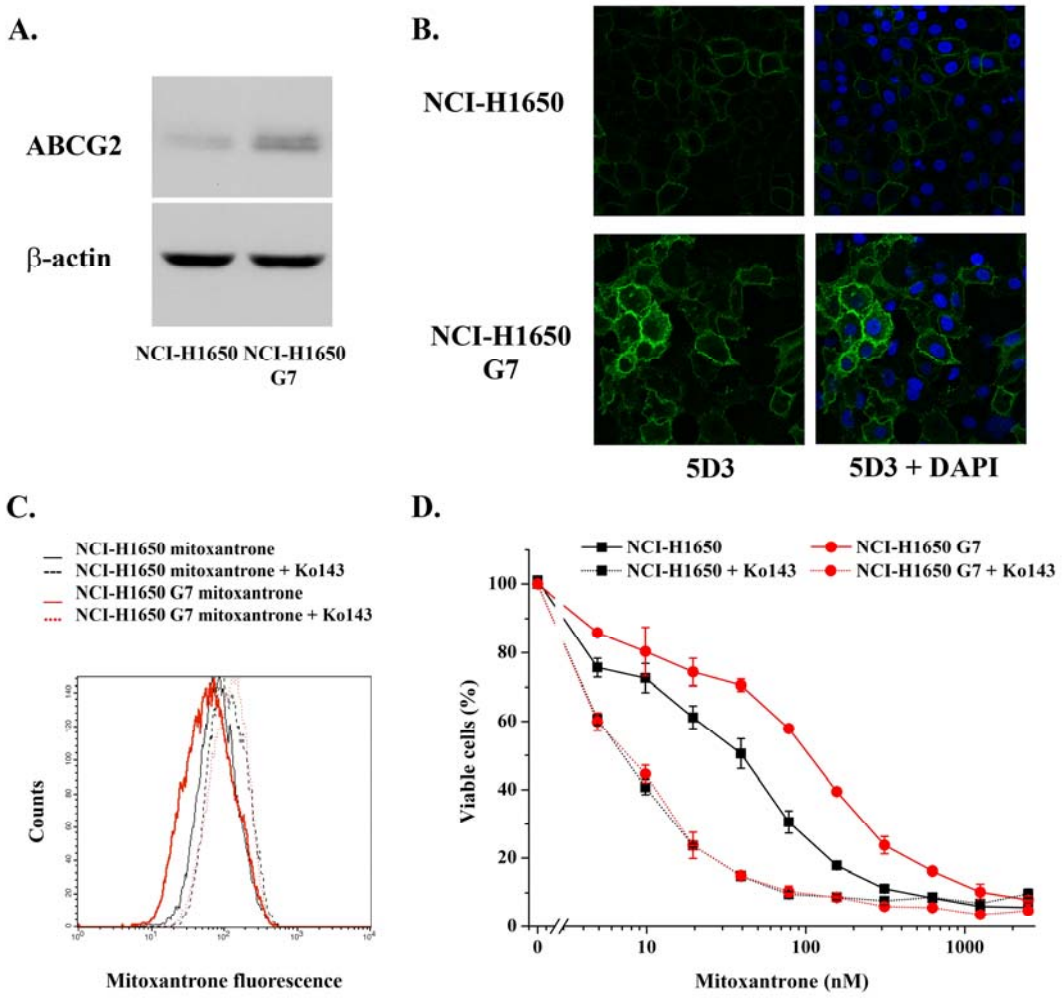

Figure 21. Enhanced expression and function of ABCG2 in gefitinib-resistant NCI-H1650 cells. ***(A)*** *Total ABCG2 protein levels in NCI-H1650 and gefitinib-resistant NCI-H1650 G7 cells were determined by Western blot using 50 μg cellular protein extracts and the BXP-21 antibody. A representative blot of three independent experiments is shown.* ***(B)*** *Cell surface expression of ABCG2 was measured by confocal microscopy using the 5D3 antibody. A representative image of two independent experiments is shown.* ***(C)*** *$2*10^5$ cells were incubated with 2 μM mitoxantrone in the absence or presence of 1 μM Ko143 at 37 °C for 30 minutes. Cellular fluorescence of mitoxantrone in live cells was determined by flow cytometry. A representative histogram of eight independent measurements is shown.* ***(D)*** *$4*10^3$ NCI-H1650 or NCI-H1650 G7 cells were exposed to mitoxantrone in the absence or the presence of 1 μM Ko143 for 72 hours. Cellular viability was determined by the MTT assay. Mean ± SE values of three independent experiments (each performed in quadruplicates) are shown.*

5.2.6. Effect of the investigated pharmacological PI3K/Akt/mTOR inhibitors on the ATPase activity of ABCG2

The PI3K/Akt/mTOR signaling cascade, which is downstream of activated EGFR (Fig. 15), has been implicated in the regulation of the ABCG2 transporter. Inhibition of Akt signaling was reported to provoke rapid translocation of ABCG2 from the plasma membrane to intracellular compartments in several cell types (79-84), a phenomenon which has also been associated with attenuated ABCG2 function (79,81,83,84) and subsequent reversal of drug resistance caused by the transporter (83,84). Nevertheless, opposing data regarding the involvement of the PI3K/Akt axis and the downstream mTOR kinase in the regulation of the plasma membrane localization of ABCG2 has also been published (78,81). In our study, we also intended to address whether PI3K/Akt/mTOR signaling was involved in the rapid regulation of the plasma membrane localization of ABCG2 in our available model systems. In the above referenced reports, wortmannin, LY294002 and rapamycin were applied for the pharmacological inhibition of the PI3K and mTOR kinases, respectively (Fig. 15), to manipulate cellular signal transduction. Given the multispecific drug recognition capability of ABCG2, however, as a first step, we tested whether these compounds directly interacted with the transporter.

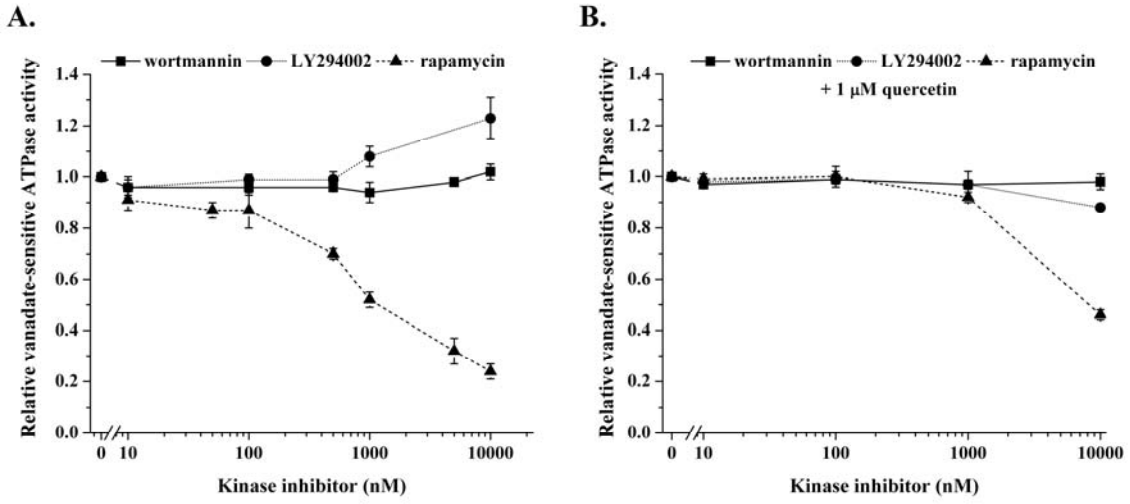

Figure 22. Modulation of the ATPase activity of ABCG2 by the investigated pharmacological PI3K/Akt/mTOR inhibitors. *Concentration-dependent effect of the investigated PI3K/Akt/mTOR inhibitors on the* ***(A)*** *basal and the* ***(B)*** *stimulated (with 1 μM quercetin) ATPase activity of ABCG2 were measured using isolated cholesterol-loaded Sf9 membranes containing ABCG2. Data were normalized to the ABCG2 ATPase activities measured in the absence of PI3K/Akt/mTOR inhibitors. Mean ± SE values of at least three independent experiments (each performed in duplicates) are shown*

Modulation of the basal (Fig. 22A) and the stimulated (Fig. 22B) ATPase activity of ABCG2 by increasing concentrations of wortmannin, LY294002 and rapamycin were measured in Sf9 membranes containing ABCG2. At its experimentally relevant 10 μM concentration, LY294002 slightly stimulated the basal ABCG2 ATPase, whereas the other PI3K inhibitor wortmannin showed no modulatory effect at all (Fig. 22A). The mTOR kinase inhibitor rapamycin decreased the basal ATPase activity of the transporter in a concentration-dependent manner and produced a pronounced inhibition when applied at 10 μM concentration (Fig. 22A). Accordingly, marked inhibition of the quercetin-stimulated ABCG2 ATPase activity could be measured only in the case of 10 μM rapamycin (Fig. 22B). In contrast, 10 μM LY294002 displayed only a slight inhibitory effect, whereas wortmannin showed no effect on the quercetin-stimulated ATPase activity of the transporter (Fig. 22B). As GFP-ABCG2 was also used in some experiments, we also tested the effect of the investigated drugs on the basal (Fig. 23A) and the stimulated (Fig. 23B) ATPase activity of GFP-ABCG2. In these measurements, similar ATPase modulatory patterns by the investigated compounds were detected to those obtained in the case of the untagged ABCG2 protein variant (Fig. 22).

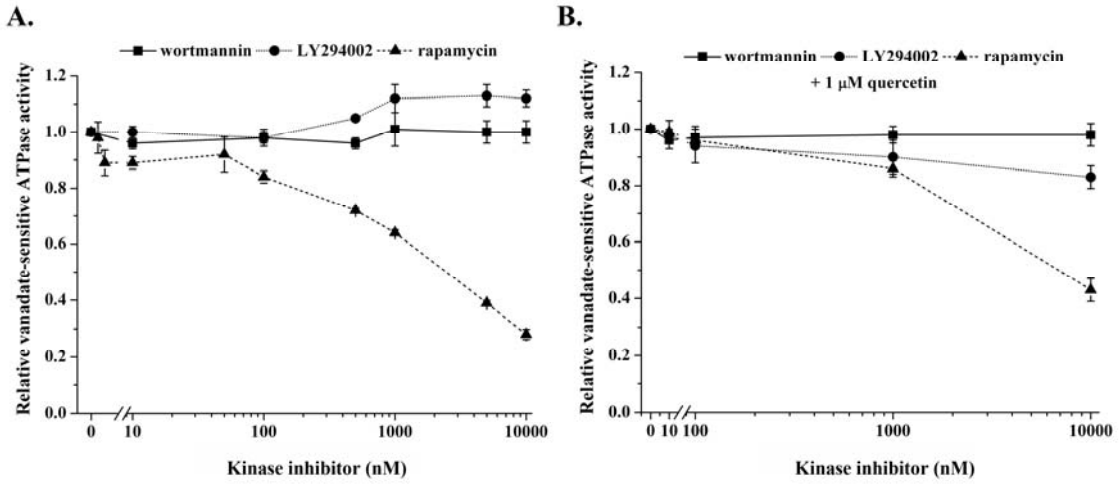

Figure 23. Modulation of the ATPase activity of GFP-ABCG2 by the investigated pharmacological PI3K/Akt/mTOR inhibitors. *Concentration-dependent effect of the investigated PI3K/Akt/mTOR inhibitors on the* ***(A)*** *basal and the* ***(B)*** *stimulated (with 1 μM quercetin) ATPase activity of GFP-ABCG2 were measured using isolated cholesterol-loaded Sf9 membranes containing GFP-ABCG2. Data were normalized to the GFP-ABCG2 ATPase activities measured in the absence of PI3K/Akt/mTOR inhibitors. Mean ± SE values of at least three independent experiments (each performed in duplicates) are shown.*

Collectively, these data suggest that in contrast to wortmannin, LY294002 and rapamycin interact with ABCG2. Nevertheless, both stimulation and inhibition of the basal ABCG2 ATPase activity by substrates transported at higher or lower rates, respectively has been described (41). Moreover, some compounds which interact with the transporter do not modulate the ABCG2 ATPase activity at all (127,222). Therefore, based on these results we could not determine the nature of the interaction between ABCG2 and rapamycin, and could not exclude a potential interaction of wortmannin with ABCG2 either. Also, it remained to be determined whether the potential interaction between the transporter and LY294002, which only slightly influenced the ABCG2 ATPase or rapamycin is also relevant in a cellular context.

5.2.7. The presence of ABCG2 does not influence target kinase inhibition by the investigated PI3K/Akt/mTOR inhibitors

As a next step, we aimed to determine whether the presence of ABCG2 could restrict the intracellular action of the applied PI3K/Akt/mTOR inhibitors at their relevant target kinase sites (Fig. 15), which would suggest active ABCG2-mediated transport of the drugs. Stimulation of EGFR-overexpressing A431 cells with hEGF results in activation of the downstream PI3K/Akt signaling cascade (203,234); therefore, we investigated Akt and p70S6 kinase phosphorylation patterns in hEGF-stimulated A431 and A431/ABCG2 cells treated with wortmannin, LY294002 or rapamycin. Drugs were used at their experimentally relevant concentrations (235), as indicated in Fig. 24. In addition, the effect of 10 μM rapamycin was also tested, since it showed inhibition of the ATPase activity of ABCG2 at this concentration. Phosphorylation of the Akt kinase and p70S6 kinase were probed by Western blot using antibodies which react with Akt when it is phosphorylated at Ser473 or p70S6 kinase when it is phosphorylated at Thr389. As expected, hEGF treatment resulted in enhanced phosphorylation of both Akt and p70S6 kinases in A431 and A431/ABCG2 cells (Fig. 24A-B). Phosphorylation of Akt in hEGF-treated A431 cells could be fully prevented by wortmannin treatment, and we also detected decreased levels of phosphorylated Akt in hEGF-treated A431 cells exposed to LY294002 (Fig. 24A). Phosphorylation of the downstream p70S6 kinase was also attenuated in hEGF-stimulated A431 cells exposed to wortmannin or LY294002, whereas

it could be fully abolished by exposure to rapamycin (Fig. 24B). Phosphorylation patterns of Akt and p70S6 kinases were similar in A431/ABCG2 cells exposed to the respective drug treatments to those measured in A431 cells (Fig. 24A-B), suggesting that the intracellular efficiencies of wortmannin, LY294002 or rapamycin are unaltered by the presence of ABCG2. These findings render it unlikely that any of these compounds, when applied at the experimentally relevant drug concentrations, is transported by ABCG2 efficiently enough to reduce their intracellular concentrations below the drug efficacy threshold.

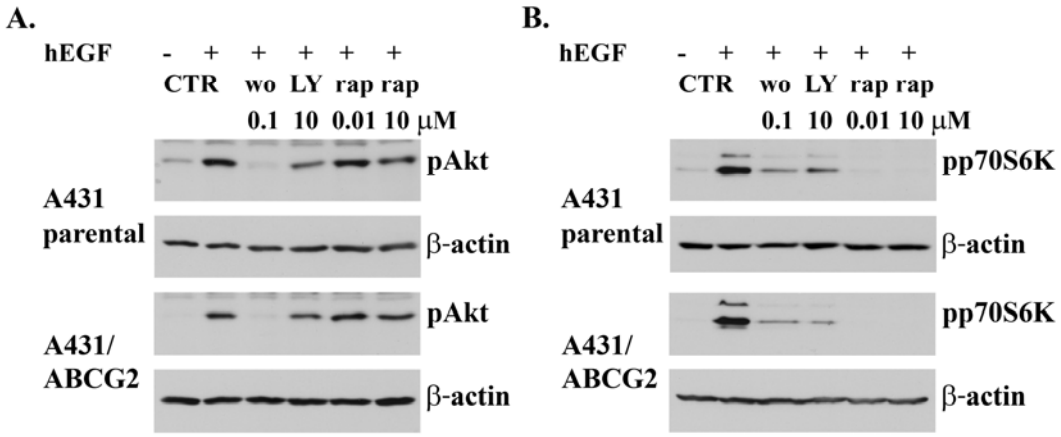

Figure 24. Effect of the investigated pharmacological PI3K/Akt/mTOR inhibitors on the phosphorylation of Akt or p70S6 kinases in A431 and A431/ABCG2 cells. *$7.5*10^5$/mL cells were seeded in serum-free medium. After 16 hours, cells were stimulated with 20 ng/mL hEGF for 15 minutes then were exposed to wortmannin, LY294002 or rapamycin at the indicated concentrations for additional 15 minutes. Cell lysates were prepared and 20 μg protein extracts were probed for phosphorylation of* ***(A)*** *Akt kinase at Ser473 and* ***(B)*** *p70S6 kinase at Thr389 by Western blot. Beta-actin was stained to check sample loading. Representative blots of three independent experiments are shown.*

5.2.8. LY294002 and rapamycin directly inhibit ABCG2 function

Next, we investigated whether wortmannin, LY294002 or rapamycin could inhibit the function of the ABCG2 transporter. To this end, we tested if the presence of the investigated inhibitors could generate a conformational change in the ABCG2 protein similarly to Ko143, which thereby would increase the 5D3 binding affinity of the transporter (215,223). 5D3 binding of various cell lines overexpressing ABCG2 was measured in the presence of increasing concentrations of wortmannin, LY294002 or

rapamycin. Geometric mean values of the histograms representing specific 5D3 binding were corrected with those obtained in cells labeled with isotype control antibodies in the presence of the respective drug. None of the investigated compounds provoked a remarkable increase in 5D3 binding of the ABCG2 expressing cells at 0.1 μM or 1 μM concentrations (data not shown). Wortmannin did not affect the 5D3 binding affinity of ABCG2 at 10 μM concentration either (Table 7). In contrast, both LY294002 and rapamycin, when applied at 10 μM concentration, highly increased the 5D3 binding of ABCG2 in A431/ABCG2 cells (Table 7), and also in MDCKII/GFP-ABCG2 and PLB/ABCG2 cells (data not shown). These results imply that in contrast to wortmannin, LY294002 and rapamycin might efficiently inhibit the function of the ABCG2 transporter.

	Wortmannin	**LY294002**	**Rapamycin**
Aliases	-	-	Sirolimus
Target	PI3K	PI3K	mTOR
5D3 binding in A431/ABCG2 cells (% relative to Ko143; mean ± SD)	no effect	63.2 ± 4.2	61.9 ± 10.6
EC50 of inhibition of Hst 33342 efflux in PLB/ABCG2 cells (μM; mean ± SD)	no effect	11.2 ± 2.0	1.6 ± 0.2

Table 7. Modulation of the 5D3 binding and Hoechst 33342 efflux capacity of ABCG2 by the investigated pharmacological PI3K/Akt/mTOR inhibitors.

Therefore, next we studied whether the investigated PI3K/Akt/mTOR inhibitors could inhibit the transport of Hoechst 33342 and mitoxantrone, both of which are substrates of ABCG2. As shown in Table 7, in correlation with the 5D3 binding data, wortmannin had no effect on the Hoechst 33342 transport capacity of PLB/ABCG2 cells; whereas LY294002 and rapamycin inhibited Hoechst 33342 efflux from PLB/ABCG2 cells in a concentration-dependent manner. Similar results were obtained using A431/ABCG2 cells (data not shown). Similarly, 10 μM LY294002 and 10 μM rapamycin completely abrogated the efflux of mitoxantrone from A431/ABCG2 cells (Fig. 25A). In contrast, wortmannin showed no inhibitory effect on mitoxantrone transport in A431/ABCG2 cells, even when applied at a 100-fold excess to its experimentally used 0.1 μM

concentration (Fig. 25A). Collectively, these results suggest that LY294002 and rapamycin directly inhibit the function of ABCG2, while wortmannin does not interact with the protein.

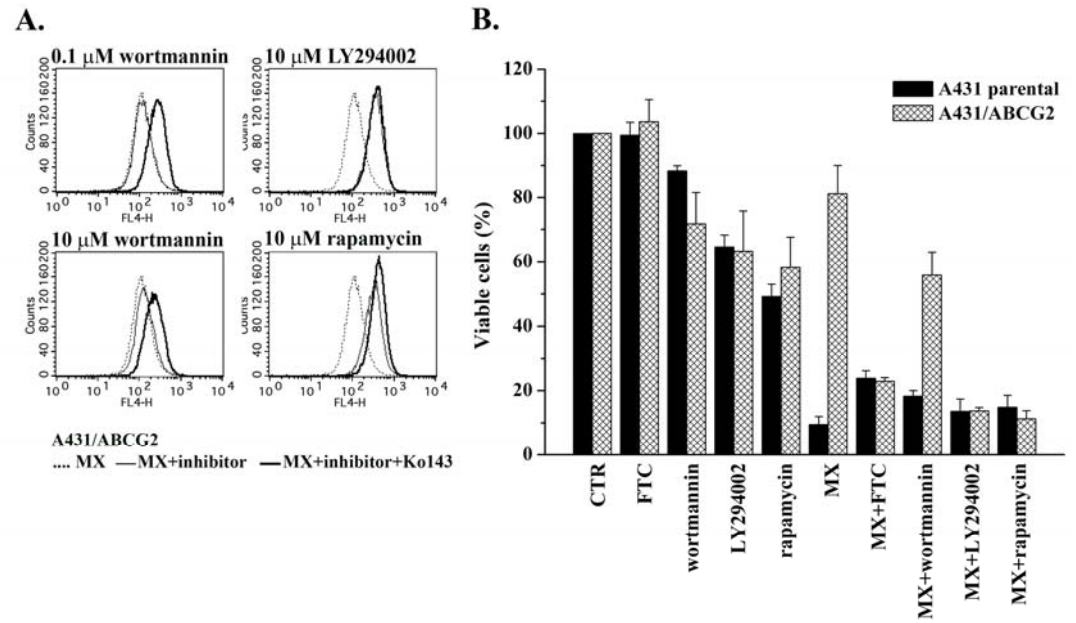

Figure 25. Inhibition of ABCG2-mediated mitoxantrone (MX) efflux and restoration of MX-sensitivity by the investigated pharmacological PI3K/Akt/mTOR inhibitors. (A) *$2*10^5$ A431/ABCG2 cells were incubated with 5 μM MX (dotted line), 5 μM MX with PI3K/Akt/mTOR inhibitors at the indicated concentrations (solid line) or 5 μM MX with inhibitors and 1 μM Ko143 (solid, bold line) at 37 °C for 30 minutes. Cellular fluorescence of MX in live cells was determined by flow cytometry. Representative histograms of three independent experiments are shown.* ***(B)*** *$4*10^3$ A431 or A431/ABCG2 cells were treated with 5 μM FTC, 10 μM wortmannin, 10 μM LY294002, 10 μM rapamycin or 50 nM MX either as a single agent or in combination for 72 hours. Cellular viability was assessed by the MTT assay. Mean ± SE values of three independent experiments (each performed in quadruplicates) are shown.*

In order to reveal whether inhibition of ABCG2 function by LY294002 or rapamycin also results in the reversal of drug resistance caused by the transporter, we measured the cellular toxicity of mitoxantrone in A431 and A431/ABCG2 cells in the presence of the drugs indicated in Fig. 25B. Cells were exposed to the indicated treatments for 72 hours, and cellular viability was determined by the MTT assay. Treatment with wortmannin, LY294002 or rapamycin reduced the viability of both A431 and A431/ABCG2 cells. As we expected, A431/ABCG2 cells were resistant to mitoxantrone, and this resistance could be similarly reversed by administration of the specific ABCG2 inhibitor FTC, and

also by LY294002 and rapamycin. Re-sensitization of mitoxantrone-resistant A431/ABCG2 cells by LY294002 or rapamycin suggests that these compounds are indeed capable of long-term functional inhibition of the transporter thereby reversing multidrug resistance. In contrast, mitoxantrone resistance of A431/ABCG2 cells was unaffected by wortmannin, confirming results of the 5D3 binding (Table 7) and dye uptake (Table 7, Fig. 25A) experiments showing that wortmannin could not inhibit the function of ABCG2. Notably, cellular viability in the case of wortmannin, LY294002 and rapamycin treatment was similar in both A431 and A431/ABCG2 samples, further supporting that ABCG2 is not capable of hindering intracellular action of these PI3K/Akt/mTOR inhibitors by active efflux at the applied drug concentrations. Moreover, as wortmannin and LY294002, which both inhibit PI3K thereby preventing phosphorylation of Akt and the downstream p70S6 kinase (Fig. 24), produced distinct effects on reversing ABCG2-mediated mitoxantrone resistance (Fig. 25B), we concluded that the observed effects correlated with direct inhibition of ABCG2 function rather than with alterations in PI3K/Akt/mTOR signaling and subsequent potential changes in functional ABCG2 protein levels.

5.2.9. Pharmacological inhibition of the EGFR/PI3K/Akt/mTOR cascade does not result in rapid internalization of ABCG2

Inhibition of Akt signaling was shown to induce rapid translocation of ABCG2 from the plasma membrane to intracellular compartments in various cell types (79-84). This phenomenon has also been associated with attenuated ABCG2 transporter function (79,81,83,84) and subsequent reversal of ABCG2-mediated drug resistance (83,84). Nevertheless, opposing data has also been published showing that inhibition of PI3K/Akt signaling in human leukemia cells down-regulated overall ABCG2 protein levels rather than affecting only its plasma membrane localization (78). Involvement of the downstream mTOR kinase in the regulation of the plasma membrane insertion of ABCG2 has also been controversial (81,233). Employing cell lines with either endogenous or forced ABCG2 or GFP-ABCG2 protein expression, in the current study we also addressed the issue concerning involvement of the PI3K/Akt/mTOR signaling axis in the regulation of ABCG2.

As a first approach, we used the anti-ABCG2 5D3 antibody to monitor cell surface transporter level in cells treated with pharmacological inhibitors of the PI3K/Akt signaling cascade. 5D3 is a conformation sensitive antibody which reacts with an epitope located in the third extracellular loop of ABCG2 (70,71,215). Fixation with PFA or incubation with FTC or Ko143 has been shown to induce a protein conformation of ABCG2 which bears maximum 5D3 antibody binding affinity (215).

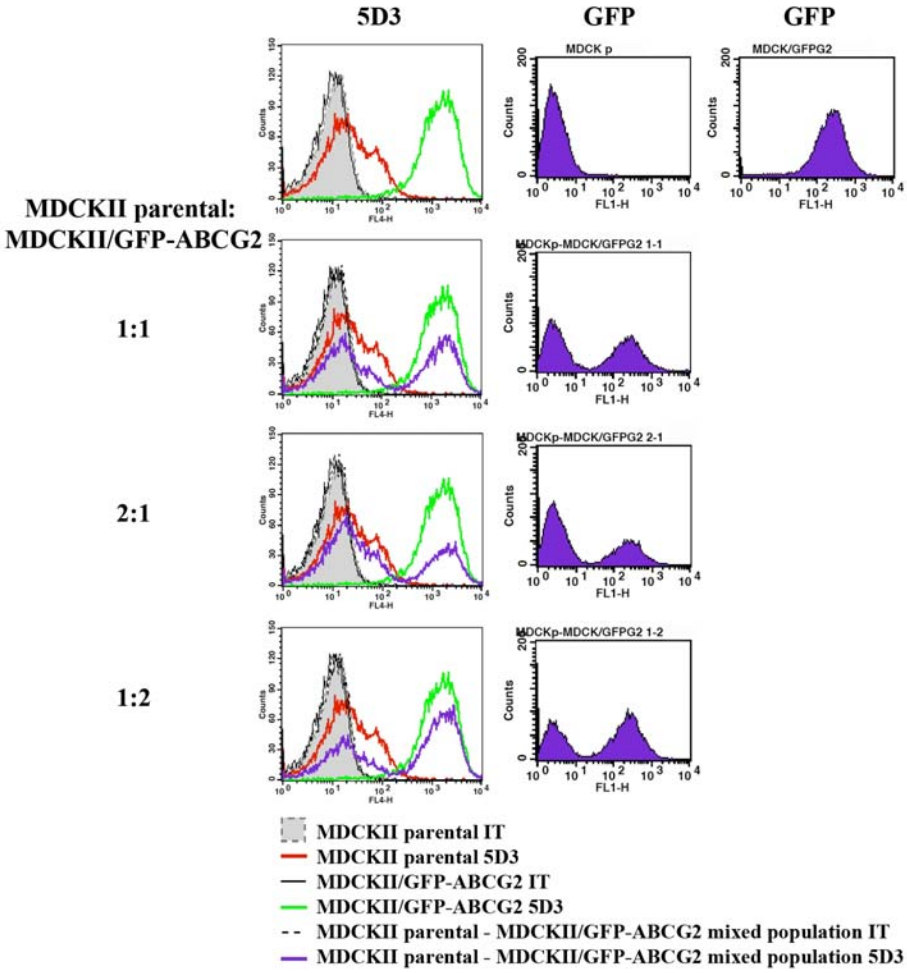

Figure 26. Detection of the appearance of an ABCG2-negative cell population in paraformaldehyde (PFA)-fixed cells with the conformation-sensitive anti-ABCG2 5D3 antibody. *$2.5*10^5$ parental or GFP-ABCG2-expressing MDCKII cells or the mixture of the two cell types at the indicated ratios were fixed with PFA and were labeled with IgG2b (isotype control, IT) or 5D3 primary antibodies and Alexa-Fluor-647-conjugated secondary antibodies. Samples were analyzed by flow cytometry. Representative histograms of two independent experiments are shown.*

In the experiments aiming to elucidate the role of PI3K/Akt signaling in the plasma membrane localization of ABCG2, we planned to use PFA-fixed cells. Therefore in the first control measurements we wanted to prove that 5D3 labeling quantitatively correlates with the amount of ABCG2 in the cell surface under PFA-fixed conditions and that it is also applicable to co-detect PFA-fixed cell populations showing decreased or abolished plasma membrane ABCG2 levels together with those showing maximum 5D3 binding. Parental and GFP-ABCG2 overexpressing MDCKII cells (Fig. 16B-C) were mixed in different ratios then were fixed with PFA and were subsequently stained with 5D3. As 5D3 signals corresponded with the GFP-fluorescence intensities of the respective cell populations, we concluded that 5D3 labeling allows for sensitive and quantitative detection of plasma membrane ABCG2 levels in PFA-fixed cells (Fig. 26).

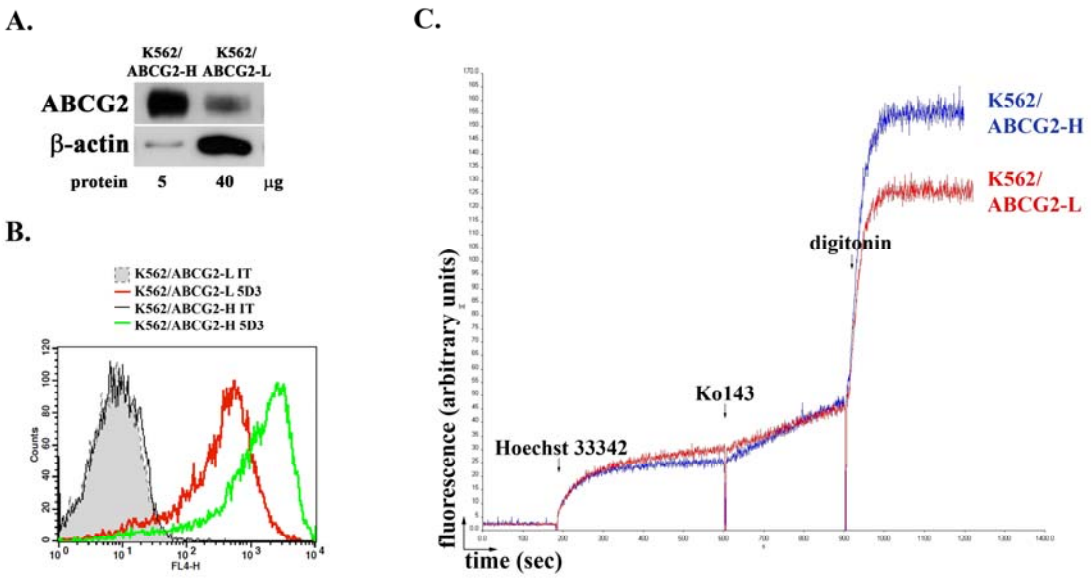

Figure 27. Detection and functional consequences of decreased plasma membrane ABCG2 levels. ***(A)*** *Total ABCG2 protein levels of K562/ABCG2 cells stably expressing high (K562/ABCG2-H) or low (K562/ABCG2-L) amounts of the transporter were evaluated by Western blot using the BXP-21 antibody. Beta-actin was stained to check sample loading. A representative blot of three independent experiments is shown.* ***(B)*** *Cell surface expression of ABCG2 in K562/ABCG2-L or K562/ABCG2-H cells were measured by fixation with paraformaldehyde and labeling with IgG2b (isotype control, IT) or 5D3 primary antibodies and Alexa-Fluor-647-conjugated secondary antibodies. Samples were analyzed by flow cytometry. A representative histogram of two independent experiments is shown.* ***(C)*** *Specific ABCG2 function in K562/ABCG2-L or K562/ABCG2-H cells was followed by real-time spectrofluorometric detection of the cellular accumulation of the ABCG2 substrate dye, Hoechst 33342. A representative image of at least three independent measurements is shown.*

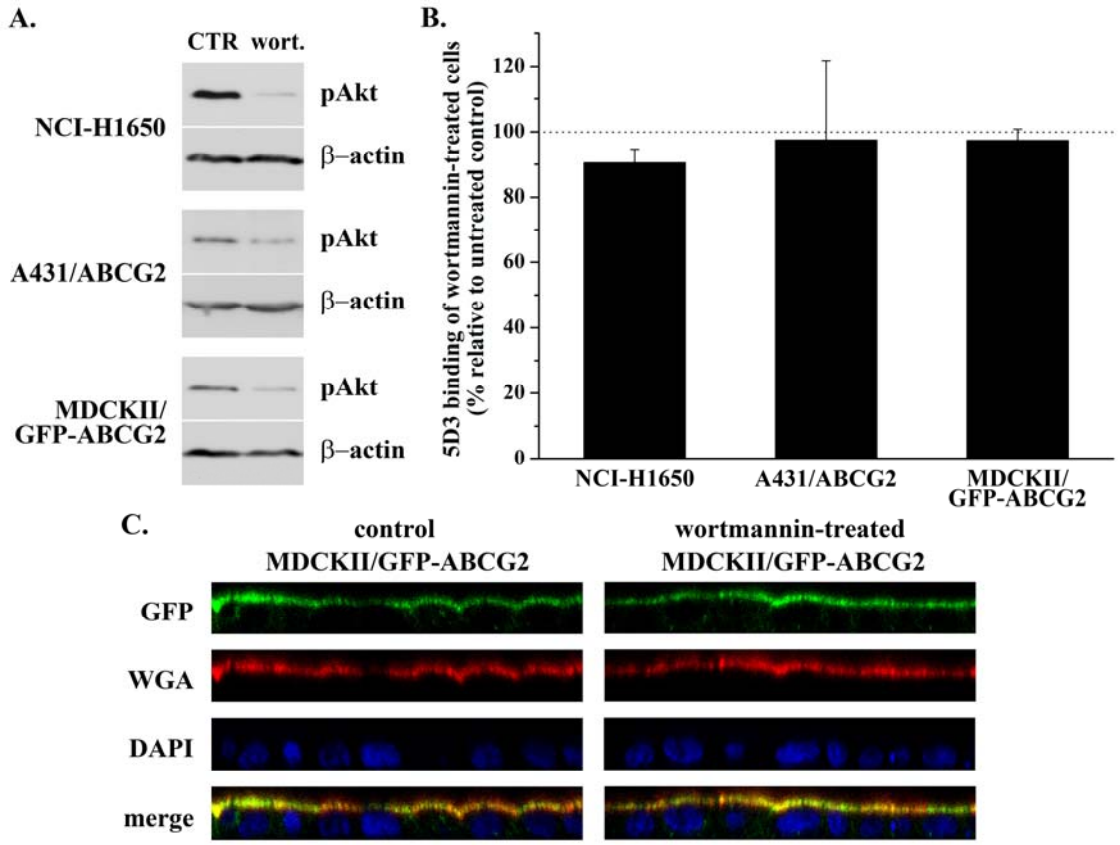

Figure 28. Localization of ABCG2 in wortmannin-treated NCI-H1650, A431/ABCG2 and MDCKII/GFP-ABCG2 cells. *Cells were treated with 100 nM wortmannin for 90 minutes at 37 °C.* ***(A)*** *Phosphorylation of Akt at Ser473 was probed by Western blot. Beta-actin was stained to check sample loading. Representative blots of two independent experiments are shown.* ***(B)*** *$2.5*10^5$ untreated control and wortmannin-treated cells were fixed with paraformaldehyde (PFA), and were labeled with 5D3 or IgG2b primary antibodies and Alexa-Fluor-647-conjugated secondary antibodies. Samples were analyzed by flow cytometry. Geometric mean values of the histograms representing 5D3-labeled cells were corrected with those of IgG2b-labeled cells, and data were plotted as the percentage of 5D3 binding measured in untreated cells (100%). Mean ± SD values of three independent experiments are shown.* ***(C)*** *Control and wortmannin-treated polarized MDCKII/GFP-ABCG2 cells were fixed with PFA and were stained with the apical marker Alexa-Fluor-633-conjugated WGA and the nuclear stain DAPI. Subcellular distribution of GFP-ABCG2 was evaluated by confocal microscopy. Representative images of three independent experiments are shown.*

Next, K562 cells stably expressing high (K562/ABCG2-H) or low (K562/ABCG2-L) amounts of ABCG2 (Fig. 27A) were fixed with PFA and then were labeled with 5D3. Flow cytometry analysis of the K562/ABCG2-H and K562/ABCG2-L samples again revealed that 5D3 labeling of PFA-fixed cells quantitatively reflected the amount of the ABCG2 transporter in the plasma membrane (Fig. 27B). Notably, K562/ABCG2-L cells

which showed approximately one order of magnitude decrease in cell surface ABCG2 levels as compared to K562/ABCG2-H cells still showed remarkable ABCG2-mediated Hoechst 33342 transport capacity (Fig. 27C).

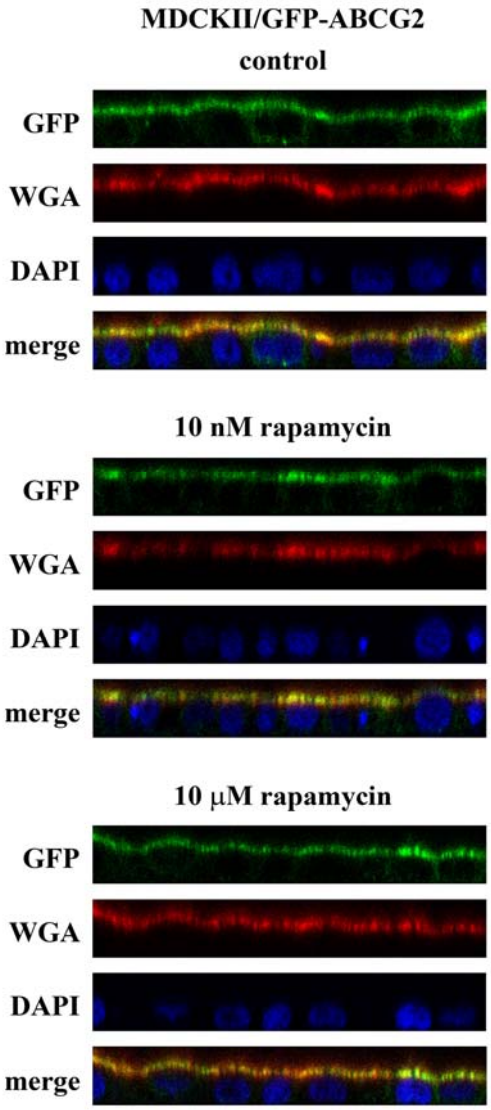

Figure 29. Subcellular distribution of GFP-ABCG2 in rapamycin-treated polarized MDCKII/GFP-ABCG2 cells. *Polarized MDCKII/GFP-ABCG2 cells were untreated or treated with 10 nM or 10 μM rapamycin for 90 minutes at 37 °C. Cells were fixed with paraformaldehyde and were stained with the apical marker Alexa-Fluor-633-conjugated WGA and the nuclear stain DAPI. Subcellular distribution of GFP-ABCG2 was evaluated by confocal microscopy. Representative images of three independent experiments are shown.*

In order to investigate whether PI3K/Akt/mTOR signaling is involved in the rapid regulation of the plasma membrane localization of ABCG2, NCI-H1650 cells showing endogenous ABCG2 expression (Fig. 21A-B), or A431/ABCG2 cells engineered to overexpress ABCG2 and MDCKII/GFP-ABCG2 (Fig. 16B-C) were exposed to the PI3K inhibitor wortmannin for 90 minutes at 37 °C. Wortmannin was used because it does not

interact with ABCG2; therefore, PI3K/Akt signaling could be manipulated without direct functional modulation of the transporter. Under these conditions, wortmannin could efficiently prevent phosphorylation of Akt (Fig. 28A). Cells were fixed with PFA, and were then labeled with 5D3. As shown in Fig. 28B, wortmannin treatment did not significantly decrease 5D3 binding, therefore cell surface expression of ABCG2 in any of the cell lines tested, as compared to the untreated cells (100 %). In addition, treatment with either 10 μM LY294002 or 1 μM Ko143 for 90 minutes at 37 °C did not reduce the 5D3 binding capacity and the corresponding cell surface levels of ABCG2 in any of the cell lines applied (data not shown). Moreover, we did not find any rapid effect of the investigated EGFR inhibitors on the plasma membrane insertion of ABCG2 either (data not shown).

As a second approach, subcellular distribution of GFP-ABCG2 was followed in polarized MDCKII/GFP-ABCG2 cells by confocal microscopy (Fig. 28C). GFP-ABCG2 co-localized with the apical marker WGA in untreated cells. Major apical localization and subcellular distribution of GFP-ABCG2 was not altered by wortmannin treatment. Brief exposure of MDCKII/GFP-ABCG2 cells to the downstream mTOR inhibitor rapamycin applied at the experimentally relevant 10 nM concentration (which does not inhibit ABCG2) or 10 μM concentration (which inhibits ABCG2) did not alter subcellular distribution of GFP-ABCG2 either (Fig. 29).

In summary, in the model cells used we found no impact of pharmacological PI3K/Akt/mTOR inhibitor treatment on plasma membrane localization of ABCG2. Pharmacological inhibition of EGFR upstream of the PI3K/Akt/mTOR signaling axis did not rapidly regulate cell surface levels of ABCG2 either. On the other hand, we provide biochemical evidence that ABCG2 is directly inhibited by LY294002 and rapamycin. Direct functional modulation of the transporter by these compounds should be taken into consideration when regulation of ABCG2 and a subsequent reversal of drug resistance by PI3K/Akt/mTOR signaling is investigated using these pharmacological signal transduction inhibitors.

6. DISCUSSION

The ABCG2 efflux transporter is expressed in cancer cells and putative cancer stem cells (CSCs) and is responsible for conferring multiple drug resistance. Being expressed at pharmacological tissue barriers, such as the gut, the liver, the kidney, the blood-brain barrier or the blood-testis barrier, ABCG2 also has a major influence on the absorption, distribution, metabolism, excretion and toxicity (ADME-Tox) of orally administered drugs. The constitutive tyrosine kinase activity of Bcr-Abl or the Epidermal Growth Factor Receptor (EGFR) plays a causal role in the oncogenesis of chronic myeloid leukemia (CML) and various solid tumors, respectively. The Bcr-Abl and EGFR kinase enzymes are therefore intensively pursued as molecular drug targets. Currently, several small molecule inhibitors are available at the clinic for the specific targeting and elimination of kinase-addicted cancer cells. Clinically available inhibitors of Bcr-Abl include imatinib, and the second generation drugs nilotinib, dasatinib and bosutinib indicated in the treatment of CML (178,179) (Table 3). The EGFR inhibitor compounds gefitinib, vandetanib, pelitinib and neratinib are presently under clinical evaluation or use for treating a histologically diverse range of solid tumors, including lung cancer (183), breast cancer (187-189) and colorectal cancer (190) (Table 4). Similarly to conventional chemotherapeutics, resistance to targeted small molecule inhibitors represents a major impediment to successful cancer therapy. Together with genetic alterations of the target molecule or engagement of redundant signaling pathways, the ABCG2 multidrug transporter has also been implicated in the emergence of resistance against targeted drugs. Here, we provided detailed biochemical characterization regarding the interaction of ABCG2 with the aforementioned small molecule inhibitors of Bcr-Abl and EGFR. We analyzed whether ABCG2 modifies the intracellular action of these inhibitors; and whether the inhibitors are capable of inhibiting the function of the transporter. Given that ABCG2 is expressed on the targeted cancer cells or putative CSCs and also at pharmacological tissue barriers, interaction of these drugs with ABCG2 might significantly modify both the cellular anti-cancer efficiency at the target tumor site and the systemic biodistribution of the compounds *in vivo*. Importantly, as ABCG2 is currently considered to be a key contributor to drug resistance of CSCs, it is also reasonable to speculate that drugs which are not effluxed by ABCG2, or drugs which

inhibit the function of the transporter, may be efficient in chemo-sensitization and also in eradication of the drug resistant CSC compartment.

In order to study the cellular effects of the small molecule inhibitors of Bcr-Abl, we generated and characterized a CML-derived Bcr-Abl+ K562 cellular model system, which stably expresses ABCG2 (Fig. 5-6). Using these model cells, we showed that ABCG2 prevented imatinib-induced cell death and erythroid differentiation in K562 cells (Fig. 7-8), confirming the findings of others (78,196,198) suggesting that imatinib is a substrate for the ABCG2 transporter. Similarly, ABCG2 conferred cellular resistance to the second generation Bcr-Abl inhibitors nilotinib and dasatinib that could be fully reversed by administration of the specific ABCG2 inhibitor FTC (Fig. 9). In contrast, the cellular toxicity of bosutinib was unaltered by the presence of ABCG2 (Fig. 9). Analysis of the phosphorylation of Bcr-Abl at Tyr177 in drug-treated K562 and K562/ABCG2 cells revealed that in the presence of ABCG2 imatinib, nilotinib and dasatinib did not reach their intracellular target kinase and therefore could not inhibit its autophosphorylation (Fig. 10). In contrast, when K562/ABCG2 cells were simultaneously exposed to one of these Bcr-Abl inhibitors and FTC, decreased phosphorylation and an accompanying decrease in the levels of the Bcr-Abl kinase could be detected, similarly to those measured in parental K562 cells (Fig. 10-11). Levels of phosphorylated and total Bcr-Abl proteins were similar in K562 and K562/ABCG2 cells treated with bosutinib alone or in combination with FTC (Fig. 10-11). These results strongly suggested that ABCG2 restricts the intracellular efficiency of imatinib, nilotinib and dasatinib by active efflux, whereas rendered it unlikely that ABCG2 could reduce the intracellular concentration of bosutinib below the drug efficacy threshold in the applied concentration range. In lack of fluorescently or radioactively labeled Bcr-Abl inhibitors, we set out to develop a transport measurement protocol that relies on HPLC-MS based detection of the unlabeled drugs. Using this novel approach, we proved that ABCG2 efficiently transported nilotinib and dasatinib, while bosutinib proved not to be susceptible to ABCG2-mediated recognition and efflux (Fig. 12). Applying a similar experimental setup, in another study we could also demonstrate the ABCG2-mediated active transport of imatinib (223).

Notably, modulation of the ATPase activity of ABCG2 by the Bcr-Abl inhibitors measured in Sf9 insect cells could not precisely predict whether the drug was an ABCG2 substrate. ABCG2 expressed in insect cells exhibits a relatively high ATPase activity in the absence of drugs, which had previously been believed to represent either an uncoupled state of the transporter or its ATPase stimulation by an unknown substrate resident in the insect membrane (41). An uncoupled ATPase activity was also suggested to be important for the promiscuous drug recognition capability of multidrug transporters (236). Studies performed on purified and reconstituted functional ABCG2 proposed that the basal ABCG2 ATPase is dependent on the lipid environment and especially on the presence of cholesterol but might not be coupled to any transport activity (237). It is widely accepted that drugs which can stimulate the relatively high ABCG2 ATPase in Sf9 insect membrane fragments are most probably transported substrates, as was seen in the case of nilotinib (Fig. 13). However, known ABCG2 substrates most probably transported at a lower rate have been described to decrease or not affect the basal ATPase activity of the transporter, as was also detected in our study in the case of imatinib and dasatinib, respectively (Fig. 4, 13). It is therefore important to highlight, that a combination of *in vitro* measurements are required to determine whether a drug interacts with ABCG2 and to further distinguish between substrates and inhibitors of the transporter.

The cellular efficiency of gefitinib and the second generation inhibitors of EGFR were investigated in A431 epidermoid carcinoma cells which rely on mitogenic and survival signaling mediated by the overexpressed EGFR and therefore are sensitive to inhibition of the receptor. A431 cells stably expressing ABCG2 had been generated previously, and were applied to study the interaction of gefitinib and the transporter (203) (Fig. 16-17). Here, we showed that similarly to gefitinib, ABCG2 conferred resistance to pelitinib by limiting the access of the drugs (most probably by means of active efflux) to the intracellular kinase domain of EGFR and therefore preventing inhibition of EGFR autophosphorylation at Tyr1068 (Table 5, Fig. 19). Specific involvement of ABCG2 in the cellular resistance to gefitinib and pelitinib was verified by re-sensitization with FTC (Table 5). We also measured slightly increased resistance to neratinib in A431/ABCG2 cells; however, it was not reversible with FTC (Table 5). It is possible, that

A431/ABCG2 cells acquired genetic alterations during the retroviral delivery of ABCG2, leading to the appearance of additional resistance mechanisms. Nevertheless the impact of ABCG2 could clearly be distinguished by administration of its specific inhibitor. Therefore, we concluded that susceptibility of A431 cells to vandetanib and neratinib was not influenced by the presence of ABCG2 (Table 5, Fig. 19). In case of the EGFR inhibitors, the ABCG2 ATPase data correlated with the results obtained in model cells, as we measured pronounced stimulation of the basal ABCG2 ATPase activity by gefitinib and pelitinib (Fig. 18A), which were also strongly suggested to be transported substrates of ABCG2 by the cellular toxicity (Table 5) and EGFR phosphorylation analyses (Fig. 19A-B).

In another series of experiments, we aimed to determine whether the small molecule kinase inhibitors could interfere with the function of ABCG2. In the case of nilotinib, dasatinib and bosutinib, we measured a concentration dependent inhibitory effect on the ABCG2-mediated transport of Hoechst 33342 (Fig. 14). Gefitinib, pelitinib, vandetanib and neratinib also inhibited ABCG2 function in a concentration-dependent manner. Besides inhibition of the quercetin-stimulated ABCG2 ATPase activity (Fig. 18B), we also detected increased 5D3 binding affinity of ABCG2 upon EGFR inhibitor treatment (Table 6), which corresponds to the inhibited conformation of the transporter (215,223). Accordingly, we showed that at relatively high concentrations, all four EGFR inhibitors were capable of inhibiting ABCG2-mediated transport of Hoechst 33342 (Table 6) and mitoxantrone (Fig. 20). Our cellular toxicity data strongly suggest that nilotinib, dasatinib, gefitinib and pelitinib are transported substrates of ABCG2 (Fig. 9A-B, Table 5); therefore, blockade of ABCG2-mediated efflux by these compounds most probably occur via competitive inhibition. In the case of bosutinib, vandetanib and neratinib, additional direct transport or kinetic measurements involving various drug doses would be needed to determine whether these compounds are also competitive inhibitors of the transporter. The ATPase and 5D3 binding data strongly support that ABCG2 is directly inhibited by these drugs. In summary, all the herein investigated small molecule kinase inhibitors display potency to enhance accumulation and thereby restore cellular sensitivity toward ABCG2 substrate cytotoxic drugs by directly blocking ABCG2 function. This finding highlights the possible clinical benefit of combining targeted Bcr-

Abl or EGFR inhibitor-based therapies with conventional chemotherapeutic drugs that are substrates for ABCG2.

Treatment-induced enhancement of functional ABCG2 expression could hamper the therapeutic efficacy of administered drugs. Therefore, we also investigated whether functional ABCG2 expression was altered in gefitinib-resistant NCI-H1650 G7 cells of non-small cell lung cancer (NSCLC) origin (Fig. 21). Gefitinib-resistant subclones of NCI-H1650 cells were reported to be devoid of secondary point mutations in EGFR and also lacked additional mutations in other oncogenes such as ErbB2, PTEN, KRAS or p53 (214). Interestingly, we found enhanced ABCG2 protein expression in 3 out of 5 gefitinib-resistant NCI-H1650 clones, and a corresponding resistance to an additional cytotoxic drug, mitoxantrone (Fig. 21). Although, only one case report described association of ABCG2 expression and acquired gefitinib-resistance in an NSCLC patient (125), our *in vitro* data point out, that in addition to acquired alterations in the target kinase or engagement of redundant signaling pathways, the involvement of ABCG2 in acquired EGFR inhibitor resistance and a corresponding emergence of a MDR phenotype could also be clinically relevant. Additionally, these cells might also serve as good models to investigate the molecular mechanism of gefitinib-mediated upregulation of ABCG2. Enhancement of ABCG2 protein expression by nuclear EGFR in gefitinib-resistant A431 cells has recently been reported (238); therefore it is tempting to speculate that a similar mechanism is responsible for ABCG2 upregulation in NCI-H1650 G7 cells, which displayed increased internalization of ligand-activated EGFR (214). On the other hand, based on the chemoimmunity concept, gefitinib could also be recognized as a xenobiotic by the cellular detoxifying network, which might lead to ABCG2 upregulation independently from simultaneous alterations in EGFR signaling (46,194).

Finally, we addressed the issue concerning the rapid regulation of the cell surface localization of ABCG2 by the PI3K/Akt signaling axis. Inhibition of Akt signaling was reported to result in rapid translocation of ABCG2 from the plasma membrane to intracellular compartments (79-84), which has also been associated with attenuated ABCG2 function (79,81,83,84) and subsequent reversal of drug resistance caused by the transporter (83,84). Nevertheless, opposing data regarding the involvement of the PI3K/Akt axis and the downstream mTOR kinase in the regulation of the plasma

membrane localization of ABCG2 has also been published (78,81). Here, using the 5D3 antibody that recognizes an external epitope of ABCG2 or the fluorescently tagged GFP-ABCG2 molecule, we demonstrated that pharmacological inhibition of the PI3K/Akt axis, or EGFR and mTOR upstream and downstream of PI3K/Akt, respectively, did not alter the cell surface localization and subcellular distribution of ABCG2 (Fig. 28-29). Interestingly, in the course of these studies we found that besides inhibiting their respective target kinases, the pharmacological PI3K inhibitor LY294002 and the downstream mTOR kinase inhibitor rapamycin also directly inhibit ABCG2 function (Table 7, Fig. 22, 25). In contrast, wortmannin, another commonly used pharmacological inhibitor of PI3K does not interact with the transporter. Therefore, we suggested that direct functional modulation of ABCG2 should also be taken into consideration when pharmacological inhibitors are applied to dissect the specific role of PI3K/Akt/mTOR signaling in the MDR phenomenon. A report, which appeared online exactly the same time as our paper was accepted, presented similar findings; and proposed that the versatile PI3K and ABCG2 inhibitory potential of LY294002 should be exploited to design novel therapeutic strategies for the targeting of drug resistant cancer cells or cancer stem cells which rely on Akt signaling for survival (239).

In summary, we found that the herein investigated small molecule Bcr-Abl or EGFR inhibitors all interact with ABCG2. If local drug concentrations are low (due to poor bioavailability, or the size, stage, vascularization and poor penetration of the solid tumor), ABCG2 can confer imatinib, nilotinib, dasatinib, gefitinib or pelitinib resistance; however, anti-cancer efficiency of bosutinib, neratinib and vandetanib will most probably not be restricted by ABCG2. On the other hand, in ABCG2-expressing tissues where local drug concentrations are high (either at pharmacological tissue barriers or in tumor tissues where drug penetration is not limited), all of the investigated drugs can inhibit ABCG2 function and promote improved systemic distribution, intracellular accumulation and cytotoxic action of simultaneously administered ABCG2 substrate chemotherapeutics, thereby reversing multidrug resistance. These phenomena might significantly influence Bcr-Abl or EGFR inhibitor treatment outcomes in case of kinase-addicted cancer cells or putative cancer stem cells with inherent or acquired ABCG2 expression.

7. SUMMARY

Human ABCG2 is a plasma membrane glycoprotein that provides physiological tissue protection against xenobiotics. ABCG2 influences the biodistribution of drugs through pharmacological tissue barriers, and confers multidrug resistance (MDR) to cancer cells. ABCG2 is the molecular determinant of the side population (SP) that is characteristically enriched in normal or cancer stem cells. Cancer cells often rely on unregulated kinase signaling, and small molecule kinase inhibitors are clinically applied to specifically target and eliminate kinase-addicted malignant cells. The constitutive tyrosine kinase activity of Bcr-Abl and Epidermal Growth Factor Receptor (EGFR) are required for the oncogenesis of chronic myeloid leukemia (CML) and various solid tumors, respectively. Here, we provided detailed biochemical characterization regarding the interaction of ABCG2 with clinically relevant small molecule inhibitors of Bcr-Abl and EGFR. We found that in Bcr-Abl+ K562 cells, ABCG2 restricted the intracellular cytotoxic action of imatinib, nilotinib and dasatinib by limiting their intracellular access to their target kinase Bcr-Abl. In K562 cells, the cellular toxicity of bosutinib was unaltered by the presence of ABCG2. We proved that in contrast to bosutinib, ABCG2 actively transported nilotinib and dasatinib. In EGFR+ A431 cells, ABCG2 conferred cellular resistance to gefitinib and pelitinib, whereas it did not modify the intracellular action of vandetanib and neratinib. The molecular basis of resistance in A431/ABCG2 cells was the highly phosphorylated EGFR even in the presence of gefitinib and pelitinib. At higher doses, all of the investigated Bcr-Abl and EGFR inhibitors blocked ABCG2 function, thereby promoting accumulation of the ABCG2 substrates Hoechst 33342 and mitoxantrone. In addition, we demonstrated that gefitinib exposure enhanced the cell surface expression of ABCG2, whereas inhibition of the EGFR/PI3K/Akt/mTOR signaling axis did not result in rapid internalization of the transporter. In the course of these studies, we also found that LY294002 and rapamycin, inhibitors of the PI3-kinase and mTOR kinase respectively, directly inhibit the function of ABCG2. Our results should provide useful information about the therapeutic applicability of the clinically relevant drugs. Moreover, the finding that the investigated small molecule kinase inhibitors efficiently block ABCG2 function may help to design novel drug-combination therapeutic strategies.

8. ÖSSZEFOGLALÁS

A humán ABCG2 egy plazmamembrán glikoprotein, amely fontos fiziológiás szerepet játszik a szervezet idegen anyagokkal szembeni védelmében. A farmakológiai barriereken kifejeződő ABCG2 befolyásolja a gyógyszerek szöveti eloszlását, túltermelődése pedig a rákos sejtek multidrog rezisztencia fenotípusának (MDR) kialakulásához vezet. Az ABCG2 funkciója alapján definiálható a normál és tumorszövetekből is elkülöníthető, jellemzően őssejtekben illetve tumor őssejtekben gazdag ún. side populáció (SP). Tumorsejtekben gyakran megfigyelhető bizonyos kináz enzimek szabályozatlan működése, ezért a klinikumban számos kis molekulasúlyú kináz inhibitor vegyületet alkalmaznak a kinázfüggő rosszindulatú sejtek célzott elpusztítására. A Bcr-Abl fehérje konstitutív tirozin kináz aktivitása a krónikus mieloid leukémia (CML), míg az Epidermális Növekedési Faktor Receptor (EGFR) szabályozatlan tirozin kináz aktivitása számos szolid tumor kialakításában játszik kulcsszerepet. Munkánkban biokémiai módszerek segítségével részletesen jellemeztük az ABCG2 kölcsönhatását a Bcr-Abl illetve az EGFR klinikumban alkalmazott kis molekulasúlyú gátlószereivel. Bcr-Abl+ K562 sejtekben az ABCG2 csökkentette az imatinib, a nilotinib és a dasatinib sejten belüli toxikus hatását azáltal, hogy megakadályozta a Bcr-Abl célfehérjére kifejtett gátló hatásukat. Az ABCG2 nem befolyásolta a bosutinib K562 sejtekben kifejtett sejtpusztító hatását. Igazoltuk, hogy a bosutinibbel ellentétben a nilotinib és a dasatinib az ABCG2 transzportált szubsztrátja. EGFR+ A431 sejtekben az ABCG2 gefitinib és pelitinib rezisztenciát okozott, míg a vandetanib és a neratinib toxikus hatásától nem védte meg a sejteket. A rezisztencia hátterében A431/ABCG2 sejtekben a gefitinib és pelitinib jelenlétében is kimutatható fokozott EGFR foszforiláció állt. Magasabb koncentrációkban az összes vizsgált vegyület gátolta az ABCG2 funkcióját, elősegítve az ABCG2 szubsztrát Hoechst 33342 és mitoxantron akkumulációját. Bemutattuk, hogy gefitinib kezelés hatására megnő az ABCG2 kifejeződése a sejtfelszínen, ugyanakkor az EGFR/PI3K/Akt/mTOR jelpálya gátlása nem vezet a fehérje gyors internalizációjához. Munkánk során igazoltuk, hogy a PI3 kináz gátló LY294002 és az mTOR kináz gátló rapamycin gátolja az ABCG2 fehérje működését is. Eredményeink hasznosak lehetnek a vegyületek terápiás alkalmazhatóságának felmérésében, illetve az ABCG2 fehérje gátlásán keresztül hatékonyabbnak ígérkező kombinációs kezelések kidolgozásában.

9. PUBLICATIONS

9.1. Publications related to the subject of the thesis

9.1.1. Research papers

Hegedüs C, Özvegy-Laczka C, Apáti A, Magócsi M, Német K, Őrfi L, Kéri G, Katona M, Takáts Z, Váradi A, Szakács G, Sarkadi B. Interaction of nilotinib, dasatinib and bosutinib with ABCB1 and ABCG2: implications for altered anti-cancer effects and pharmacological properties. Br J Pharmacol. 2009 Oct;158(4):1153-64.

Hegedüs C*, Truta-Feles K*, Antalffy G, Brózik A, Kasza I, Német K, Orbán TI, Özvegy-Laczka C, Váradi A, Sarkadi B. PI3-kinase and mTOR inhibitors differently modulate the function of the ABCG2 multidrug transporter. Biochem Biophys Res Commun. 2012 Apr 20;420(4):869-74. (* joint first authors)

Hegedüs C*, Truta-Feles K*, Antalffy G, Várady G, Német K, Özvegy-Laczka C, Kéri G, Őrfi L, Szakács G, Settleman J, Váradi A, Sarkadi B. Interaction of the EGFR inhibitors gefitinib, vandetanib, pelitinib and neratinib with the ABCG2 multidrug transporter: Implications for the emergence and reversal of cancer drug resistance. Biochem Pharmacol. 2012 Aug 1;84(3):260-7. (* joint first authors)

9.1.2. Reviews

Hegedüs C, Özvegy-Laczka C, Szakács G, Sarkadi B. Interaction of ABC multidrug transporters with anticancer protein kinase inhibitors: substrates and/or inhibitors? Curr Cancer Drug Targets. 2009 May;9(3):252-72.

Brózik A, **Hegedüs C**, Erdei Z, Hegedűs T, Özvegy-Laczka C, Szakács G, Sarkadi B. Tyrosine kinase inhibitors as modulators of ATP binding cassette multidrug transporters: substrates, chemosensitizers or inducers of acquired multidrug resistance? Expert Opin Drug Metab Toxicol. 2011 May;7(5):623-42.

9.2. Other publications

Brózik A, Casey NP, **Hegedüs C**, Bors A, Kozma A, Andrikovics H, Geiszt M, Német K, Magócsi M. Reduction of Bcr-Abl function leads to erythroid differentiation of K562 cells via downregulation of ERK. Ann N Y Acad Sci. 2006 Dec;1090:344-54.

Özvegy-Laczka C, Laczkó R, **Hegedüs C**, Litman T, Várady G, Goda K, Hegedűs T, Dokholyan NV, Sorrentino BP, Váradi A, Sarkadi B. Interaction with the 5D3 monoclonal antibody is regulated by intramolecular rearrangements but not by covalent dimer formation of the human ABCG2 multidrug transporter. J Biol Chem. 2008 Sep 19;283(38):26059-70.

Hegedüs C, Szakács G, Homolya L, Orbán TI, Telbisz A, Jani M, Sarkadi B. Ins and outs of the ABCG2 multidrug transporter: an update on in vitro functional assays. Adv Drug Deliv Rev. 2009 Jan 31;61(1):47-56.

Telbisz A, **Hegedüs C**, Özvegy-Laczka C, Goda K, Várady G, Takáts Z, Szabó E, Sorrentino BP, Váradi A, Sarkadi B. Antibody binding shift assay for rapid screening of drug interactions with the human ABCG2 multidrug transporter. Eur J Pharm Sci. 2012 Jan 23;45(1-2):101-9.

10. ACKNOWLEDGEMENTS

First, I wish to express my gratitude to my supervisors, **Csilla Laczka** and **Balázs Sarkadi**, who generously shared their time and experience with me to help navigating in the exciting field of ABC transporters. Both of them were always open to answer my questions and discuss my ideas, and were critical and supportive at the same time. I am deeply indebted to them for readily helping me even with personal matters.

I would like to thank all members of the ABCG2 Laboratory for creating a motivating and pleasant working atmosphere. All the valuable advice of **Ágnes Telbisz** is greatly appreciated. I am happy that I could have the opportunity to run a joint project with **Krisztina Truta-Feles**, whose support and friendship also helped me through the harder times. I would like to thank all the precise work of our excellent assistants **Zsuzsanna Andrási** and **Éva Krizsán**, who provide the ABCG2 Laboratory with a smooth and solid technical background. The technical help of **Katalin Mihály** is also greatly appreciated.

I would like to thank **György Kéri** and **László Őrfi** for providing the small molecule kinase inhibitor compounds for us.

I am thankful to **Judit Kis** and **Gyöngyi Bézsenyi** for the encouraging and reassuring talks and personal support and also for their valuable help regarding laboratory issues.

I feel grateful that I could have the opportunity to do some work with **Gergely Szakács**, and that I could get to know his exceptional enthusiasm for scientific questions and his unique way of thinking.

I also wish to thank **Mária Magócsi, Ágota Apáti, Anna Brózik** and **Zoltán Ondrejó**, members of the former Signal Transduction Laboratory, for introducing me the basis of scientific thinking and laboratory work.

I am thankful for all the former and present members of the **Isotope/Molecular Cell Biology/Biomembrane Department** and also for **András Váradi** and members of his group at the Institue of Enzymology, for the creative, inspiring and friendly atmosphere.

I wish to thank my **Parents** and my **Family** for their continuous support and encouragement without which this work could not have been completed. I am grateful to my husband, **Géza Antalffy** for his love, endless patience, wise criticisms and enduring sincerity. I wish to thank my daughter **Lili** that with her pure existence she magically multiplied my energies and taught me completely new dimensions of time.

11. REFERENCES

1. Welch, A.D. (1959) The problem of drug resistance in cancer chemotherapy. *Cancer research*, **19**, 359-371.
2. Gottesman, M.M. (2002) Mechanisms of cancer drug resistance. *Annu Rev Med*, **53**, 615-627.
3. Gottesman, M.M., Fojo, T. and Bates, S.E. (2002) Multidrug resistance in cancer: role of ATP-dependent transporters. *Nature reviews. Cancer*, **2**, 48-58.
4. Dano, K. (1973) Active outward transport of daunomycin in resistant Ehrlich ascites tumor cells. *Biochimica et biophysica acta*, **323**, 466-483.
5. Ling, V. and Thompson, L.H. (1974) Reduced permeability in CHO cells as a mechanism of resistance to colchicine. *Journal of cellular physiology*, **83**, 103-116.
6. Bech-Hansen, N.T., Till, J.E. and Ling, V. (1976) Pleiotropic phenotype of colchicine-resistant CHO cells: cross-resistance and collateral sensitivity. *J Cell Physiol*, **88**, 23-31.
7. See, Y.P., Carlsen, S.A., Till, J.E. and Ling, V. (1974) Increased drug permeability in Chinese hamster ovary cells in the presence of cyanide. *Biochimica et biophysica acta*, **373**, 242-252.
8. Juliano, R.L. and Ling, V. (1976) A surface glycoprotein modulating drug permeability in Chinese hamster ovary cell mutants. *Biochim Biophys Acta*, **455**, 152-162.
9. Kartner, N., Shales, M., Riordan, J.R. and Ling, V. (1983) Daunorubicin-resistant Chinese hamster ovary cells expressing multidrug resistance and a cell-surface P-glycoprotein. *Cancer research*, **43**, 4413-4419.
10. Kartner, N., Riordan, J.R. and Ling, V. (1983) Cell surface P-glycoprotein associated with multidrug resistance in mammalian cell lines. *Science*, **221**, 1285-1288.
11. Kartner, N., Evernden-Porelle, D., Bradley, G. and Ling, V. (1985) Detection of P-glycoprotein in multidrug-resistant cell lines by monoclonal antibodies. *Nature*, **316**, 820-823.
12. Bell, D.R., Gerlach, J.H., Kartner, N., Buick, R.N. and Ling, V. (1985) Detection of P-glycoprotein in ovarian cancer: a molecular marker associated with multidrug resistance. *J Clin Oncol*, **3**, 311-315.
13. Riordan, J.R., Deuchars, K., Kartner, N., Alon, N., Trent, J. and Ling, V. (1985) Amplification of P-glycoprotein genes in multidrug-resistant mammalian cell lines. *Nature*, **316**, 817-819.
14. Shen, D.W., Fojo, A., Chin, J.E., Roninson, I.B., Richert, N., Pastan, I. and Gottesman, M.M. (1986) Human multidrug-resistant cell lines: increased mdr1 expression can precede gene amplification. *Science*, **232**, 643-645.
15. Higgins, C.F., Hiles, I.D., Salmond, G.P., Gill, D.R., Downie, J.A., Evans, I.J., Holland, I.B., Gray, L., Buckel, S.D., Bell, A.W. *et al.* (1986) A family of related ATP-binding subunits coupled to many distinct biological processes in bacteria. *Nature*, **323**, 448-450.

16. Roninson, I.B., Chin, J.E., Choi, K.G., Gros, P., Housman, D.E., Fojo, A., Shen, D.W., Gottesman, M.M. and Pastan, I. (1986) Isolation of human mdr DNA sequences amplified in multidrug-resistant KB carcinoma cells. *Proceedings of the National Academy of Sciences of the United States of America*, **83**, 4538-4542.
17. Gros, P., Ben Neriah, Y.B., Croop, J.M. and Housman, D.E. (1986) Isolation and expression of a complementary DNA that confers multidrug resistance. *Nature*, **323**, 728-731.
18. Chen, C.J., Chin, J.E., Ueda, K., Clark, D.P., Pastan, I., Gottesman, M.M. and Roninson, I.B. (1986) Internal duplication and homology with bacterial transport proteins in the mdr1 (P-glycoprotein) gene from multidrug-resistant human cells. *Cell*, **47**, 381-389.
19. Ueda, K., Cornwell, M.M., Gottesman, M.M., Pastan, I., Roninson, I.B., Ling, V. and Riordan, J.R. (1986) The mdr1 gene, responsible for multidrug-resistance, codes for P-glycoprotein. *Biochemical and biophysical research communications*, **141**, 956-962.
20. Ueda, K., Cardarelli, C., Gottesman, M.M. and Pastan, I. (1987) Expression of a full-length cDNA for the human "MDR1" gene confers resistance to colchicine, doxorubicin, and vinblastine. *Proceedings of the National Academy of Sciences of the United States of America*, **84**, 3004-3008.
21. Gerlach, J.H., Endicott, J.A., Juranka, P.F., Henderson, G., Sarangi, F., Deuchars, K.L. and Ling, V. (1986) Homology between P-glycoprotein and a bacterial haemolysin transport protein suggests a model for multidrug resistance. *Nature*, **324**, 485-489.
22. Gros, P., Croop, J. and Housman, D. (1986) Mammalian multidrug resistance gene: complete cDNA sequence indicates strong homology to bacterial transport proteins. *Cell*, **47**, 371-380.
23. McGrath, T. and Center, M.S. (1988) Mechanisms of multidrug resistance in HL60 cells: evidence that a surface membrane protein distinct from P-glycoprotein contributes to reduced cellular accumulation of drug. *Cancer research*, **48**, 3959-3963.
24. Cole, S.P., Bhardwaj, G., Gerlach, J.H., Mackie, J.E., Grant, C.E., Almquist, K.C., Stewart, A.J., Kurz, E.U., Duncan, A.M. and Deeley, R.G. (1992) Overexpression of a transporter gene in a multidrug-resistant human lung cancer cell line. *Science*, **258**, 1650-1654.
25. Cole, S.P., Sparks, K.E., Fraser, K., Loe, D.W., Grant, C.E., Wilson, G.M. and Deeley, R.G. (1994) Pharmacological characterization of multidrug resistant MRP-transfected human tumor cells. *Cancer research*, **54**, 5902-5910.
26. Chen, Y.N., Mickley, L.A., Schwartz, A.M., Acton, E.M., Hwang, J.L. and Fojo, A.T. (1990) Characterization of adriamycin-resistant human breast cancer cells which display overexpression of a novel resistance-related membrane protein. *J Biol Chem*, **265**, 10073-10080.
27. Lee, J.S., Scala, S., Matsumoto, Y., Dickstein, B., Robey, R., Zhan, Z., Altenberg, G. and Bates, S.E. (1997) Reduced drug accumulation and multidrug resistance in human breast cancer cells without associated P-glycoprotein or MRP overexpression. *J Cell Biochem*, **65**, 513-526.

28. Doyle, L.A., Yang, W., Abruzzo, L.V., Krogmann, T., Gao, Y., Rishi, A.K. and Ross, D.D. (1998) A multidrug resistance transporter from human MCF-7 breast cancer cells. *Proc Natl Acad Sci U S A*, **95**, 15665-15670.
29. Miyake, K., Mickley, L., Litman, T., Zhan, Z., Robey, R., Cristensen, B., Brangi, M., Greenberger, L., Dean, M., Fojo, T. *et al.* (1999) Molecular cloning of cDNAs which are highly overexpressed in mitoxantrone-resistant cells: demonstration of homology to ABC transport genes. *Cancer Res*, **59**, 8-13.
30. Allikmets, R., Schriml, L.M., Hutchinson, A., Romano-Spica, V. and Dean, M. (1998) A human placenta-specific ATP-binding cassette gene (ABCP) on chromosome 4q22 that is involved in multidrug resistance. *Cancer Res*, **58**, 5337-5339.
31. Higgins, C.F. (1992) ABC transporters: from microorganisms to man. *Annu Rev Cell Biol*, **8**, 67-113.
32. Dean, M., Rzhetsky, A. and Allikmets, R. (2001) The human ATP-binding cassette (ABC) transporter superfamily. *Genome Res*, **11**, 1156-1166.
33. Dean, M., Hamon, Y. and Chimini, G. (2001) The human ATP-binding cassette (ABC) transporter superfamily. *J Lipid Res*, **42**, 1007-1017.
34. Dean, M. (2005) The genetics of ATP-binding cassette transporters. *Methods in enzymology*, **400**, 409-429.
35. Bailey-Dell, K.J., Hassel, B., Doyle, L.A. and Ross, D.D. (2001) Promoter characterization and genomic organization of the human breast cancer resistance protein (ATP-binding cassette transporter G2) gene. *Biochimica et biophysica acta*, **1520**, 234-241.
36. Hyde, S.C., Emsley, P., Hartshorn, M.J., Mimmack, M.M., Gileadi, U., Pearce, S.R., Gallagher, M.P., Gill, D.R., Hubbard, R.E. and Higgins, C.F. (1990) Structural model of ATP-binding proteins associated with cystic fibrosis, multidrug resistance and bacterial transport. *Nature*, **346**, 362-365.
37. Walker, J.E., Saraste, M., Runswick, M.J. and Gay, N.J. (1982) Distantly related sequences in the alpha- and beta-subunits of ATP synthase, myosin, kinases and other ATP-requiring enzymes and a common nucleotide binding fold. *Embo J*, **1**, 945-951.
38. Tusnady, G.E., Sarkadi, B., Simon, I. and Varadi, A. (2006) Membrane topology of human ABC proteins. *FEBS Lett*, **580**, 1017-1022.
39. Wang, H., Lee, E.W., Cai, X., Ni, Z., Zhou, L. and Mao, Q. (2008) Membrane topology of the human breast cancer resistance protein (BCRP/ABCG2) determined by epitope insertion and immunofluorescence. *Biochemistry*, **47**, 13778-13787.
40. Rosenberg, M.F., Bikadi, Z., Chan, J., Liu, X., Ni, Z., Cai, X., Ford, R.C. and Mao, Q. (2010) The human breast cancer resistance protein (BCRP/ABCG2) shows conformational changes with mitoxantrone. *Structure*, **18**, 482-493.
41. Ozvegy, C., Litman, T., Szakacs, G., Nagy, Z., Bates, S., Varadi, A. and Sarkadi, B. (2001) Functional characterization of the human multidrug transporter, ABCG2, expressed in insect cells. *Biochemical and biophysical research communications*, **285**, 111-117.

42. Xu, J., Liu, Y., Yang, Y., Bates, S. and Zhang, J.T. (2004) Characterization of oligomeric human half-ABC transporter ATP-binding cassette G2. *The Journal of biological chemistry*, **279**, 19781-19789.
43. Bhatia, A., Schafer, H.J. and Hrycyna, C.A. (2005) Oligomerization of the human ABC transporter ABCG2: evaluation of the native protein and chimeric dimers. *Biochemistry*, **44**, 10893-10904.
44. Ni, Z., Mark, M.E., Cai, X. and Mao, Q. (2010) Fluorescence resonance energy transfer (FRET) analysis demonstrates dimer/oligomer formation of the human breast cancer resistance protein (BCRP/ABCG2) in intact cells. *Int J Biochem Mol Biol*, **1**, 1-11.
45. Smith, P.C., Karpowich, N., Millen, L., Moody, J.E., Rosen, J., Thomas, P.J. and Hunt, J.F. (2002) ATP binding to the motor domain from an ABC transporter drives formation of a nucleotide sandwich dimer. *Mol Cell*, **10**, 139-149.
46. Sarkadi, B., Homolya, L., Szakacs, G. and Varadi, A. (2006) Human multidrug resistance ABCB and ABCG transporters: participation in a chemoimmunity defense system. *Physiol Rev*, **86**, 1179-1236.
47. Loo, T.W. and Clarke, D.M. (2005) Recent progress in understanding the mechanism of P-glycoprotein-mediated drug efflux. *J Membr Biol*, **206**, 173-185.
48. Seeger, M.A. and van Veen, H.W. (2009) Molecular basis of multidrug transport by ABC transporters. *Biochimica et biophysica acta*, **1794**, 725-737.
49. Locher, K.P. (2009) Review. Structure and mechanism of ATP-binding cassette transporters. *Philos Trans R Soc Lond B Biol Sci*, **364**, 239-245.
50. Senior, A.E., al-Shawi, M.K. and Urbatsch, I.L. (1995) The catalytic cycle of P-glycoprotein. *FEBS Lett*, **377**, 285-289.
51. Sauna, Z.E. and Ambudkar, S.V. (2001) Characterization of the catalytic cycle of ATP hydrolysis by human P-glycoprotein. The two ATP hydrolysis events in a single catalytic cycle are kinetically similar but affect different functional outcomes. *The Journal of biological chemistry*, **276**, 11653-11661.
52. Homolya, L., Orban, T.I., Csanady, L. and Sarkadi, B. (2011) Mitoxantrone is expelled by the ABCG2 multidrug transporter directly from the plasma membrane. *Biochimica et biophysica acta*, **1808**, 154-163.
53. Dawson, R.J. and Locher, K.P. (2006) Structure of a bacterial multidrug ABC transporter. *Nature*, **443**, 180-185.
54. Dawson, R.J. and Locher, K.P. (2007) Structure of the multidrug ABC transporter Sav1866 from Staphylococcus aureus in complex with AMP-PNP. *FEBS Lett*, **581**, 935-938.
55. Aller, S.G., Yu, J., Ward, A., Weng, Y., Chittaboina, S., Zhuo, R., Harrell, P.M., Trinh, Y.T., Zhang, Q., Urbatsch, I.L. *et al.* (2009) Structure of P-glycoprotein reveals a molecular basis for poly-specific drug binding. *Science*, **323**, 1718-1722.
56. Natarajan, K., Xie, Y., Baer, M.R. and Ross, D.D. (2012) Role of breast cancer resistance protein (BCRP/ABCG2) in cancer drug resistance. *Biochemical pharmacology*, **83**, 1084-1103.
57. Nakanishi, T., Bailey-Dell, K.J., Hassel, B.A., Shiozawa, K., Sullivan, D.M., Turner, J. and Ross, D.D. (2006) Novel 5' untranslated region variants of BCRP mRNA are differentially expressed in drug-selected cancer cells and in normal

human tissues: implications for drug resistance, tissue-specific expression, and alternative promoter usage. *Cancer research*, **66**, 5007-5011.

58. Apati, A., Orban, T.I., Varga, N., Nemeth, A., Schamberger, A., Krizsik, V., Erdelyi-Belle, B., Homolya, L., Varady, G., Padanyi, R. *et al.* (2008) High level functional expression of the ABCG2 multidrug transporter in undifferentiated human embryonic stem cells. *Biochimica et biophysica acta*, **1778**, 2700-2709.
59. Campbell, P.K., Zong, Y., Yang, S., Zhou, S., Rubnitz, J.E. and Sorrentino, B.P. (2011) Identification of a novel, tissue-specific ABCG2 promoter expressed in pediatric acute megakaryoblastic leukemia. *Leuk Res*, **35**, 1321-1329.
60. de Boussac, H., Orban, T.I., Varady, G., Tihanyi, B., Bacquet, C., Brozik, A., Varadi, A., Sarkadi, B. and Aranyi, T. (2012) Stimulus-induced expression of the ABCG2 multidrug transporter in HepG2 hepatocarcinoma model cells involves the ERK1/2 cascade and alternative promoters. *Biochemical and biophysical research communications*, **426**, 172-176.
61. To, K.K., Zhan, Z., Litman, T. and Bates, S.E. (2008) Regulation of ABCG2 expression at the 3' untranslated region of its mRNA through modulation of transcript stability and protein translation by a putative microRNA in the S1 colon cancer cell line. *Mol Cell Biol*, **28**, 5147-5161.
62. To, K.K., Robey, R.W., Knutsen, T., Zhan, Z., Ried, T. and Bates, S.E. (2009) Escape from hsa-miR-519c enables drug-resistant cells to maintain high expression of ABCG2. *Molecular cancer therapeutics*, **8**, 2959-2968.
63. Diop, N.K. and Hrycyna, C.A. (2005) N-Linked glycosylation of the human ABC transporter ABCG2 on asparagine 596 is not essential for expression, transport activity, or trafficking to the plasma membrane. *Biochemistry*, **44**, 5420-5429.
64. Mohrmann, K., van Eijndhoven, M.A., Schinkel, A.H. and Schellens, J.H. (2005) Absence of N-linked glycosylation does not affect plasma membrane localization of breast cancer resistance protein (BCRP/ABCG2). *Cancer chemotherapy and pharmacology*, **56**, 344-350.
65. Wakabayashi-Nakao, K., Tamura, A., Furukawa, T., Nakagawa, H. and Ishikawa, T. (2009) Quality control of human ABCG2 protein in the endoplasmic reticulum: ubiquitination and proteasomal degradation. *Advanced drug delivery reviews*, **61**, 66-72.
66. Henriksen, U., Fog, J.U., Litman, T. and Gether, U. (2005) Identification of intra- and intermolecular disulfide bridges in the multidrug resistance transporter ABCG2. *The Journal of biological chemistry*, **280**, 36926-36934.
67. Wakabayashi, K., Nakagawa, H., Adachi, T., Kii, I., Kobatake, E., Kudo, A. and Ishikawa, T. (2006) Identification of cysteine residues critically involved in homodimer formation and protein expression of human ATP-binding cassette transporter ABCG2: a new approach using the flp recombinase system. *J Exp Ther Oncol*, **5**, 205-222.
68. Takada, T., Suzuki, H. and Sugiyama, Y. (2005) Characterization of polarized expression of point- or deletion-mutated human BCRP/ABCG2 in LLC-PK1 cells. *Pharm Res*, **22**, 458-464.
69. Wakabayashi, K., Nakagawa, H., Tamura, A., Koshiba, S., Hoshijima, K., Komada, M. and Ishikawa, T. (2007) Intramolecular disulfide bond is a critical check point determining degradative fates of ATP-binding cassette (ABC)

transporter ABCG2 protein. *The Journal of biological chemistry*, **282**, 27841-27846.

70. Zhou, S., Schuetz, J.D., Bunting, K.D., Colapietro, A.M., Sampath, J., Morris, J.J., Lagutina, I., Grosveld, G.C., Osawa, M., Nakauchi, H. *et al.* (2001) The ABC transporter Bcrp1/ABCG2 is expressed in a wide variety of stem cells and is a molecular determinant of the side-population phenotype. *Nat Med*, **7**, 1028-1034.
71. Ozvegy-Laczka, C., Laczko, R., Hegedus, C., Litman, T., Varady, G., Goda, K., Hegedus, T., Dokholyan, N.V., Sorrentino, B.P., Varadi, A. *et al.* (2008) Interaction with the 5D3 monoclonal antibody is regulated by intramolecular rearrangements but not by covalent dimer formation of the human ABCG2 multidrug transporter. *The Journal of biological chemistry*, **283**, 26059-26070.
72. Kage, K., Fujita, T. and Sugimoto, Y. (2005) Role of Cys-603 in dimer/oligomer formation of the breast cancer resistance protein BCRP/ABCG2. *Cancer Sci*, **96**, 866-872.
73. Liu, Y., Yang, Y., Qi, J., Peng, H. and Zhang, J.T. (2008) Effect of cysteine mutagenesis on the function and disulfide bond formation of human ABCG2. *J Pharmacol Exp Ther*, **326**, 33-40.
74. Desuzinges-Mandon, E., Arnaud, O., Martinez, L., Huche, F., Di Pietro, A. and Falson, P. (2010) ABCG2 transports and transfers heme to albumin through its large extracellular loop. *The Journal of biological chemistry*, **285**, 33123-33133.
75. Xie, Y., Xu, K., Linn, D.E., Yang, X., Guo, Z., Shimelis, H., Nakanishi, T., Ross, D.D., Chen, H., Fazli, L. *et al.* (2008) The 44-kDa Pim-1 kinase phosphorylates BCRP/ABCG2 and thereby promotes its multimerization and drug-resistant activity in human prostate cancer cells. *The Journal of biological chemistry*, **283**, 3349-3356.
76. Meyer zu Schwabedissen, H.E., Grube, M., Dreisbach, A., Jedlitschky, G., Meissner, K., Linnemann, K., Fusch, C., Ritter, C.A., Volker, U. and Kroemer, H.K. (2006) Epidermal growth factor-mediated activation of the map kinase cascade results in altered expression and function of ABCG2 (BCRP). *Drug metabolism and disposition: the biological fate of chemicals*, **34**, 524-533.
77. Imai, Y., Ohmori, K., Yasuda, S., Wada, M., Suzuki, T., Fukuda, K. and Ueda, Y. (2009) Breast cancer resistance protein/ABCG2 is differentially regulated downstream of extracellular signal-regulated kinase. *Cancer Sci*, **100**, 1118-1127.
78. Nakanishi, T., Shiozawa, K., Hassel, B.A. and Ross, D.D. (2006) Complex interaction of BCRP/ABCG2 and imatinib in BCR-ABL-expressing cells: BCRP-mediated resistance to imatinib is attenuated by imatinib-induced reduction of BCRP expression. *Blood*, **108**, 678-684.
79. Mogi, M., Yang, J., Lambert, J.F., Colvin, G.A., Shiojima, I., Skurk, C., Summer, R., Fine, A., Quesenberry, P.J. and Walsh, K. (2003) Akt signaling regulates side population cell phenotype via Bcrp1 translocation. *J Biol Chem*, **278**, 39068-39075.
80. Takada, T., Suzuki, H., Gotoh, Y. and Sugiyama, Y. (2005) Regulation of the cell surface expression of human BCRP/ABCG2 by the phosphorylation state of Akt in polarized cells. *Drug Metab Dispos*, **33**, 905-909.
81. Bleau, A.M., Hambardzumyan, D., Ozawa, T., Fomchenko, E.I., Huse, J.T., Brennan, C.W. and Holland, E.C. (2009) PTEN/PI3K/Akt pathway regulates the

side population phenotype and ABCG2 activity in glioma tumor stem-like cells. *Cell Stem Cell*, **4**, 226-235.

82. Aust, S., Obrist, P., Jaeger, W., Klimpfinger, M., Tucek, G., Wrba, F., Penner, E. and Thalhammer, T. (2004) Subcellular localization of the ABCG2 transporter in normal and malignant human gallbladder epithelium. *Lab Invest*, **84**, 1024-1036.
83. Hu, C., Li, H., Li, J., Zhu, Z., Yin, S., Hao, X., Yao, M., Zheng, S. and Gu, J. (2008) Analysis of ABCG2 expression and side population identifies intrinsic drug efflux in the HCC cell line MHCC-97L and its modulation by Akt signaling. *Carcinogenesis*, **29**, 2289-2297.
84. Goler-Baron, V., Sladkevich, I. and Assaraf, Y.G. (2012) Inhibition of the PI3K-Akt signaling pathway disrupts ABCG2-rich extracellular vesicles and overcomes multidrug resistance in breast cancer cells. *Biochemical pharmacology*, **83**, 1340-1348.
85. Wang, X., Wu, X., Wang, C., Zhang, W., Ouyang, Y., Yu, Y. and He, Z. (2010) Transcriptional suppression of breast cancer resistance protein (BCRP) by wild-type p53 through the NF-kappaB pathway in MCF-7 cells. *FEBS Lett*, **584**, 3392-3397.
86. Sims-Mourtada, J., Izzo, J.G., Ajani, J. and Chao, K.S. (2007) Sonic Hedgehog promotes multiple drug resistance by regulation of drug transport. *Oncogene*, **26**, 5674-5679.
87. Singh, R.R., Kunkalla, K., Qu, C., Schlette, E., Neelapu, S.S., Samaniego, F. and Vega, F. (2011) ABCG2 is a direct transcriptional target of hedgehog signaling and involved in stroma-induced drug tolerance in diffuse large B-cell lymphoma. *Oncogene*, **30**, 4874-4886.
88. Litman, T., Brangi, M., Hudson, E., Fetsch, P., Abati, A., Ross, D.D., Miyake, K., Resau, J.H. and Bates, S.E. (2000) The multidrug-resistant phenotype associated with overexpression of the new ABC half-transporter, MXR (ABCG2). *J Cell Sci*, **113 (Pt 11)**, 2011-2021.
89. Rocchi, E., Khodjakov, A., Volk, E.L., Yang, C.H., Litman, T., Bates, S.E. and Schneider, E. (2000) The product of the ABC half-transporter gene ABCG2 (BCRP/MXR/ABCP) is expressed in the plasma membrane. *Biochem Biophys Res Commun*, **271**, 42-46.
90. Scheffer, G.L., Maliepaard, M., Pijnenborg, A.C., van Gastelen, M.A., de Jong, M.C., Schroeijers, A.B., van der Kolk, D.M., Allen, J.D., Ross, D.D., van der Valk, P. *et al.* (2000) Breast cancer resistance protein is localized at the plasma membrane in mitoxantrone- and topotecan-resistant cell lines. *Cancer Res*, **60**, 2589-2593.
91. Rajagopal, A. and Simon, S.M. (2003) Subcellular localization and activity of multidrug resistance proteins. *Mol Biol Cell*, **14**, 3389-3399.
92. Solazzo, M., Fantappie, O., D'Amico, M., Sassoli, C., Tani, A., Cipriani, G., Bogani, C., Formigli, L. and Mazzanti, R. (2009) Mitochondrial expression and functional activity of breast cancer resistance protein in different multiple drug-resistant cell lines. *Cancer research*, **69**, 7235-7242.
93. Kobuchi, H., Moriya, K., Ogino, T., Fujita, H., Inoue, K., Shuin, T., Yasuda, T., Utsumi, K. and Utsumi, T. (2012) Mitochondrial localization of ABC transporter

ABCG2 and its function in 5-aminolevulinic acid-mediated protoporphyrin IX accumulation. *PLoS One*, **7**, e50082.

94. Maliepaard, M., Scheffer, G.L., Faneyte, I.F., van Gastelen, M.A., Pijnenborg, A.C., Schinkel, A.H., van De Vijver, M.J., Scheper, R.J. and Schellens, J.H. (2001) Subcellular localization and distribution of the breast cancer resistance protein transporter in normal human tissues. *Cancer research*, **61**, 3458-3464.
95. Robey, R.W., To, K.K., Polgar, O., Dohse, M., Fetsch, P., Dean, M. and Bates, S.E. (2009) ABCG2: a perspective. *Advanced drug delivery reviews*, **61**, 3-13.
96. Scharenberg, C.W., Harkey, M.A. and Torok-Storb, B. (2002) The ABCG2 transporter is an efficient Hoechst 33342 efflux pump and is preferentially expressed by immature human hematopoietic progenitors. *Blood*, **99**, 507-512.
97. Krishnamurthy, P., Ross, D.D., Nakanishi, T., Bailey-Dell, K., Zhou, S., Mercer, K.E., Sarkadi, B., Sorrentino, B.P. and Schuetz, J.D. (2004) The stem cell marker Bcrp/ABCG2 enhances hypoxic cell survival through interactions with heme. *The Journal of biological chemistry*, **279**, 24218-24225.
98. Erdei, Z., Sarkadi, B., Brozik, A., Szebenyi, K., Varady, G., Mako, V., Pentek, A., Orban, T.I. and Apati, A. (2012) Dynamic ABCG2 expression in human embryonic stem cells provides the basis for stress response. *Eur Biophys J*.
99. Zelinski, T., Coghlan, G., Liu, X.Q. and Reid, M.E. (2012) ABCG2 null alleles define the Jr(a-) blood group phenotype. *Nat Genet*, **44**, 131-132.
100. Saison, C., Helias, V., Ballif, B.A., Peyrard, T., Puy, H., Miyazaki, T., Perrot, S., Vayssier-Taussat, M., Waldner, M., Le Pennec, P.Y. *et al.* (2012) Null alleles of ABCG2 encoding the breast cancer resistance protein define the new blood group system Junior. *Nat Genet*, **44**, 174-177.
101. Zhou, S., Morris, J.J., Barnes, Y., Lan, L., Schuetz, J.D. and Sorrentino, B.P. (2002) Bcrp1 gene expression is required for normal numbers of side population stem cells in mice, and confers relative protection to mitoxantrone in hematopoietic cells in vivo. *Proceedings of the National Academy of Sciences of the United States of America*, **99**, 12339-12344.
102. Jonker, J.W., Buitelaar, M., Wagenaar, E., Van Der Valk, M.A., Scheffer, G.L., Scheper, R.J., Plosch, T., Kuipers, F., Elferink, R.P., Rosing, H. *et al.* (2002) The breast cancer resistance protein protects against a major chlorophyll-derived dietary phototoxin and protoporphyria. *Proceedings of the National Academy of Sciences of the United States of America*, **99**, 15649-15654.
103. Robey, R.W., Steadman, K., Polgar, O., Morisaki, K., Blayney, M., Mistry, P. and Bates, S.E. (2004) Pheophorbide a is a specific probe for ABCG2 function and inhibition. *Cancer research*, **64**, 1242-1246.
104. van Herwaarden, A.E., Jonker, J.W., Wagenaar, E., Brinkhuis, R.F., Schellens, J.H., Beijnen, J.H. and Schinkel, A.H. (2003) The breast cancer resistance protein (Bcrp1/Abcg2) restricts exposure to the dietary carcinogen 2-amino-1-methyl-6-phenylimidazo[4,5-b]pyridine. *Cancer research*, **63**, 6447-6452.
105. Sarkadi, B., Muller, M. and Hollo, Z. (1996) The multidrug transporters--proteins of an ancient immune system. *Immunol Lett*, **54**, 215-219.
106. Ebert, B., Seidel, A. and Lampen, A. (2005) Identification of BCRP as transporter of benzo[a]pyrene conjugates metabolically formed in Caco-2 cells and its induction by Ah-receptor agonists. *Carcinogenesis*, **26**, 1754-1763.

107. Tan, K.P., Wang, B., Yang, M., Boutros, P.C., Macaulay, J., Xu, H., Chuang, A.I., Kosuge, K., Yamamoto, M., Takahashi, S. *et al.* (2010) Aryl hydrocarbon receptor is a transcriptional activator of the human breast cancer resistance protein (BCRP/ABCG2). *Molecular pharmacology*, **78**, 175-185.
108. Tompkins, L.M., Li, H., Li, L., Lynch, C., Xie, Y., Nakanishi, T., Ross, D.D. and Wang, H. (2010) A novel xenobiotic responsive element regulated by aryl hydrocarbon receptor is involved in the induction of BCRP/ABCG2 in LS174T cells. *Biochemical pharmacology*, **80**, 1754-1761.
109. Zhang, M., Mathur, A., Zhang, Y., Xi, S., Atay, S., Hong, J.A., Datrice, N., Upham, T., Kemp, C.D., Ripley, R.T. *et al.* (2012) Mithramycin represses basal and cigarette smoke-induced expression of ABCG2 and inhibits stem cell signaling in lung and esophageal cancer cells. *Cancer research*, **72**, 4178-4192.
110. Jigorel, E., Le Vee, M., Boursier-Neyret, C., Parmentier, Y. and Fardel, O. (2006) Differential regulation of sinusoidal and canalicular hepatic drug transporter expression by xenobiotics activating drug-sensing receptors in primary human hepatocytes. *Drug metabolism and disposition: the biological fate of chemicals*, **34**, 1756-1763.
111. Wang, X., Sykes, D.B. and Miller, D.S. (2010) Constitutive androstane receptor-mediated up-regulation of ATP-driven xenobiotic efflux transporters at the blood-brain barrier. *Molecular pharmacology*, **78**, 376-383.
112. Maliepaard, M., van Gastelen, M.A., de Jong, L.A., Pluim, D., van Waardenburg, R.C., Ruevekamp-Helmers, M.C., Floot, B.G. and Schellens, J.H. (1999) Overexpression of the BCRP/MXR/ABCP gene in a topotecan-selected ovarian tumor cell line. *Cancer Res*, **59**, 4559-4563.
113. Ross, D.D., Yang, W., Abruzzo, L.V., Dalton, W.S., Schneider, E., Lage, H., Dietel, M., Greenberger, L., Cole, S.P. and Doyle, L.A. (1999) Atypical multidrug resistance: breast cancer resistance protein messenger RNA expression in mitoxantrone-selected cell lines. *J Natl Cancer Inst*, **91**, 429-433.
114. Ross, D.D., Karp, J.E., Chen, T.T. and Doyle, L.A. (2000) Expression of breast cancer resistance protein in blast cells from patients with acute leukemia. *Blood*, **96**, 365-368.
115. van den Heuvel-Eibrink, M.M., Wiemer, E.A., Prins, A., Meijerink, J.P., Vossebeld, P.J., van der Holt, B., Pieters, R. and Sonneveld, P. (2002) Increased expression of the breast cancer resistance protein (BCRP) in relapsed or refractory acute myeloid leukemia (AML). *Leukemia*, **16**, 833-839.
116. van der Kolk, D.M., Vellenga, E., Scheffer, G.L., Muller, M., Bates, S.E., Scheper, R.J. and de Vries, E.G. (2002) Expression and activity of breast cancer resistance protein (BCRP) in de novo and relapsed acute myeloid leukemia. *Blood*, **99**, 3763-3770.
117. Steinbach, D., Sell, W., Voigt, A., Hermann, J., Zintl, F. and Sauerbrey, A. (2002) BCRP gene expression is associated with a poor response to remission induction therapy in childhood acute myeloid leukemia. *Leukemia*, **16**, 1443-1447.
118. Abbott, B.L., Colapietro, A.M., Barnes, Y., Marini, F., Andreeff, M. and Sorrentino, B.P. (2002) Low levels of ABCG2 expression in adult AML blast samples. *Blood*, **100**, 4594-4601.

119. Raaijmakers, M.H., de Grouw, E.P., Heuver, L.H., van der Reijden, B.A., Jansen, J.H., Scheper, R.J., Scheffer, G.L., de Witte, T.J. and Raymakers, R.A. (2005) Breast cancer resistance protein in drug resistance of primitive CD34+38- cells in acute myeloid leukemia. *Clin Cancer Res*, **11**, 2436-2444.
120. Suvannasankha, A., Minderman, H., O'Loughlin, K.L., Nakanishi, T., Ford, L.A., Greco, W.R., Wetzler, M., Ross, D.D. and Baer, M.R. (2004) Breast cancer resistance protein (BCRP/MXR/ABCG2) in adult acute lymphoblastic leukaemia: frequent expression and possible correlation with shorter disease-free survival. *Br J Haematol*, **127**, 392-398.
121. Sauerbrey, A., Sell, W., Steinbach, D., Voigt, A. and Zintl, F. (2002) Expression of the BCRP gene (ABCG2/MXR/ABCP) in childhood acute lymphoblastic leukaemia. *Br J Haematol*, **118**, 147-150.
122. Jordanides, N.E., Jorgensen, H.G., Holyoake, T.L. and Mountford, J.C. (2006) Functional ABCG2 is overexpressed on primary CML CD34+ cells and is inhibited by imatinib mesylate. *Blood*, **108**, 1370-1373.
123. Jiang, X., Zhao, Y., Smith, C., Gasparetto, M., Turhan, A., Eaves, A. and Eaves, C. (2007) Chronic myeloid leukemia stem cells possess multiple unique features of resistance to BCR-ABL targeted therapies. *Leukemia*, **21**, 926-935.
124. Diestra, J.E., Scheffer, G.L., Catala, I., Maliepaard, M., Schellens, J.H., Scheper, R.J., Germa-Lluch, J.R. and Izquierdo, M.A. (2002) Frequent expression of the multi-drug resistance-associated protein BCRP/MXR/ABCP/ABCG2 in human tumours detected by the BXP-21 monoclonal antibody in paraffin-embedded material. *J Pathol*, **198**, 213-219.
125. Usuda, J., Ohira, T., Suga, Y., Oikawa, T., Ichinose, S., Inoue, T., Ohtani, K., Maehara, S., Imai, K., Kubota, M. *et al.* (2007) Breast cancer resistance protein (BCRP) affected acquired resistance to gefitinib in a "never-smoked" female patient with advanced non-small cell lung cancer. *Lung Cancer*, **58**, 296-299.
126. Tamaki, A., Ierano, C., Szakacs, G., Robey, R.W. and Bates, S.E. (2011) The controversial role of ABC transporters in clinical oncology. *Essays Biochem*, **50**, 209-232.
127. Szakacs, G., Varadi, A., Ozvegy-Laczka, C. and Sarkadi, B. (2008) The role of ABC transporters in drug absorption, distribution, metabolism, excretion and toxicity (ADME-Tox). *Drug Discov Today*, **13**, 379-393.
128. Abbott, B.L. (2006) ABCG2 (BCRP): a cytoprotectant in normal and malignant stem cells. *Clin Adv Hematol Oncol*, **4**, 63-72.
129. Hirschmann-Jax, C., Foster, A.E., Wulf, G.G., Nuchtern, J.G., Jax, T.W., Gobel, U., Goodell, M.A. and Brenner, M.K. (2004) A distinct "side population" of cells with high drug efflux capacity in human tumor cells. *Proc Natl Acad Sci U S A*, **101**, 14228-14233.
130. Visvader, J.E. and Lindeman, G.J. (2008) Cancer stem cells in solid tumours: accumulating evidence and unresolved questions. *Nat Rev Cancer*, **8**, 755-768.
131. Reya, T., Morrison, S.J., Clarke, M.F. and Weissman, I.L. (2001) Stem cells, cancer, and cancer stem cells. *Nature*, **414**, 105-111.
132. Dean, M., Fojo, T. and Bates, S. (2005) Tumour stem cells and drug resistance. *Nat Rev Cancer*, **5**, 275-284.

133. Dehghan, A., Kottgen, A., Yang, Q., Hwang, S.J., Kao, W.L., Rivadeneira, F., Boerwinkle, E., Levy, D., Hofman, A., Astor, B.C. *et al.* (2008) Association of three genetic loci with uric acid concentration and risk of gout: a genome-wide association study. *Lancet*, **372**, 1953-1961.
134. Kolz, M., Johnson, T., Sanna, S., Teumer, A., Vitart, V., Perola, M., Mangino, M., Albrecht, E., Wallace, C., Farrall, M. *et al.* (2009) Meta-analysis of 28,141 individuals identifies common variants within five new loci that influence uric acid concentrations. *PLoS Genet*, **5**, e1000504.
135. Woodward, O.M., Kottgen, A., Coresh, J., Boerwinkle, E., Guggino, W.B. and Kottgen, M. (2009) Identification of a urate transporter, ABCG2, with a common functional polymorphism causing gout. *Proceedings of the National Academy of Sciences of the United States of America*, **106**, 10338-10342.
136. Szakacs, G., Paterson, J.K., Ludwig, J.A., Booth-Genthe, C. and Gottesman, M.M. (2006) Targeting multidrug resistance in cancer. *Nat Rev Drug Discov*, **5**, 219-234.
137. Kerr, I.D., Haider, A.J. and Gelissen, I.C. (2011) The ABCG family of membrane-associated transporters: you don't have to be big to be mighty. *Br J Pharmacol*, **164**, 1767-1779.
138. Honjo, Y., Hrycyna, C.A., Yan, Q.W., Medina-Perez, W.Y., Robey, R.W., van de Laar, A., Litman, T., Dean, M. and Bates, S.E. (2001) Acquired mutations in the MXR/BCRP/ABCP gene alter substrate specificity in MXR/BCRP/ABCP-overexpressing cells. *Cancer research*, **61**, 6635-6639.
139. Ozvegy, C., Varadi, A. and Sarkadi, B. (2002) Characterization of drug transport, ATP hydrolysis, and nucleotide trapping by the human ABCG2 multidrug transporter. Modulation of substrate specificity by a point mutation. *J Biol Chem*, **277**, 47980-47990.
140. Robey, R.W., Honjo, Y., Morisaki, K., Nadjem, T.A., Runge, S., Risbood, M., Poruchynsky, M.S. and Bates, S.E. (2003) Mutations at amino-acid 482 in the ABCG2 gene affect substrate and antagonist specificity. *Br J Cancer*, **89**, 1971-1978.
141. Miwa, M., Tsukahara, S., Ishikawa, E., Asada, S., Imai, Y. and Sugimoto, Y. (2003) Single amino acid substitutions in the transmembrane domains of breast cancer resistance protein (BCRP) alter cross resistance patterns in transfectants. *International journal of cancer. Journal international du cancer*, **107**, 757-763.
142. Ozvegy-Laczka, C., Koblos, G., Sarkadi, B. and Varadi, A. (2005) Single amino acid (482) variants of the ABCG2 multidrug transporter: major differences in transport capacity and substrate recognition. *Biochimica et biophysica acta*, **1668**, 53-63.
143. Honjo, Y., Morisaki, K., Huff, L.M., Robey, R.W., Hung, J., Dean, M. and Bates, S.E. (2002) Single-nucleotide polymorphism (SNP) analysis in the ABC half-transporter ABCG2 (MXR/BCRP/ABCP1). *Cancer biology & therapy*, **1**, 696-702.
144. Rabindran, S.K., He, H., Singh, M., Brown, E., Collins, K.I., Annable, T. and Greenberger, L.M. (1998) Reversal of a novel multidrug resistance mechanism in human colon carcinoma cells by fumitremorgin C. *Cancer Res*, **58**, 5850-5858.

145. Rabindran, S.K., Ross, D.D., Doyle, L.A., Yang, W. and Greenberger, L.M. (2000) Fumitremorgin C reverses multidrug resistance in cells transfected with the breast cancer resistance protein. *Cancer Res*, **60**, 47-50.
146. Allen, J.D., van Loevezijn, A., Lakhai, J.M., van der Valk, M., van Tellingen, O., Reid, G., Schellens, J.H., Koomen, G.J. and Schinkel, A.H. (2002) Potent and specific inhibition of the breast cancer resistance protein multidrug transporter in vitro and in mouse intestine by a novel analogue of fumitremorgin C. *Molecular cancer therapeutics*, **1**, 417-425.
147. Szakacs, G., Annereau, J.P., Lababidi, S., Shankavaram, U., Arciello, A., Bussey, K.J., Reinhold, W., Guo, Y., Kruh, G.D., Reimers, M. *et al.* (2004) Predicting drug sensitivity and resistance: profiling ABC transporter genes in cancer cells. *Cancer Cell*, **6**, 129-137.
148. Ludwig, J.A., Szakacs, G., Martin, S.E., Chu, B.F., Cardarelli, C., Sauna, Z.E., Caplen, N.J., Fales, H.M., Ambudkar, S.V., Weinstein, J.N. *et al.* (2006) Selective toxicity of NSC73306 in MDR1-positive cells as a new strategy to circumvent multidrug resistance in cancer. *Cancer research*, **66**, 4808-4815.
149. Turk, D., Hall, M.D., Chu, B.F., Ludwig, J.A., Fales, H.M., Gottesman, M.M. and Szakacs, G. (2009) Identification of compounds selectively killing multidrug-resistant cancer cells. *Cancer research*, **69**, 8293-8301.
150. Deeken, J.F., Robey, R.W., Shukla, S., Steadman, K., Chakraborty, A.R., Poonkuzhali, B., Schuetz, E.G., Holbeck, S., Ambudkar, S.V. and Bates, S.E. (2009) Identification of compounds that correlate with ABCG2 transporter function in the National Cancer Institute Anticancer Drug Screen. *Molecular pharmacology*, **76**, 946-956.
151. Sawyers, C. (2004) Targeted cancer therapy. *Nature*, **432**, 294-297.
152. Sharma, S.V. and Settleman, J. (2007) Oncogene addiction: setting the stage for molecularly targeted cancer therapy. *Genes Dev*, **21**, 3214-3231.
153. Weinstein, I.B. and Joe, A. (2008) Oncogene addiction. *Cancer research*, **68**, 3077-3080; discussion 3080.
154. Zhang, J., Yang, P.L. and Gray, N.S. (2009) Targeting cancer with small molecule kinase inhibitors. *Nature reviews. Cancer*, **9**, 28-39.
155. Blume-Jensen, P. and Hunter, T. (2001) Oncogenic kinase signalling. *Nature*, **411**, 355-365.
156. Futreal, P.A., Coin, L., Marshall, M., Down, T., Hubbard, T., Wooster, R., Rahman, N. and Stratton, M.R. (2004) A census of human cancer genes. *Nature reviews. Cancer*, **4**, 177-183.
157. Santarius, T., Shipley, J., Brewer, D., Stratton, M.R. and Cooper, C.S. (2010) A census of amplified and overexpressed human cancer genes. *Nature reviews. Cancer*, **10**, 59-64.
158. Manning, G., Whyte, D.B., Martinez, R., Hunter, T. and Sudarsanam, S. (2002) The protein kinase complement of the human genome. *Science*, **298**, 1912-1934.
159. Davies, H., Hunter, C., Smith, R., Stephens, P., Greenman, C., Bignell, G., Teague, J., Butler, A., Edkins, S., Stevens, C. *et al.* (2005) Somatic mutations of the protein kinase gene family in human lung cancer. *Cancer research*, **65**, 7591-7595.

160. Greenman, C., Stephens, P., Smith, R., Dalgliesh, G.L., Hunter, C., Bignell, G., Davies, H., Teague, J., Butler, A., Stevens, C. *et al.* (2007) Patterns of somatic mutation in human cancer genomes. *Nature*, **446**, 153-158.
161. Faderl, S., Talpaz, M., Estrov, Z., O'Brien, S., Kurzrock, R. and Kantarjian, H.M. (1999) The biology of chronic myeloid leukemia. *N Engl J Med*, **341**, 164-172.
162. Deininger, M.W., Goldman, J.M. and Melo, J.V. (2000) The molecular biology of chronic myeloid leukemia. *Blood*, **96**, 3343-3356.
163. Quintas-Cardama, A. and Cortes, J. (2009) Molecular biology of bcr-abl1-positive chronic myeloid leukemia. *Blood*, **113**, 1619-1630.
164. Smith, K.M., Yacobi, R. and Van Etten, R.A. (2003) Autoinhibition of Bcr-Abl through its SH3 domain. *Mol Cell*, **12**, 27-37.
165. Liu, J., Campbell, M., Guo, J.Q., Lu, D., Xian, Y.M., Andersson, B.S. and Arlinghaus, R.B. (1993) BCR-ABL tyrosine kinase is autophosphorylated or transphosphorylates P160 BCR on tyrosine predominantly within the first BCR exon. *Oncogene*, **8**, 101-109.
166. Pendergast, A.M., Quilliam, L.A., Cripe, L.D., Bassing, C.H., Dai, Z., Li, N., Batzer, A., Rabun, K.M., Der, C.J., Schlessinger, J. *et al.* (1993) BCR-ABL-induced oncogenesis is mediated by direct interaction with the SH2 domain of the GRB-2 adaptor protein. *Cell*, **75**, 175-185.
167. Puil, L., Liu, J., Gish, G., Mbamalu, G., Bowtell, D., Pelicci, P.G., Arlinghaus, R. and Pawson, T. (1994) Bcr-Abl oncoproteins bind directly to activators of the Ras signalling pathway. *The EMBO journal*, **13**, 764-773.
168. Ren, R. (2005) Mechanisms of BCR-ABL in the pathogenesis of chronic myelogenous leukaemia. *Nat Rev Cancer*, **5**, 172-183.
169. Buchdunger, E., Zimmermann, J., Mett, H., Meyer, T., Muller, M., Druker, B.J. and Lydon, N.B. (1996) Inhibition of the Abl protein-tyrosine kinase in vitro and in vivo by a 2-phenylaminopyrimidine derivative. *Cancer Res*, **56**, 100-104.
170. Druker, B.J., Tamura, S., Buchdunger, E., Ohno, S., Segal, G.M., Fanning, S., Zimmermann, J. and Lydon, N.B. (1996) Effects of a selective inhibitor of the Abl tyrosine kinase on the growth of Bcr-Abl positive cells. *Nat Med*, **2**, 561-566.
171. Carroll, M., Ohno-Jones, S., Tamura, S., Buchdunger, E., Zimmermann, J., Lydon, N.B., Gilliland, D.G. and Druker, B.J. (1997) CGP 57148, a tyrosine kinase inhibitor, inhibits the growth of cells expressing BCR-ABL, TEL-ABL, and TEL-PDGFR fusion proteins. *Blood*, **90**, 4947-4952.
172. Deininger, M.W., Goldman, J.M., Lydon, N. and Melo, J.V. (1997) The tyrosine kinase inhibitor CGP57148B selectively inhibits the growth of BCR-ABL-positive cells. *Blood*, **90**, 3691-3698.
173. Gambacorti-Passerini, C., le Coutre, P., Mologni, L., Fanelli, M., Bertazzoli, C., Marchesi, E., Di Nicola, M., Biondi, A., Corneo, G.M., Belotti, D. *et al.* (1997) Inhibition of the ABL kinase activity blocks the proliferation of BCR/ABL+ leukemic cells and induces apoptosis. *Blood Cells Mol Dis*, **23**, 380-394.
174. Weisberg, E., Manley, P.W., Cowan-Jacob, S.W., Hochhaus, A. and Griffin, J.D. (2007) Second generation inhibitors of BCR-ABL for the treatment of imatinib-resistant chronic myeloid leukaemia. *Nat Rev Cancer*, **7**, 345-356.
175. Druker, B.J., Guilhot, F., O'Brien, S.G., Gathmann, I., Kantarjian, H., Gattermann, N., Deininger, M.W., Silver, R.T., Goldman, J.M., Stone, R.M. *et al.*

(2006) Five-year follow-up of patients receiving imatinib for chronic myeloid leukemia. *N Engl J Med*, **355**, 2408-2417.
176. Hochhaus, A., O'Brien, S.G., Guilhot, F., Druker, B.J., Branford, S., Foroni, L., Goldman, J.M., Muller, M.C., Radich, J.P., Rudoltz, M. *et al.* (2009) Six-year follow-up of patients receiving imatinib for the first-line treatment of chronic myeloid leukemia. *Leukemia*, **23**, 1054-1061.
177. Milojkovic, D. and Apperley, J. (2009) Mechanisms of Resistance to Imatinib and Second-Generation Tyrosine Inhibitors in Chronic Myeloid Leukemia. *Clin Cancer Res*, **15**, 7519-7527.
178. Santos, F.P., Kantarjian, H., Quintas-Cardama, A. and Cortes, J. (2011) Evolution of therapies for chronic myelogenous leukemia. *Cancer J*, **17**, 465-476.
179. Khoury, H.J., Cortes, J.E., Kantarjian, H.M., Gambacorti-Passerini, C., Baccarani, M., Kim, D.W., Zaritskey, A., Countouriotis, A., Besson, N., Leip, E. *et al.* (2012) Bosutinib is active in chronic phase chronic myeloid leukemia after imatinib and dasatinib and/or nilotinib therapy failure. *Blood*, **119**, 3403-3412.
180. Holbro, T. and Hynes, N.E. (2004) ErbB receptors: directing key signaling networks throughout life. *Annu Rev Pharmacol Toxicol*, **44**, 195-217.
181. Hynes, N.E. and Lane, H.A. (2005) ERBB receptors and cancer: the complexity of targeted inhibitors. *Nat Rev Cancer*, **5**, 341-354.
182. Hynes, N.E. and MacDonald, G. (2009) ErbB receptors and signaling pathways in cancer. *Curr Opin Cell Biol*, **21**, 177-184.
183. Wheeler, D.L., Dunn, E.F. and Harari, P.M. (2010) Understanding resistance to EGFR inhibitors-impact on future treatment strategies. *Nature reviews. Clinical oncology*, **7**, 493-507.
184. Ryan, A.J. and Wedge, S.R. (2005) ZD6474--a novel inhibitor of VEGFR and EGFR tyrosine kinase activity. *Br J Cancer*, **92 Suppl 1**, S6-13.
185. Torrance, C.J., Jackson, P.E., Montgomery, E., Kinzler, K.W., Vogelstein, B., Wissner, A., Nunes, M., Frost, P. and Discafani, C.M. (2000) Combinatorial chemoprevention of intestinal neoplasia. *Nature medicine*, **6**, 1024-1028.
186. Rabindran, S.K., Discafani, C.M., Rosfjord, E.C., Baxter, M., Floyd, M.B., Golas, J., Hallett, W.A., Johnson, B.D., Nilakantan, R., Overbeek, E. *et al.* (2004) Antitumor activity of HKI-272, an orally active, irreversible inhibitor of the HER-2 tyrosine kinase. *Cancer research*, **64**, 3958-3965.
187. Ocana, A. and Amir, E. (2009) Irreversible pan-ErbB tyrosine kinase inhibitors and breast cancer: current status and future directions. *Cancer Treat Rev*, **35**, 685-691.
188. Perez, E.A. and Spano, J.P. (2012) Current and emerging targeted therapies for metastatic breast cancer. *Cancer*, **118**, 3014-3025.
189. Awada, A., Bozovic-Spasojevic, I. and Chow, L. (2012) New therapies in HER2-positive breast cancer: a major step towards a cure of the disease? *Cancer Treat Rev*, **38**, 494-504.
190. Rocha-Lima, C.M., Soares, H.P., Raez, L.E. and Singal, R. (2007) EGFR targeting of solid tumors. *Cancer Control*, **14**, 295-304.
191. Sharma, S.V., Bell, D.W., Settleman, J. and Haber, D.A. (2007) Epidermal growth factor receptor mutations in lung cancer. *Nat Rev Cancer*, **7**, 169-181.

192. Janne, P.A., Gray, N. and Settleman, J. (2009) Factors underlying sensitivity of cancers to small-molecule kinase inhibitors. *Nat Rev Drug Discov*, **8**, 709-723.
193. Hegedus, C., Ozvegy-Laczka, C., Szakacs, G. and Sarkadi, B. (2009) Interaction of ABC multidrug transporters with anticancer protein kinase inhibitors: substrates and/or inhibitors? *Curr Cancer Drug Targets*, **9**, 252-272.
194. Brozik, A., Hegedus, C., Erdei, Z., Hegedus, T., Ozvegy-Laczka, C., Szakacs, G. and Sarkadi, B. (2011) Tyrosine kinase inhibitors as modulators of ATP binding cassette multidrug transporters: substrates, chemosensitizers or inducers of acquired multidrug resistance? *Expert Opin Drug Metab Toxicol*, **7**, 623-642.
195. Ozvegy-Laczka, C., Hegedus, T., Varady, G., Ujhelly, O., Schuetz, J.D., Varadi, A., Keri, G., Orfi, L., Nemet, K. and Sarkadi, B. (2004) High-affinity interaction of tyrosine kinase inhibitors with the ABCG2 multidrug transporter. *Mol Pharmacol*, **65**, 1485-1495.
196. Burger, H., van Tol, H., Boersma, A.W., Brok, M., Wiemer, E.A., Stoter, G. and Nooter, K. (2004) Imatinib mesylate (STI571) is a substrate for the breast cancer resistance protein (BCRP)/ABCG2 drug pump. *Blood*, **104**, 2940-2942.
197. Houghton, P.J., Germain, G.S., Harwood, F.C., Schuetz, J.D., Stewart, C.F., Buchdunger, E. and Traxler, P. (2004) Imatinib mesylate is a potent inhibitor of the ABCG2 (BCRP) transporter and reverses resistance to topotecan and SN-38 in vitro. *Cancer Res*, **64**, 2333-2337.
198. Brendel, C., Scharenberg, C., Dohse, M., Robey, R.W., Bates, S.E., Shukla, S., Ambudkar, S.V., Wang, Y., Wennemuth, G., Burchert, A. *et al.* (2007) Imatinib mesylate and nilotinib (AMN107) exhibit high-affinity interaction with ABCG2 on primitive hematopoietic stem cells. *Leukemia*, **21**, 1267-1275.
199. Shukla, S., Sauna, Z.E. and Ambudkar, S.V. (2007) Evidence for the interaction of imatinib at the transport-substrate site(s) of the multidrug-resistance-linked ABC drug transporters ABCB1 (P-glycoprotein) and ABCG2. *Leukemia*.
200. Tamura, A., Onishi, Y., An, R., Koshiba, S., Wakabayashi, K., Hoshijima, K., Priebe, W., Yoshida, T., Kometani, S., Matsubara, T. *et al.* (2007) In vitro evaluation of photosensitivity risk related to genetic polymorphisms of human ABC transporter ABCG2 and inhibition by drugs. *Drug Metab Pharmacokinet*, **22**, 428-440.
201. Pick, A., Klinkhammer, W. and Wiese, M. (2010) Specific inhibitors of the breast cancer resistance protein (BCRP). *ChemMedChem*, **5**, 1498-1505.
202. Hiwase, D.K., Saunders, V., Hewett, D., Frede, A., Zrim, S., Dang, P., Eadie, L., To, L.B., Melo, J., Kumar, S. *et al.* (2008) Dasatinib cellular uptake and efflux in chronic myeloid leukemia cells: therapeutic implications. *Clin Cancer Res*, **14**, 3881-3888.
203. Elkind, N.B., Szentpetery, Z., Apati, A., Ozvegy-Laczka, C., Varady, G., Ujhelly, O., Szabo, K., Homolya, L., Varadi, A., Buday, L. *et al.* (2005) Multidrug transporter ABCG2 prevents tumor cell death induced by the epidermal growth factor receptor inhibitor Iressa (ZD1839, Gefitinib). *Cancer Res*, **65**, 1770-1777.
204. Yanase, K., Tsukahara, S., Asada, S., Ishikawa, E., Imai, Y. and Sugimoto, Y. (2004) Gefitinib reverses breast cancer resistance protein-mediated drug resistance. *Mol Cancer Ther*, **3**, 1119-1125.

205. Stewart, C.F., Leggas, M., Schuetz, J.D., Panetta, J.C., Cheshire, P.J., Peterson, J., Daw, N., Jenkins, J.J., 3rd, Gilbertson, R., Germain, G.S. *et al.* (2004) Gefitinib enhances the antitumor activity and oral bioavailability of irinotecan in mice. *Cancer Res*, **64**, 7491-7499.
206. Nakamura, Y., Oka, M., Soda, H., Shiozawa, K., Yoshikawa, M., Itoh, A., Ikegami, Y., Tsurutani, J., Nakatomi, K., Kitazaki, T. *et al.* (2005) Gefitinib ("Iressa", ZD1839), an epidermal growth factor receptor tyrosine kinase inhibitor, reverses breast cancer resistance protein/ABCG2-mediated drug resistance. *Cancer Res*, **65**, 1541-1546.
207. Leggas, M., Panetta, J.C., Zhuang, Y., Schuetz, J.D., Johnston, B., Bai, F., Sorrentino, B., Zhou, S., Houghton, P.J. and Stewart, C.F. (2006) Gefitinib modulates the function of multiple ATP-binding cassette transporters in vivo. *Cancer Res*, **66**, 4802-4807.
208. Li, J., Cusatis, G., Brahmer, J., Sparreboom, A., Robey, R.W., Bates, S.E., Hidalgo, M. and Baker, S.D. (2007) Association of variant ABCG2 and the pharmacokinetics of epidermal growth factor receptor tyrosine kinase inhibitors in cancer patients. *Cancer Biol Ther*, **6**, 432-438.
209. Zheng, L.S., Wang, F., Li, Y.H., Zhang, X., Chen, L.M., Liang, Y.J., Dai, C.L., Yan, Y.Y., Tao, L.Y., Mi, Y.J. *et al.* (2009) Vandetanib (Zactima, ZD6474) antagonizes ABCC1- and ABCG2-mediated multidrug resistance by inhibition of their transport function. *PLoS One*, **4**, e5172.
210. Ujhelly, O., Ozvegy, C., Varady, G., Cervenak, J., Homolya, L., Grez, M., Scheffer, G., Roos, D., Bates, S.E., Varadi, A. *et al.* (2003) Application of a human multidrug transporter (ABCG2) variant as selectable marker in gene transfer to progenitor cells. *Hum Gene Ther*, **14**, 403-412.
211. Orban, T.I., Seres, L., Ozvegy-Laczka, C., Elkind, N.B., Sarkadi, B. and Homolya, L. (2008) Combined localization and real-time functional studies using a GFP-tagged ABCG2 multidrug transporter. *Biochemical and biophysical research communications*, **367**, 667-673.
212. Ivics, Z., Hackett, P.B., Plasterk, R.H. and Izsvak, Z. (1997) Molecular reconstruction of Sleeping Beauty, a Tc1-like transposon from fish, and its transposition in human cells. *Cell*, **91**, 501-510.
213. Izsvak, Z. and Ivics, Z. (2004) Sleeping beauty transposition: biology and applications for molecular therapy. *Mol Ther*, **9**, 147-156.
214. Kwak, E.L., Sordella, R., Bell, D.W., Godin-Heymann, N., Okimoto, R.A., Brannigan, B.W., Harris, P.L., Driscoll, D.R., Fidias, P., Lynch, T.J. *et al.* (2005) Irreversible inhibitors of the EGF receptor may circumvent acquired resistance to gefitinib. *Proc Natl Acad Sci U S A*, **102**, 7665-7670.
215. Ozvegy-Laczka, C., Varady, G., Koblos, G., Ujhelly, O., Cervenak, J., Schuetz, J.D., Sorrentino, B.P., Koomen, G.J., Varadi, A., Nemet, K. *et al.* (2005) Function-dependent conformational changes of the ABCG2 multidrug transporter modify its interaction with a monoclonal antibody on the cell surface. *J Biol Chem*, **280**, 4219-4227.
216. Sarkadi, B., Price, E.M., Boucher, R.C., Germann, U.A. and Scarborough, G.A. (1992) Expression of the human multidrug resistance cDNA in insect cells

generates a high activity drug-stimulated membrane ATPase. *The Journal of biological chemistry*, **267**, 4854-4858.
217. Telbisz, A., Muller, M., Ozvegy-Laczka, C., Homolya, L., Szente, L., Varadi, A. and Sarkadi, B. (2007) Membrane cholesterol selectively modulates the activity of the human ABCG2 multidrug transporter. *Biochimica et biophysica acta*, **1768**, 2698-2713.
218. Bensadoun, A. and Weinstein, D. (1976) Assay of proteins in the presence of interfering materials. *Anal Biochem*, **70**, 241-250.
219. Luftig, R.B., Conscience, J.F., Skoultchi, A., McMillan, P., Revel, M. and Ruddle, F.H. (1977) Effect of interferon on dimethyl sulfoxide-stimulated Friend erythroleukemic cells: ultrastructural and biochemical study. *J Virol*, **23**, 799-810.
220. Kolonics, A., Apati, A., Janossy, J., Brozik, A., Gati, R., Schaefer, A. and Magocsi, M. (2001) Activation of Raf/ERK1/2 MAP kinase pathway is involved in GM-CSF-induced proliferation and survival but not in erythropoietin-induced differentiation of TF-1 cells. *Cell Signal*, **13**, 743-754.
221. Hollo, Z., Homolya, L., Davis, C.W. and Sarkadi, B. (1994) Calcein accumulation as a fluorometric functional assay of the multidrug transporter. *Biochimica et biophysica acta*, **1191**, 384-388.
222. Hegedus, C., Szakacs, G., Homolya, L., Orban, T.I., Telbisz, A., Jani, M. and Sarkadi, B. (2009) Ins and outs of the ABCG2 multidrug transporter: an update on in vitro functional assays. *Adv Drug Deliv Rev*, **61**, 47-56.
223. Telbisz, A., Hegedus, C., Ozvegy-Laczka, C., Goda, K., Varady, G., Takats, Z., Szabo, E., Sorrentino, B.P., Varadi, A. and Sarkadi, B. (2012) Antibody binding shift assay for rapid screening of drug interactions with the human ABCG2 multidrug transporter. *Eur J Pharm Sci*, **45**, 101-109.
224. Lozzio, C.B. and Lozzio, B.B. (1975) Human chronic myelogenous leukemia cell-line with positive Philadelphia chromosome. *Blood*, **45**, 321-334.
225. Ben-Neriah, Y., Daley, G.Q., Mes-Masson, A.M., Witte, O.N. and Baltimore, D. (1986) The chronic myelogenous leukemia-specific P210 protein is the product of the bcr/abl hybrid gene. *Science*, **233**, 212-214.
226. Kloetzer, W., Kurzrock, R., Smith, L., Talpaz, M., Spiller, M., Gutterman, J. and Arlinghaus, R. (1985) The human cellular abl gene product in the chronic myelogenous leukemia cell line K562 has an associated tyrosine protein kinase activity. *Virology*, **140**, 230-238.
227. Kurzrock, R., Kloetzer, W.S., Talpaz, M., Blick, M., Walters, R., Arlinghaus, R.B. and Gutterman, J.U. (1987) Identification of molecular variants of p210bcr-abl in chronic myelogenous leukemia. *Blood*, **70**, 233-236.
228. Brozik, A., Casey, N.P., Hegedus, C., Bors, A., Kozma, A., Andrikovics, H., Geiszt, M., Nemet, K. and Magocsi, M. (2006) Reduction of Bcr-Abl function leads to erythroid differentiation of K562 cells via downregulation of ERK. *Ann N Y Acad Sci*, **1090**, 344-354.
229. Kim, M., Turnquist, H., Jackson, J., Sgagias, M., Yan, Y., Gong, M., Dean, M., Sharp, J.G. and Cowan, K. (2002) The multidrug resistance transporter ABCG2 (breast cancer resistance protein 1) effluxes Hoechst 33342 and is overexpressed in hematopoietic stem cells. *Clin Cancer Res*, **8**, 22-28.

230. Shapiro, A.B. and Ling, V. (1995) Reconstitution of drug transport by purified P-glycoprotein. *The Journal of biological chemistry*, **270**, 16167-16175.
231. Gambacorti-Passerini, C., le Coutre, P., Mologni, L., Fanelli, M., Bertazzoli, C., Marchesi, E., Di Nicola, M., Biondi, A., Corneo, G.M., Belotti, D. *et al.* (1997) Inhibition of the ABL kinase activity blocks the proliferation of BCR/ABL+ leukemic cells and induces apoptosis. *Blood Cells Mol Dis*, **23**, 380-394.
232. Jacquel, A., Herrant, M., Legros, L., Belhacene, N., Luciano, F., Pages, G., Hofman, P. and Auberger, P. (2003) Imatinib induces mitochondria-dependent apoptosis of the Bcr-Abl-positive K562 cell line and its differentiation toward the erythroid lineage. *Faseb J*, **17**, 2160-2162.
233. Pawarode, A., Shukla, S., Minderman, H., Fricke, S.M., Pinder, E.M., O'Loughlin, K.L., Ambudkar, S.V. and Baer, M.R. (2007) Differential effects of the immunosuppressive agents cyclosporin A, tacrolimus and sirolimus on drug transport by multidrug resistance proteins. *Cancer Chemother Pharmacol*, **60**, 179-188.
234. Brazil, D.P. and Hemmings, B.A. (2001) Ten years of protein kinase B signalling: a hard Akt to follow. *Trends Biochem Sci*, **26**, 657-664.
235. Davies, S.P., Reddy, H., Caivano, M. and Cohen, P. (2000) Specificity and mechanism of action of some commonly used protein kinase inhibitors. *Biochem J*, **351**, 95-105.
236. Krupka, R.M. (1999) Uncoupled active transport mechanisms accounting for low selectivity in multidrug carriers: P-glycoprotein and SMR antiporters. *J Membr Biol*, **172**, 129-143.
237. Telbisz, A., Ozvegy-Laczka, C., Hegedus, T., Varadi, A. and Sarkadi, B. (2012) Effects of the lipid environment, cholesterol and bile acids on the function of purified, reconstituted human ABCG2 protein. *Biochem J.*
238. Huang, W.C., Chen, Y.J., Li, L.Y., Wei, Y.L., Hsu, S.C., Tsai, S.L., Chiu, P.C., Huang, W.P., Wang, Y.N., Chen, C.H. *et al.* (2011) Nuclear translocation of epidermal growth factor receptor by Akt-dependent phosphorylation enhances breast cancer-resistant protein expression in gefitinib-resistant cells. *The Journal of biological chemistry*, **286**, 20558-20568.
239. Imai, Y., Yoshimori, M., Fukuda, K., Yamagishi, H. and Ueda, Y. (2012) The PI3K/Akt inhibitor LY294002 reverses BCRP-mediated drug resistance without affecting BCRP translocation. *Oncol Rep*, **27**, 1703-1709.